

## Louisiana State University LSU Digital Commons

---

LSU Doctoral Dissertations

Graduate School

---

2006

# Synthesis, characterization and properties of cooper(II) beta-diketonate macrocycles

Sylvester Burton

*Louisiana State University and Agricultural and Mechanical College, [sburton@lsu.edu](mailto:sburton@lsu.edu)*

Follow this and additional works at: [https://digitalcommons.lsu.edu/gradschool\\_dissertations](https://digitalcommons.lsu.edu/gradschool_dissertations)



Part of the [Chemistry Commons](#)

---

### Recommended Citation

Burton, Sylvester, "Synthesis, characterization and properties of cooper(II) beta-diketonate macrocycles" (2006). *LSU Doctoral Dissertations*. 3273.

[https://digitalcommons.lsu.edu/gradschool\\_dissertations/3273](https://digitalcommons.lsu.edu/gradschool_dissertations/3273)

This Dissertation is brought to you for free and open access by the Graduate School at LSU Digital Commons. It has been accepted for inclusion in LSU Doctoral Dissertations by an authorized graduate school editor of LSU Digital Commons. For more information, please contact [gradetd@lsu.edu](mailto:gradetd@lsu.edu).

# **SYNTHESIS, CHARACTERIZATION AND PROPERTIES OF COPPER(II) BETA-DIKETONATE MACROCYCLES**

A Dissertation

Submitted to the Graduate Faculty of the  
Louisiana State University and  
Agricultural and Mechanical College  
In partial fulfillment of the  
requirements for the degree of  
Doctor of Philosophy

in

The Department of Chemistry

by  
Sylvester Burton  
B.S., Southern University, 1977  
M.S., Southern University, 1986  
May 2006

**A.B., F.W.B., A.M.B., S.T.B., E.W.B. Sr., Jr.,  
S.M.D., J.R.G., A.A.R.G., R.G. and T.W-A.**

## Foreword

ANYONE WHO HAS EVER TRIED TO PRESENT A RATHER ABSTRACT scientific subject in a popular manner knows the great difficulties of such an attempt. Either he succeeds in being intelligible by concealing the core of the problem and by offering to the reader only superficial aspects or vague allusions, thus deceiving the reader by arousing in him the deceptive illusion of comprehension; or else he gives an expert account of the problem, but in such a fashion that the untrained reader is unable to follow the exposition and becomes discouraged from reading any further.

If these two categories are omitted from today's popular scientific literature, surprisingly little remains. But the little that is left is very valuable indeed. It is of great importance that the general public be given an opportunity to experience (consciously and intelligently) the efforts and results of scientific research. It is not sufficient that each result be taken up, elaborated, and applied by a few specialists in the field. Restricting the body of knowledge to a small group deadens the philosophical spirit of a people and leads to spiritual poverty.

Albert Einstein  
Princeton, New Jersey  
September 10, 1948

## **Acknowledgments**

FOR THEIR HELP AND ADVICE IN MY MATRICULATION, I wish to thank Dr. Andrew W. Maverick, Dr. Steve Watkins, Dr. Frank Fronczek for determining all of the crystal structures presented here, and my graduate committee, of the Department of Chemistry, Louisiana State University & A&M College; Dr. Robert H. Miller, Jr. of the Department of Chemistry/College of Sciences and Dr. Mildred R. Smalley of the Department of Chemistry/Office of the Vice Chancellor for Research and Strategic Initiatives, Southern University & A&M College.

And most of all, I thank GOD.

## Table of Contents

Dedication.....	ii
Foreword.....	iii
Acknowledgements.....	iv
List of Tables .....	vii
List of Figures .....	viii
List of Abbreviations.....	xi
Abstract.....	xii
Chapter 1	
Introduction .....	1
Chapter 2	
3,5-Diacetyl-2,6-Heptanedione ( $C_1BAH_2$ ) and Its Metal Complexes .....	9
2.1 Introduction .....	9
2.2 Experimental .....	11
2.2.1 Materials and Equipment.....	11
2.2.2 Preparation of 3,5-diacetyl-2,6-heptanedione ( $C_1BAH_2$ ) and 2-methyl-3,5,5-triacetyltetrahydropyran-2-ol .....	11
2.2.3 Attempted Preparation of $C_1BAH_2$ Molecular Solid.....	13
2.3 Results and Discussion .....	15
Chapter 3	
<i>p</i> -Xylylenebis(acetylacetone) ( $p-XBAH_2$ ) and Its Metal Complexes .....	23
3.1 Introduction .....	23
3.2 Experimental .....	23
3.2.1 Materials and Equipment.....	23
3.2.2 Preparation of <i>p</i> -xylylenebis(acetylacetone) ( $p-XBAH_2$ ) .....	24
3.2.3 Attempted Preparation of $Cu_3(p-XBA)_3$ Molecular Solid .....	25
3.2.4 Structural Analysis of $p-XBAH_2$ .....	27
3.3 Results and Discussion .....	28
Chapter 4	
$Cu_2(NBA)_2 \cdot [Substrate]$ Studies .....	30
4.1 Introduction .....	30

4.2 Experimental .....	31
4.2.1 Materials and Procedures.....	31
4.2.2. X-Ray Analysis of $\text{Cu}_2(\text{NBA})_2 \cdot (1,4\text{-dithiane})$ .....	32
4.3. Results and Discussion .....	36
Chapter 5	
$\text{Cu}_2(\text{XBDPr})_2$ and $\text{Cu}_2(\text{NBDPr})_2$ Studies.....	39
5.1 Introduction .....	39
5.2 Experimental .....	41
5.2.1 Materials and Procedures.....	41
5.2.2 Preparation of 4,4'-(2,7-naphthalenediylbis (methylene))bis(dipropionylmethane) (NBDPrH <sub>2</sub> ) and 4,4'-(1,3-xylenediylbis(methylene))bis (dipropionylmethane) (XBDPrH <sub>2</sub> ) .....	42
5.2.3 Preparation of $\text{Cu}_2(\text{NBDPr})_2$ and Attempted Preparation of $\text{Cu}_2(\text{XBDPr})_2$ .....	47
5.2.4 Structural Analysis of $\text{Cu}_2(\text{NBDPr})_2$ .....	48
5.3 Results and Discussion .....	50
Chapter 6	
Summary and Conclusions .....	52
References .....	56
Appendix Crystal Data in CIF Format .....	60
Vita.....	121

## List of Tables

Table 2.1. Melting points of 3,5-diacetyl-2,6-heptanedione tautomers .....	10
Table 2.2. $^1\text{H}$ NMR shifts for 3,5-diacetyl-2,6-heptanedione .....	11
Table 2.3. Crystal data for 3,5-diacetyl-2,6-heptanedione and 2-methyl-3,5,5-triacetyltetrahydropyran-2ol.....	14
Table 2.4. Elemental analysis data of $\text{Cu}(\text{C}_1\text{BA})_2$ .....	18
Table 3.1. Crystal data for $p\text{-XBAH}_2$ .....	26
Table 4.1. Crystal data of $\text{Cu}_2(\text{NBA})_2 \cdot (1,4\text{-dithiane})$ .....	33
Table 4.2. Selected bond distance comparison .....	34
Table 5.1. $^1\text{H}$ NMR shifts of (a) $\text{XBAH}_2$ , (b) $\text{XBDPrH}_2$ and (c) $\text{NBDPrH}_2$ .....	44
Table 5.2. Crystal data of $\text{Cu}_2(\text{NBDPr})_2$ .....	49
Table 5.3. Tabulation of $^1\text{H}$ NMR data of starting materials. ....	50



## List of Figures

Figure 1.1. Acetylacetonate anion (acac) <sup>-</sup> .....	2
Figure 1.2. Picture of $\Lambda$ and $\Delta$ enantiomers of a M(chelate) <sub>3</sub> complex.....	3
Figure 1.3. Trinuclear (Ni(acac) <sub>2</sub> ) <sub>3</sub> .....	4
Figure 1.4. Face to Face porphyrin .....	4
Figure 1.5. (a) Cu <sub>2</sub> (m-XBA) <sub>2</sub> , (b) cis-syn Cu <sub>2</sub> (BBI) <sub>2</sub> .....	5
Figure 1.6. (a) C <sub>1</sub> BAH <sub>2</sub> , (b) <i>p</i> -XBAH <sub>2</sub> .....	6
Figure 1.7. (a) Cu <sub>3</sub> ( <i>p</i> -XBA) <sub>3</sub> (molecular triangle) (b) Cu <sub>6</sub> (C <sub>1</sub> BA) <sub>6</sub> (molecular hexamer) .....	7
Figure 1.8. Oh's Proposed 4-coordinate polymer structures.....	8
Figure 2.1. 3,5-diacetyl-2,6-heptanedione tautomers.....	10
Figure 2.2. ORTEP diagram of 3,5-diacetyl-2,6-heptanedione (C <sub>1</sub> BAH <sub>2</sub> ) .....	12
Figure 2.3. ORTEP diagram of 2-methyl-3,5,5-triacetyltetrahydropyran-2-ol ....	13
Figure 2.4. Reaction scheme and picture of proposed Cu <sub>6</sub> (C <sub>1</sub> BA) <sub>6</sub> hexamer ...	17
Figure 2.5. Di-enol form of Cu(C <sub>1</sub> BA) <sub>2</sub> .....	18
Figure 2.6. Chemical structure drawing and molecular model of dinuclear Cu unit containing one bridging C <sub>1</sub> BA <sup>2-</sup> ligand ( $\Delta$ enantiomer shown) .....	19
Figure 2.7. Ring-shaped hexanuclear Cu complex containing alternating $\Delta$ - and $\Lambda$ - C <sub>1</sub> BA <sup>2-</sup> bridging ligands .....	20
Figure 2.8. Helical hexanuclear Cu complex containing all $\Delta$ -C <sub>1</sub> BA <sup>2-</sup> bridging Ligands .....	20
Figure 2.9. SPARTAN plot of conformational energy of the bis(enol) form of C <sub>1</sub> BAH <sub>2</sub> vs. central C-C-C-C torsion angle. Also shown is a ball- and-stick illustration of the molecule when this torsion angle is	

close to 90 deg, i.e. approximately in the highest-energy conformation required for interconversion of the two enantiomeric forms of the ligand .....	21
Figure 3.1. ORTEP diagram of <i>p</i> -XBAH <sub>2</sub> .....	24
Figure 3.2. IR Spectrum of <i>p</i> -XBAH <sub>2</sub> and Cu <sub>n</sub> ( <i>p</i> -XBA) <sub>n</sub> .....	26
Figure 3.3. View of <i>p</i> -XBAH <sub>2</sub> along the c- axis.....	28
Figure 3.4. Proposed coordination polymer structures for Cu( <i>p</i> -XBA) .....	29
Figure 4.1. Intramolecular binding of generic host by Cu <sub>2</sub> (NBA) <sub>2</sub> .....	31
Figure 4.2. CCDC Mercury diagram of Cu <sub>2</sub> (NBA) <sub>2</sub> •(1,4-dithiane), top view.....	33
Figure 4.3. ORTEP diagram of Cu <sub>2</sub> (NBA) <sub>2</sub> •(1,4-dithiane), side view.....	34
Figure 4.4. Crystal packing diagram of Cu <sub>2</sub> (NBA) <sub>2</sub> •(1,4-dithiane), view along a, showing the packing of adjacent molecules .....	35
Figure 4.5. Comparative side views of Cu <sub>2</sub> (NBA) <sub>2</sub> •(S), with S = 1,4-dithiane, dabco and 2,5-Me <sub>2</sub> pyz.....	35
Figure 4.6. Comparative top views of Cu <sub>2</sub> (NBA) <sub>2</sub> • (S), with S = 1,4-dithiane, dabco and 2,5-Me <sub>2</sub> pyz.....	36
Figure 4.7. Stick figure view of Cu <sub>2</sub> (NBA) <sub>2</sub> • (1,4-dithiane) showing the deviation from co-planarity of the (bis)β-diketonate units.....	37
Figure 5.1. Structure of alkylated XBA and NBA Ligands .....	39
Figure 5.2. Structure of Cu <sub>2</sub> (XBDPr) <sub>2</sub> and Cu <sub>2</sub> (NBA) <sub>2</sub> .....	40
Figure 5.3. Structures of XBAH <sub>2</sub> , XBDPrH <sub>2</sub> and NBDPrH <sub>2</sub> ligands .....	44
Figure 5.4. <sup>1</sup> H NMR spectrum of crude XBDPrH <sub>2</sub> .....	45
Figure 5.5. <sup>1</sup> H NMR spectrum of crude NBDPrH <sub>2</sub> .....	46
Figure 5.6. ORTEP diagram of Cu(3,5-heptanedionate).....	48
Figure 5.7. CCDC Mercury diagram of Cu <sub>2</sub> (NBDPr) <sub>2</sub> with view along b.....	49

Figure 6.1. (Z)-3,6-diacetyloct-4-ene-2,7-dione .....	53
Figure 6.2. Possible (bis) $\beta$ -diketonate precursor compared to C1BAH <sub>2</sub> .....	53

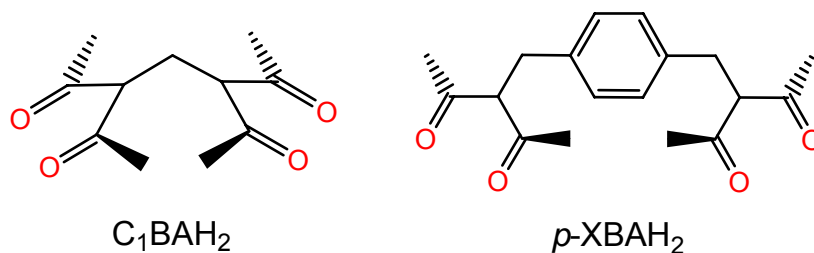
## List of Abbreviations

acacH <sub>2</sub>	acetylacetone
acacH <sup>-</sup>	acetylacetonate anion
BBi	bis(β-ketoenamine)
C <sub>1</sub> BAH <sub>2</sub>	3,5-diacetyl-2,6-heptanedione
dabco	1,4-diaza-bicyclo[2.2.2]octane
p-XBAH <sub>2</sub>	<i>p</i> -xylylenebis(acetylacetone)
ORTEP	Oak Ridge Thermal Ellipsoid Plot
NBAH <sub>2</sub>	2,7-naphthalenediylbis(methylene)bis(acetylacetone)
NBDPrH <sub>2</sub>	4,4'-(2,7-naphthalenediylbis(methylene)) bis(dipropionylmethane)
XBDPrH <sub>2</sub>	4,4'-(1,3-xylenediylbis(methylene)) bis(dipropionylmethane)
CIF	Crystallographic Information File

## Abstract

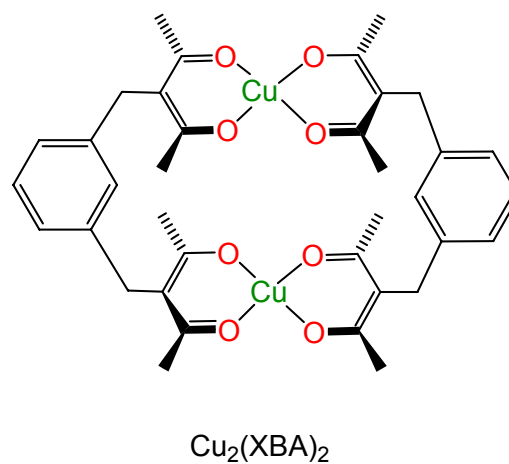
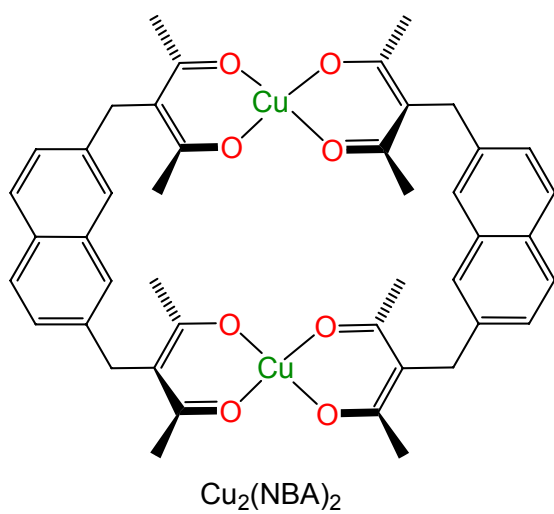
This dissertation deals with the synthesis and properties of multidentate  $\beta$ -diketone ligands and their transition-metal complexes.

(1) We prepared two bis( $\beta$ -diketones),  $C_1BAH_2$  and  $p\text{-XBAH}_2$  (see sketch below), determined their crystal structures, and studied their reactions with



copper(II). We envisioned that they would form macrocyclic complexes with 3-6 metal atoms. In both cases, although the initial products are soluble, as expected for the desired molecular products, we were unable to isolate well-behaved molecular solids. In the case of  $C_1BAH_2$ , this may be because the cyclic product requires an unusual combination of conformations of successive ligands.

(2) We studied the reactions of  $Cu_2(NBA)_2$  (shown below) with the heterocyclic sulfur bases 1,4-dithiane and 2,5-dihydroxy-1,4-dithiane. The reaction with 1,4-dithiane produces a 1:1 adduct with the guest molecule internally coordinated to the Cu atoms of the host. The affinity of the  $Cu_2(NBA)_2$  host for 1,4-dithiane is very small. The substituted derivative 2,5-dihydroxy-1,4-dithiane was also studied as a potential guest, but its solubility is not compatible with that of the  $Cu_2(NBA)_2$  host.



(3) We attempted to determine if extending the aliphatic chains of our  $\text{NBAH}_2$  and  $p\text{-XBAH}_2$  ligands would increase their solubility in organic solvents and afford us the versatility to extend our groups study of binuclear transition metal complex host-guest systems. We successfully synthesized  $\text{Cu}_2(\text{NBPr})_2$ , which contains ethyl groups in place of the methyl groups of  $\text{Cu}_2(\text{NBA})_2$ . However, the new  $\text{Cu}_2(\text{NBPr})_2$  host is not significantly more soluble in common organic solvents than the parent  $\text{Cu}_2(\text{NBA})_2$ .

# **Chapter 1**

## **Introduction**

Supramolecular chemistry has emerged from the studies of such covalent systems as cyclophanes, crown ethers, calixarenes and cryptands. This field has for over a decade been dominated by the study of non-covalent moieties which consist of transition metal motifs and coordination bonded assemblies.

Molecular manufacturing of advanced materials with specific properties and functions has become the major challenge that faces modern supramolecular nanotechnology. These properties and functions are determined by controlling the form, shape and distribution of each individual building block subunit and their precise placement within the supramolecule. Such intermolecular control imposes strict requirements on the nature, type and directionality of the bonding forces that operate within the entire aggregated structure. The chemical bonding of the subunits must be relatively weak, thermodynamically stable, and yet kinetically labile to allow the self arrangement of the subunits within the entire structure, thereby enabling the self-correction of possible defects. Another important requirement is the conformational rigidity of the building blocks in order to reduce entropic factors upon self-organization.

The more recently developed synthetic protocol, namely self-assembly, relies on critical information about the shape and properties of the target

structures being preprogrammed into each individual building block, in order to construct nanoscopic assemblies from multiple building blocks in a single step.

For many years the search for new ligands has been a prevailing goal in coordination chemistry. Through the appropriate choice of ligands, we can generally design and synthesize coordination compounds having particular specified properties. However, because of the intrinsic complexity of many of the bridging-group derivatized ligands, unexpected modes of coordination may sometimes occur, and reactions may follow undesired routes.

Beta-diketonates represent one of the oldest classes of chelating ligands, and have become one of the ligands of choice because of the recent industrial applications of several of their metal complexes. Beta-diketonates are made by

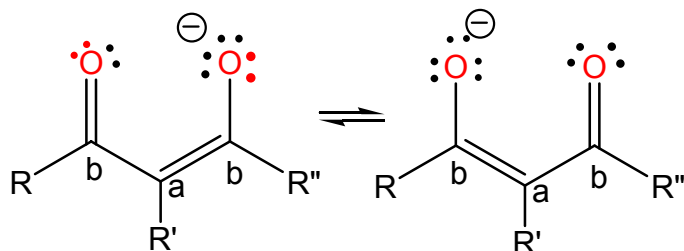


Figure 1.1. Acetylacetonate anion ( $\text{acac}^-$ ),  
 $\text{R} = \text{R}'' = \text{CH}_3$  and  $\text{R}' = \text{H}$ .

methods similar to those for the alkoxides.<sup>1.1-1.5</sup>

Beta-diketonates form anions as a result of enolization and ionization after  $\alpha$ -proton extraction by

base. These beta-ketoenolate ions form very stable chelate complexes with most metal ions.<sup>1.6</sup> The most common diketonate ionic ligand is the acetylacetonate anion ( $\text{acacH}^-$ ) (Figure 1.1), where  $\text{R} = \text{R}'' = \text{CH}_3$  and  $\text{R}' = \text{H}$ . The usual abbreviation for  $\beta$ -ketoenolate ions in general is ( $\beta$ -dike). Among the commonest types of diketonate complexes are those with the stoichiometries



$M(\beta\text{-dike})_3$  and  $M(\beta\text{-dike})_2$  tris and bis respectively. The former have structures based on an octahedral disposition of the six oxygen atoms. These tris(chelate) molecules actually have  $D_3$  symmetry and exist as enantiomers, (see  $\Lambda$  and  $\Delta$  structures in

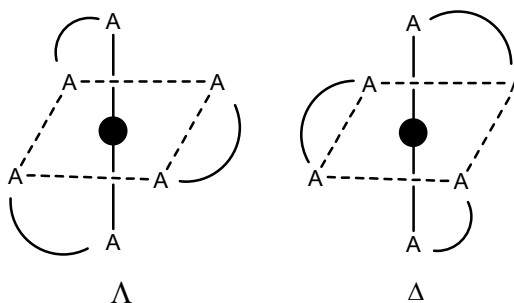


Figure 1.2. Picture of  $\Lambda$  and  $\Delta$  enantiomers of a  $M(\text{chelate})_3$  complex.

Figure 1.2). Chiral diketonate complexes have found applications in fields such as catalysis and gas-chromatographic separations of enantiomers.<sup>1,7</sup> Togni,<sup>1,8</sup> for example has demonstrated that the chiral Lewis acid bis[(1R)-3-(heptafluorobutyl)camphorato]oxovanadium(IV) can be used to promote the hetero-Diels-Alder reactions between an aldehyde and a diene of the type described by Danishefsky.<sup>1,9-1.10</sup> Tetradiketo complexes such as  $M(\beta\text{-dike})_4$  on the other hand, have usually been found to be nonrigid.<sup>1.11</sup>

Compounds with the composition  $M(\beta\text{-dike})_2$  are very often oligomeric, thereby allowing coordinative saturation of the metal. Thus, acetylacetonates of anhydrous  $Zn^{II}$ ,  $Ni^{II}$ , and  $Mn^{II}$  are trinuclear (Figure 1.3)<sup>1.23</sup> but  $Co(acac)_2$  which is expected to assume a square planar or tetrahedral arrangement, actually assumes a tetranuclear arrangement of the ligands and have bridging beta-diketonate groups. The result is a tetramer in which a pseudo-octahedral arrangement is achieved by each cobalt(II) cation. The presence of bulky substituents such as a t-butyl group on the beta-diketonate has been shown to

sterically impede oligomerization, and monomers are generally formed. These

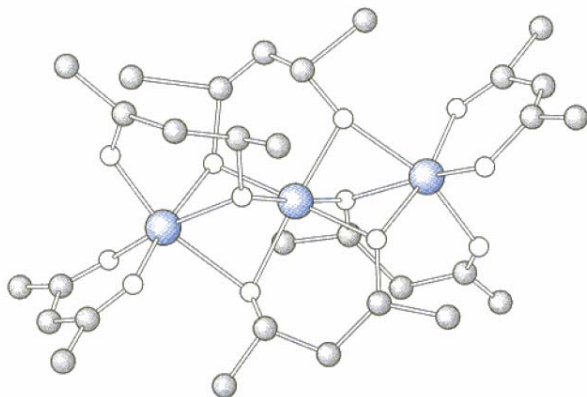


Figure 1.3. Trinuclear  $(\text{Ni}(\text{acac})_2)_3$

are commonly solvated by  $\text{H}_2\text{O}$ ,  $\text{ROH}$ , or pyridine to give 5- or 6-coordinate complexes, such as  $\text{trans-M}(\beta\text{-dike})_2\text{L}_{1,2}$ .<sup>1,11</sup>

The linking of  $\beta$ -diketonates by specific bridges allow them to form

“face-to-face” complexes similar to those of the “face-to-face” porphyrins (Figure 1.4), therefore affording the occupancy of the central cavity by small molecules.

These bridged  $\beta$ -diketonates are commonly referred to as bis-( $\beta$ -diketonates). With trivalent ions such as  $\text{Ti}^{3+}$ ,  $\text{V}^{3+}$ ,  $\text{Mn}^{3+}$ , or  $\text{Fe}^{3+}$ , triple-helical structures consisting of two 6-coordinate  $\text{M}^{\text{III}}$  ions

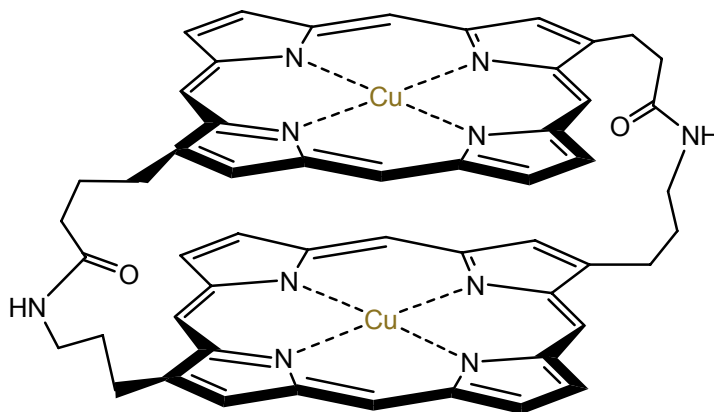


Figure 1.4. Face-to-Face porphyrin.

chelated by three bis-( $\beta$ -diketonate) ligands can be obtained.<sup>1,11</sup>

Our group has been interested in metal bis-( $\beta$ -diketonate) complexes for years because of their host-guest chemistry<sup>1.13-1.18</sup> and CVD applications to form

thin metal films. The goal of our group's study of host-guest chemistry has been directed toward the use of select bis-( $\beta$ -diketonates) and Schiff-base ligands to make binuclear metal-complexes and examine their suitability for host access, release and/or exchange.

In the examples discussed here, the metal atoms are either coordinatively unsaturated or contain ligands that can easily be displaced when the metallic moiety is introduced to other donors. This would allow the host to bind a variety of guest molecules,<sup>1,19</sup> which has been shown to be the case in some of our group's earlier work.

Therefore, the basis of our chemistry has been in the ligating ability of the acetylacetonate (acacH<sub>2</sub>) moiety, which has been extensively studied over the years, primarily because of its rich coordinating ability to metal

centers.<sup>1,13, 1,14, 1,20</sup>

Cofacial binuclear transition metal complexes derived from bis-( $\beta$ -diketonates) and bis-( $\beta$ -ketoenamine)<sup>1,13, 1,14, 1,21</sup> ligands have also been investigated by our group (Figure 1.5). The aim of this study has been to extend the usage of bis-( $\beta$ -diketonates) and construct inorganic-organic hybrid molecules

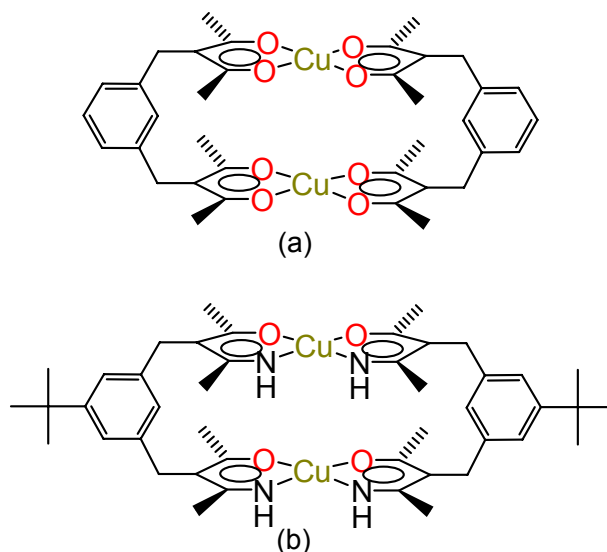


Figure 1.5. (a) Cu<sub>2</sub>(m-XBA)<sub>2</sub>,  
(b) cis-syn Cu<sub>2</sub>(BBI)<sub>2</sub>

which possess pores that are well defined by several types of nodes. My contribution for this phase of our group's research has been the preparation of a series of bis-( $\beta$ -diketonate) molecular solids having identical nodes which contain chemical functionalities that are spatially organized by covalent and/or noncovalent interactions during the synthetic process, thus designing sites for the recognition of small molecules. The resulting complexes were to be examined for their host binding ability to determine if these interactions could form the basis for nanoscale sensors and chemically active devices.

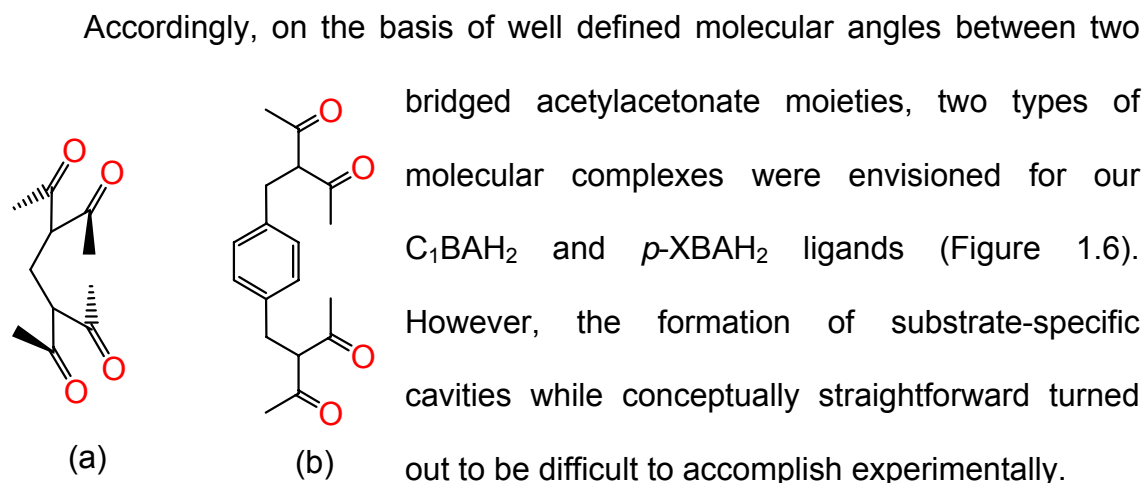


Figure 1.6. (a)  $C_1BAH_2$ ,  
(b)  $p-XBAH_2$

The synthetic difficulties that were encountered during the preparation attempts of the trimer and hexamer molecular solids (Figure 1.7) was attributed to sterics and the tendency of these ligands to form the linear monomer coordination compounds, possessing a metal to ligand ratio of 1:2,  $M(L)_2$  (Figure 1.8).

There are several literature references which indicate that when certain bridged beta-diketonates are treated with di- and tri-cationic transition metals

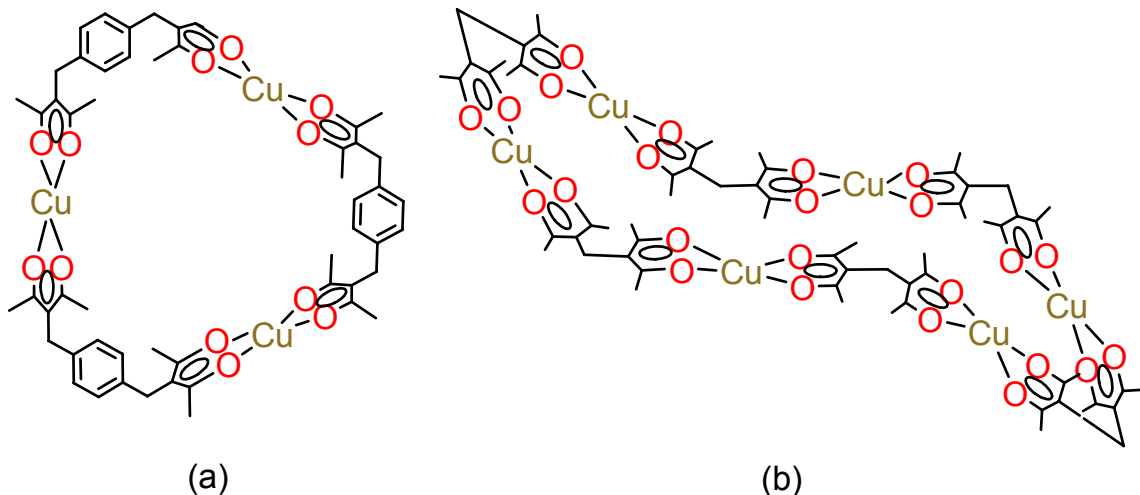


Figure 1.7. (a)  $\text{Cu}_3(\text{p-XBA})_3$  (molecular triangle),  
(b)  $\text{Cu}_6(\text{C}_1\text{BA})_6$  (molecular hexamer).

( $\text{M}^{2+}$  or  $\text{M}^{3+}$ ), they have the tendency to form 4-coordinate linear oligomers of three (Figure 1.8) types,<sup>1,22</sup> (1)  $[(\text{RCO})(\text{R}'\text{CO})\text{CH}]_2$ , (2)  $(\text{RCO})(\text{R}'\text{CO})\text{CH-Y-CH}(\text{R}'\text{CO})(\text{RCO})$  and (3)  $(\text{RCO})(\text{R}'\text{CO})\text{CH-CHR}''\text{-CH}(\text{R}'\text{CO})(\text{RCO})$  with  $\text{R} = \text{R}' = -\text{CH}_3$  and  $\text{Y} = -(\text{CH}_2)_2-$  and  $-\text{CH}_2-\text{C}_6\text{H}_6-\text{CH}_2-$ . These systematic oligomeric structures were determined based on their elemental analysis.

As previously mentioned, our group in a prior study determined that  $\text{Cu}_2(\text{NBA})_2$  intramolecularly coordinates the nitrogen bases, dabco and pyrazine. Based on that study, I undertook the task of examining the coordinating ability of  $\text{Cu}_2(\text{NBA})_2$  with heterocyclic sulfur-containing bases in order to compare the relative binding strengths of  $\text{Cu}_2(\text{NBA})_2$  with nitrogen bases and those with sulfur bases.

However, one of the challenges discovered was that in order to enhance

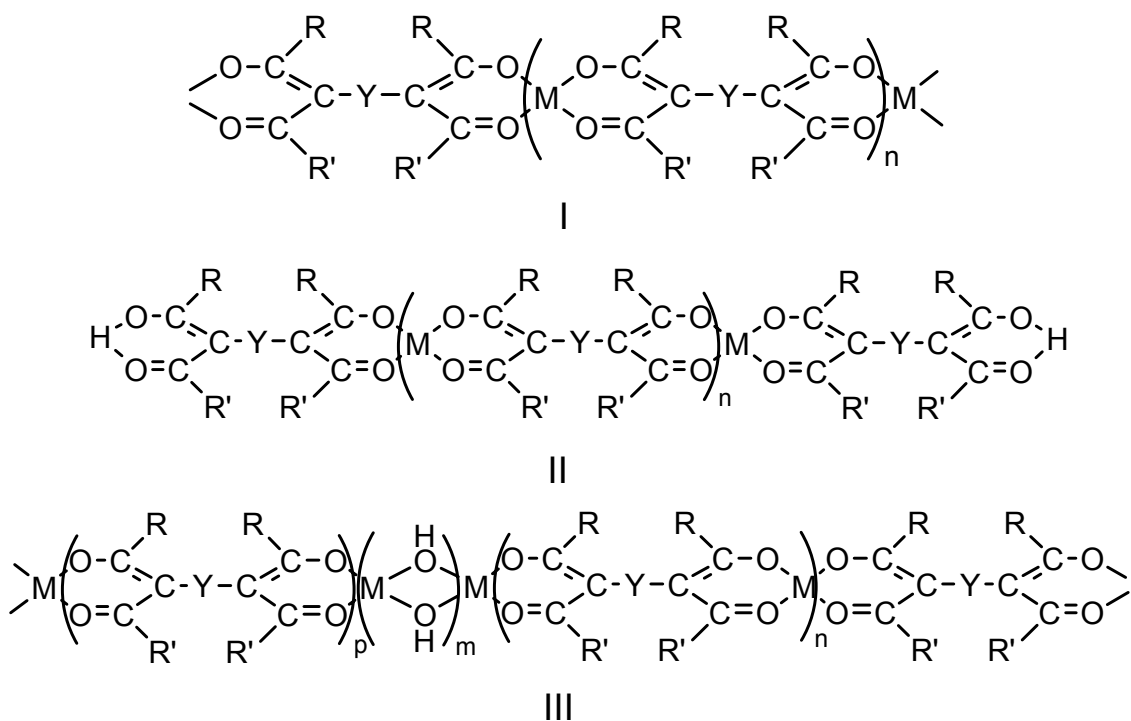


Figure 1.8. Oh's<sup>1,22</sup> proposed 4-coordinate polymer structures.

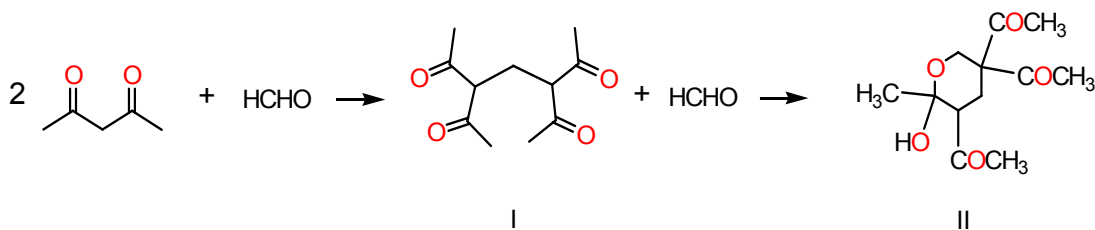
the coordination, the host and the guest should be soluble in the same solvent system. This was of concern because it had been discovered that  $\text{Cu}_2(\text{NBA})_2$  was practically insoluble in most organic solvents. Therefore, we decided to modify our  $\text{Cu}_2(\text{NBA})_2$  by alkylating the  $\text{acac}^-$  moiety in an attempt to increase its solubility in organic solvents, whereby if achieved, would allow us the potential for enhancing the coordination of our guest molecules.

## Chapter 2

### 3,5-Diacetyl-2,6 Heptanedione(C<sub>1</sub>BAH<sub>2</sub>) and Its Metal Complexes

#### 2.1. Introduction

Since the work of Knoevenagel<sup>2.1-2.2</sup> in the late nineteenth and early twentieth centuries, when he first reported the condensation products of 2,4-pentanedione with aldehydes, reactions of the compounds have been investigated extensively.<sup>2.1-2.2,2.4-2.6</sup> For example Aarna et al,<sup>2.7</sup> have shown (Scheme 2.1) that with a 2:1 ratio of acacH:HCHO the product is 3,5-diacetyl-2,6-heptanedione(I) and with a 2:2 ratio of acacH<sub>2</sub>:HCHO the undesired product, 3,5,5-triacetyl-tetrahydropyran-2-ol(II) is produced.



Scheme 2.1.

The IR for (I) shows two CO bands at 1735 cm<sup>-1</sup> and 1715 cm<sup>-1</sup>. The NMR for (I) shows chemical shifts,  $\delta$  = 2.2 (Me), 2.28 2.35 (t, CH<sub>2</sub>) and 3.58, 3.66, 3.75 ppm (t,CH). We prepared the target ligand 3,5-diacetyl-heptane-2,6-dione according to the procedure introduced by Wilson,<sup>2.4</sup> who investigated the condensation reaction between formaldehyde (HCHO) and 2,4-pentanedione, (acacH<sub>2</sub>). Because of steric effects and the terminal CH<sub>3</sub>- groups, this reaction

produces the tautomeric (or enol isomeric) forms of the 1:1 condensation product 3,5-diacetyl-2,6 heptanedione in good yield (Figure 2.1).

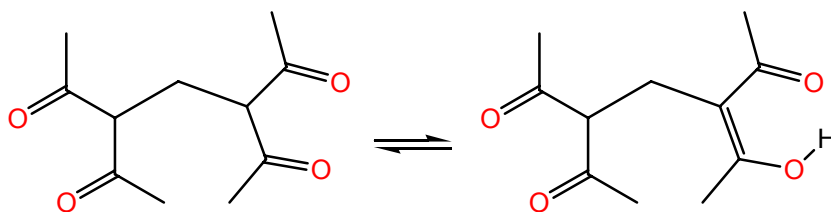


Figure 2.1. 3,5-Diacetyl-2,6-heptanedione tautomers.

Conjugated intermolecular hydrogen bonding in the enol isomer causes the extent of enolization of  $\beta$ -diketonates and  $\beta$ -ketoesters to be much greater than for other carbonyl systems. It has also been shown that the more polar keto forms are stabilized by polar solvents and protic solvents of high dielectric constant,  $\epsilon$ , because these have a tendency to disrupt the intermolecular hydrogen bonding that is present in the enol form. For example, at 298 K acetylacetone is 96% enolized in  $\text{CCl}_4$  ( $\epsilon = 2.23$ )<sup>2,8</sup>, ~80% enolized in *p*-dioxane ( $\epsilon = 2.21$ )<sup>2,9,2,10</sup>, and only 16% enolized in water ( $\epsilon = 78.5$ ).<sup>2,11,2,12</sup> Wilson and O’Loane initially characterized this compound by melting point<sup>2,4</sup> (Table 2.1) and  $^1\text{H}$  NMR spectroscopy<sup>2,5</sup> (Table 2.2) respectively.

Table 2.1. Melting points of 3,5-diacetyl-2,6-heptanedione tautomers

Keto Form	Mono-Enolic Form
41.5–42.5° C	55-56° C



Table 2.2.  $^1\text{H}$  NMR shifts for 3,5-diacetyl-2,6-heptanedione

O'Loane <sup>2.5</sup> in $\text{CDCl}_3$	Experimental ppm	Assignment
2.238(s)	2.161(s)	Keto $-\text{CH}_3$
2.275(t)	2.265(t)	$-\text{CH}_2-$
3.700(t)	3.660(t)	$\begin{array}{c}   \\ -\text{CH} \\   \end{array}$
not reported	16.891	Chelated OH

## 2.2. Experimental

### 2.2.1. Materials and Equipment

All compounds, reagents and solvents were spectrophotometric or reagent grade and were used as received unless otherwise specified.  $^1\text{H}$  NMR spectra were recorded on a Bruker 250-MHz spectrometer. UV-Visible spectra were recorded on an AVIV model 14DS UV-VIS-IR spectrophotometer. IR spectra were recorded on a Bruker Tensor-27 infrared spectrophotometer and microanalyses were performed by M-H-W Laboratories, of Phoenix, Arizona.

The molecular modeling was performed using SPARTAN (Figure 2.9) and Hyperchem version 7, and the illustrations in Figures 2.6, 2.7 and 2.8 were prepared using CCDC Mercury software.

### 2.2.2. Preparation of 3,5-diacetyl-2,6-heptanedione ( $\text{C}_7\text{BAH}_2$ ) and 2-methyl-3,5,5-triacetyltetrahydropyran-2-ol.

A mixture of 40 g (0.40 mol) 2,4-pentanedione, 15 mL. of formalin (ca. 37%) (0.20 mol) was stirred at room temperature for 5 days. At the end of the 5 day period the solvent was removed under vacuum. The residue (about 12 mL)

was diluted with an equal volume of ethyl ether and introduced to a dry ice-acetone bath which promoted crystallization of the desired product. After several

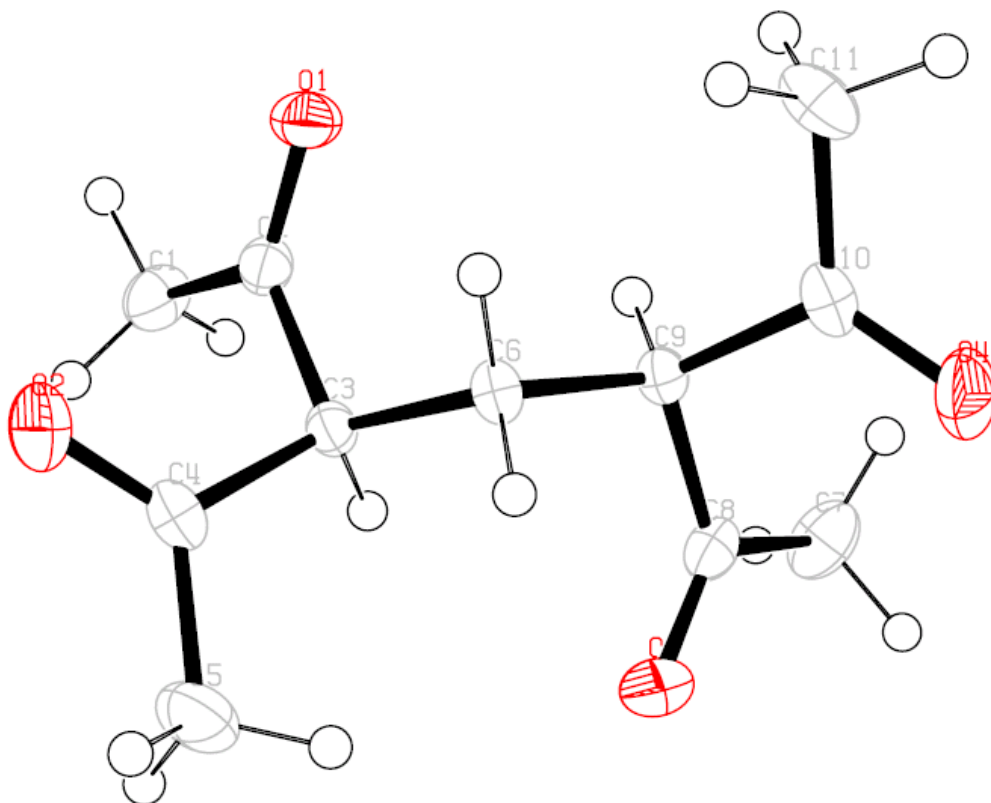


Figure 2.2. ORTEP diagram of 3,5-diacetyl-2,6-heptanedione, ( $C_1BAH_2$ ).

repeated crystallizations in a dry ice-acetone bath, several crops of  $C_1BAH_2$  colorless crystals were obtained which eventually gave a m.p. 40.5-41° C. The final product (9.03 g, 0.0425 mole) was fully characterized by its  $^1H$ -NMR and IR-spectra, and X-ray crystal structure (Figure 2.2).

When the above condensation is conducted in the presence of diethylamine as catalyst, a crystalline product was observed which was later determined by X-ray diffraction to be 2-methyl-3,5,5-triacetyltetrahydropyran-2-ol

(Figure 2.3), the 2:2 product that Aarna, et al.<sup>2.7</sup> and McMurry, et al.<sup>2.13</sup> had reported when they had conducted the reaction using a basic catalyst. Comparative crystal data for 3,5-diacetyl-2,6-heptanedione and 2-methyl-3,5,5-triacetyltetrahydropyran-2-ol are listed in Table 2.3.

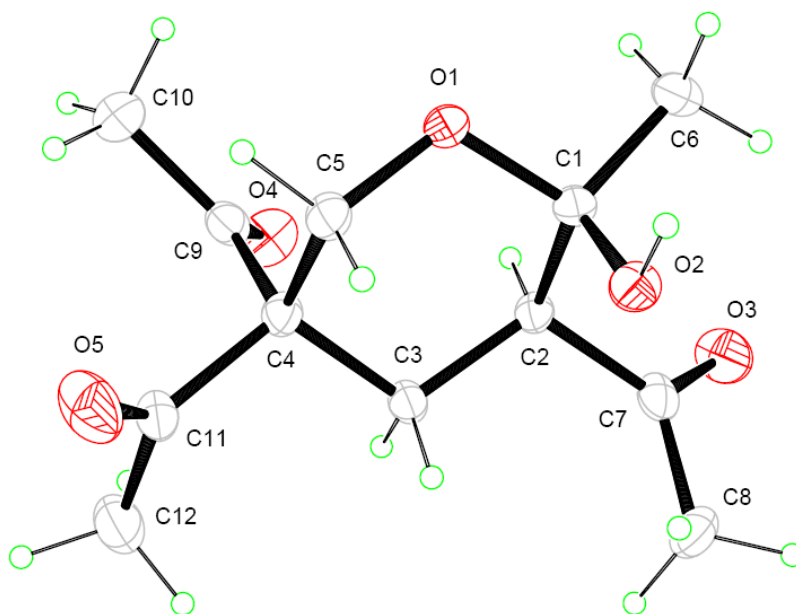


Figure 2.3. ORTEP diagram of 2-methyl-3,5,5-triacetyltetrahydropyran-2-ol.

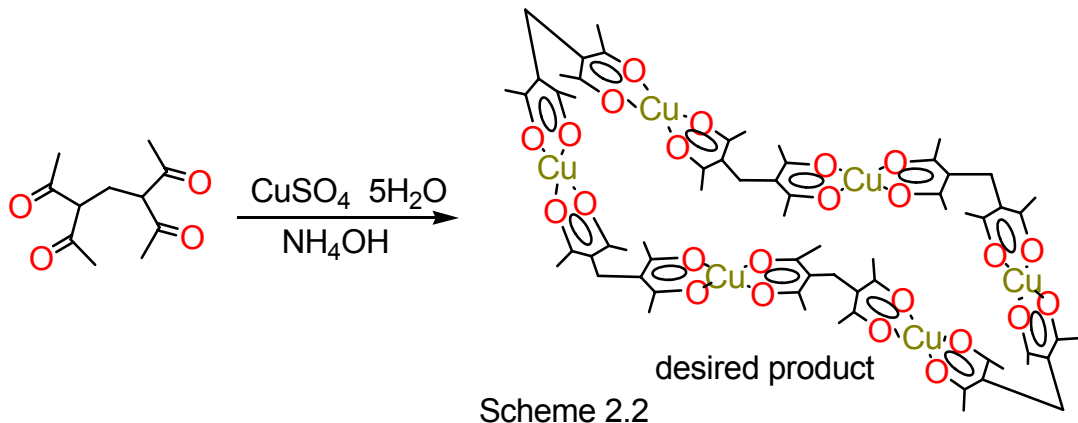
### 2.2.3 Attempted Preparation of $C_1BAH_2$ Molecular Solid

The molecular solid synthesis was initially conducted using  $Cu^{2+}$  as the metal cation. Based upon literature findings, two methods were examined in these preparative attempts with our 3,5-diacetyl-2,6-heptanedione, ( $C_1BAH_2$ ) ligand. Initially, the molecular solid synthesis was attempted by adding a

Table 2.3. Crystal data for 3,5-diacetyl-2,6-heptanedione and 2-methyl-3,5,5-triacetyltetrahydropyran-2-ol.

empirical formula	C <sub>11</sub> H <sub>16</sub> O <sub>4</sub>	C <sub>12</sub> H <sub>18</sub> O <sub>5</sub>
fw	212.24	242.26
T (K)	100	120
cryst syst	orthorhombic	monoclinic
space group	P 21 21 21	P n
a (Å)	7.810(2)	7.5981(4)
b (Å)	8.611(2)	8.8133(5)
c (Å)	17.431(4)	9.1692(4)
α (deg)	90	90
β(deg)	90	91.260(4)
γ(deg)	90	90
V (Å <sup>3</sup> )	1172.27	613.861
Z	4	2
d (calc'd) (Mg/m <sup>3</sup> )	1.203	1.311
R <sub>1</sub> (%)	4.1	4.6

chloroform solution of C<sub>1</sub>BAH<sub>2</sub> to an aqueous solution consisting of a mixture of CuSO<sub>4</sub>•5H<sub>2</sub>O and NH<sub>4</sub>OH (as proposed in Scheme 2.2). Specifically, a 1.299g (5.20 mmole) portion of CuSO<sub>4</sub>•5H<sub>2</sub>O was taken up in 10 mL of distilled water and 3 mL of NH<sub>4</sub>OH was added to the solution. The resulting blue solution was transferred to a 125 mL separatory funnel in one portion. Afterwards, a 0.121g (0.57 mmol) portion of C<sub>1</sub>BAH<sub>2</sub> was taken up in 5 mL of chloroform and introduced to the 25 mL separatory funnel. After setting for 2½ days an olive green organic layer was evident. The green organic layer was extracted over MgSO<sub>4</sub> and saved. Secondly, the molecular solid synthesis was attempted by dissolving a 0.198 g portion of CuCl<sub>2</sub>•2H<sub>2</sub>O in 2.5 mL of distilled water in a 25 mL Erlenmeyer flask. I then added dropwise over a 20 minute period, a methanol

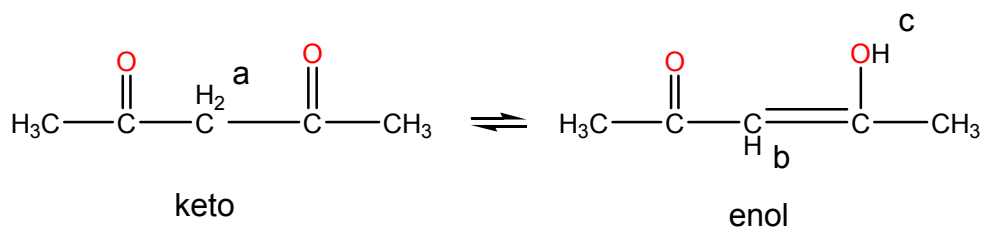


solution (0.467 g  $C_1BAH_2$  in 1.0 mL) of  $C_1baH_2$ , which resulted in a light green solution. I then added an aqueous  $NaC_2H_3O_2$  (0.348 g  $NaC_2H_3O_2$  in 1.5 mL) component in one portion and the solution turned olive green and afforded a grayish-white precipitate. After suction filtration to collect the precipitate, I allowed the suction to continue until all the MeOH solvent had evaporated from the side armed flask leaving behind a grey and a green precipitate. The gray precipitate was insoluble in water, therefore I concluded that the grey precipitate was organic. I then treated the side arm flask with 2mL of  $CHCl_3$  and separated a dark green organic layer from an apparent blue-green aqueous layer and stored it. The previously separated grey solid was taken up in 13 mL  $CHCl_3$  and combined with the 2 mL  $CHCl_3$  portion. The resulting mixture was dried over  $Na_2CO_3$  and  $Na_2SO_4$  and a 15 mL olive green portion was collected.

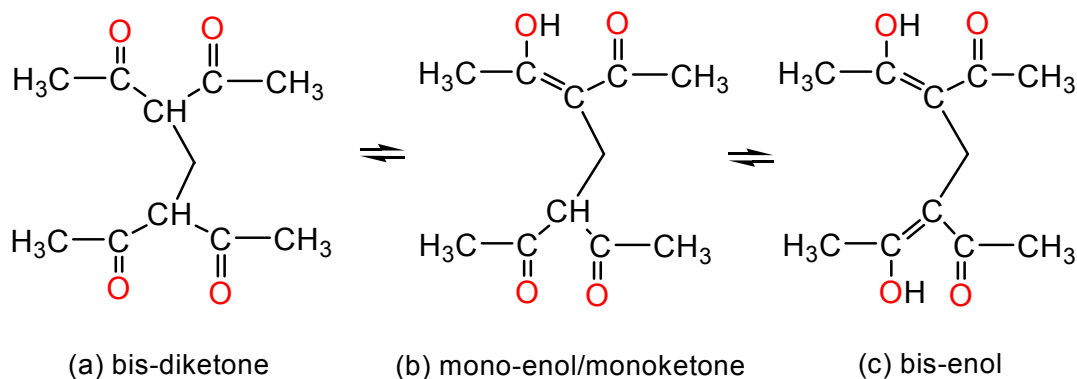
### 2.3. Results and Discussion

$^1H$  NMR analysis can be used to determine the ratio of the number of different kinds of protons in a single compound. It has also been used to

determine the the ratio of magnetically nonequivalent protons in the two different forms (keto and enol) of acetylacetone (Scheme 2.3). Because the keto



Scheme 2.3.



Scheme 2.4.

hydrogens (a) and the enol hydrogens (b and c) are magnetically nonequivalent protons, they should have different chemical shifts. According to theory there are three (3) possible isomers for 3,5-diacetyl-2,6-heptane dione (Scheme 2.4), C<sub>1</sub>BAH<sub>2</sub> (the bis-diketone, the mono-enol/mono-ketone, and the bis-enol).

Because of the 110° angle imposed on the β-diketonate groups of the C<sub>1</sub>BAH<sub>2</sub> ligand by the methylene bridge between them we believed that a six-membered hexanuclear complex similar to that shown in Scheme 2.2 and Figure 2.4 might be formed.

Because I could not produce sufficient x-ray quality crystals of the proposed  $\text{Cu}_6(\text{C}_1\text{BA})_6$  hexamer, I attempted to acquire mass spectrometer (MS) data. After numerous attempts to acquire suitable MS data failed, a sample of the olive green dendramer looking material that had resulted from each attempt to crystallize the compound was sent out for elemental analysis by M-H-W Laboratories, Phoenix, AZ.

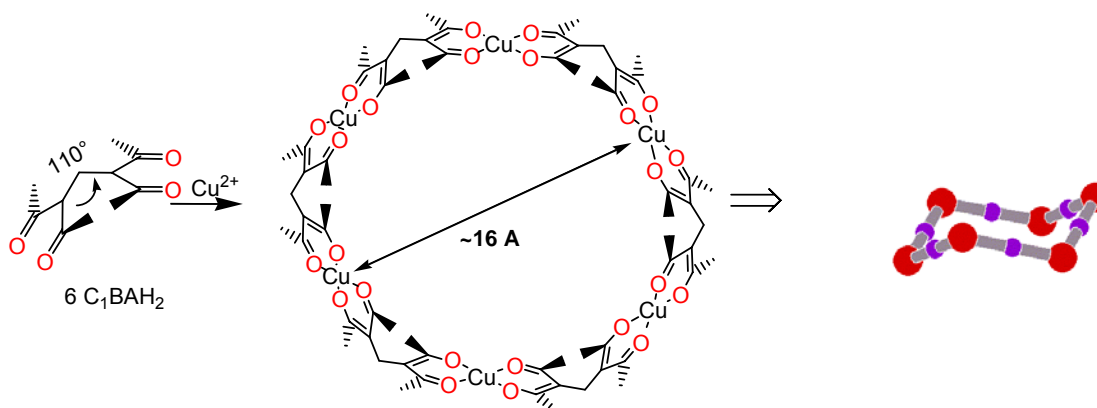


Figure 2.4. Reaction scheme and picture of proposed  $\text{Cu}_6(\text{C}_1\text{BA})_6$  hexamer

The elemental analysis did not substantiate the calculated molecular mass for the proposed hexameric structure  $\text{Cu}_6(\text{C}_1\text{BA})_6$ . However, the elemental analysis does support  $\text{Cu}(\text{C}_1\text{BA})_2$ , see Table 2.4 and Figure 2.5.

After exploring the literature and discovering the extent of work that has already been conducted with acetylacetone (our basic coordination moiety), and its coordinating behavior with numerous transition metal ions including  $\text{Co}^{2+}$ ,  $\text{Ni}^{2+}$ ,  $\text{Cu}^{2+}$ , and  $\text{Zn}^{2+}$ , I decided to examine the coordinating ability  $\text{C}_1\text{BAH}_2$  with  $\text{Co}^{2+}$ ,  $\text{Ni}^{2+}$  and  $\text{Zn}^{2+}$  metal ions as well, in order to ascertain whether either of

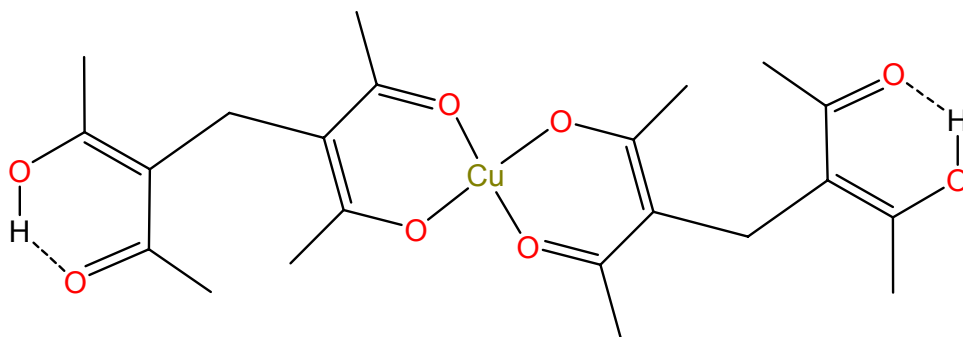


Figure 2.5. Di-enol form of  $\text{Cu}(\text{C}_1\text{BA})_2$

Table 2.4. Elemental analysis data of  $\text{Cu}(\text{C}_1\text{BA})_2$ .

Comparison of theoretical and determined elemental analysis based on $\text{Cu}_6(\text{C}_1\text{BA})_6$			
Element	Theoretical % Based on $\text{Cu}_6(\text{C}_1\text{BA})_6$	Theoretical % Based on $\text{CuO}_4\text{C}_{22}\text{H}_{30}\text{O}_4$	Determined %
Carbon	47.9	54.37	a. 54.68 b. 54.46
Hydrogen	5.86	6.22	a. 6.37 b. 6.34

these would respectively yield one of the proposed molecular solids. As with the  $\text{Cu}^{2+}$  preparation attempts, the  $\text{Co}^{2+}$ ,  $\text{Ni}^{2+}$  and  $\text{Zn}^{2+}$  preparations were also attempted by both of the mentioned synthetic methods. The only products that were generated were viscous oils, which could not be characterized.

Based on the oil formations mentioned above and Oh's<sup>2.14</sup> proposed polymer structures, I am led to believe that the metal and ligand do not coordinate in a cyclic fashion as we had envisioned for our molecular solids, but generally react to form polymers.



Because of steric interference between methyl groups, the most stable conformation of the  $C_1BA^{2-}$  ligand is twisted, as shown in Figure 2.6. This twist makes the conformation chiral, and the two possible senses of the twist can be represented as  $\Delta$  and  $\Lambda$ . The  $\Delta$  enantiomer is shown in the figure.

Assembly of a macrocyclic polynuclear complex from  $C_1BA^{2-}$  requires specific conformations of the ligand. For example, the most stable ring structure

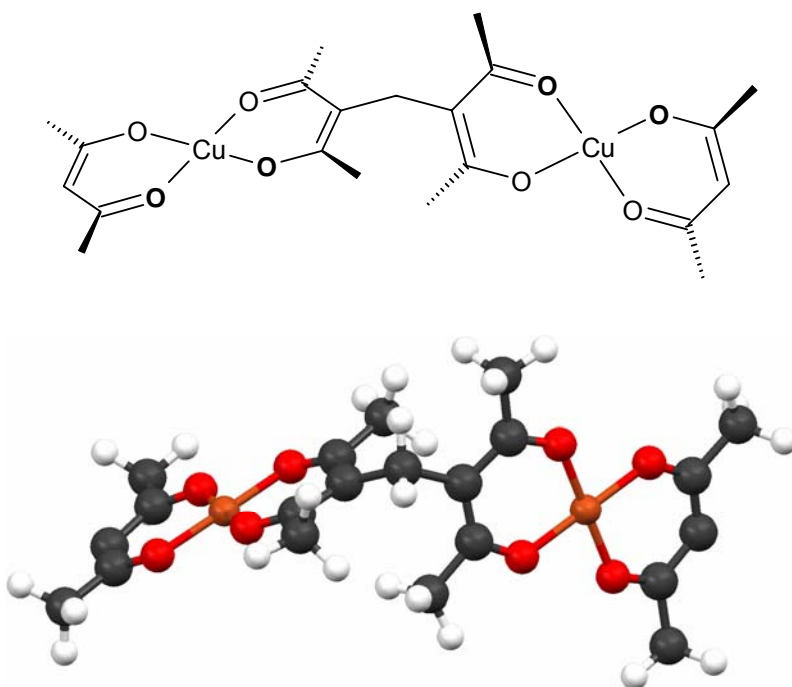


Figure 2.6. Chemical structure drawing and molecular model of dinuclear Cu unit containing one bridging  $C_1BA^{2-}$  ligand ( $\Delta$  enantiomer shown).

for  $Cu_6(C_1BA)_6$ , shown in Figure 2.7, contains alternating  $\Delta$  and  $\Lambda$  ligands. A ring structure is much more difficult to assemble using other combinations of ligand conformations; instead, a polymer is more likely to be formed (see example in Figure 2.8). Therefore, if only a few combinations of ligand conformations are

permissible in a ring structure, with most other possible combinations leading to polymers, it is not surprising that our Cu-C<sub>1</sub>BA product behaves more like a polymeric material.

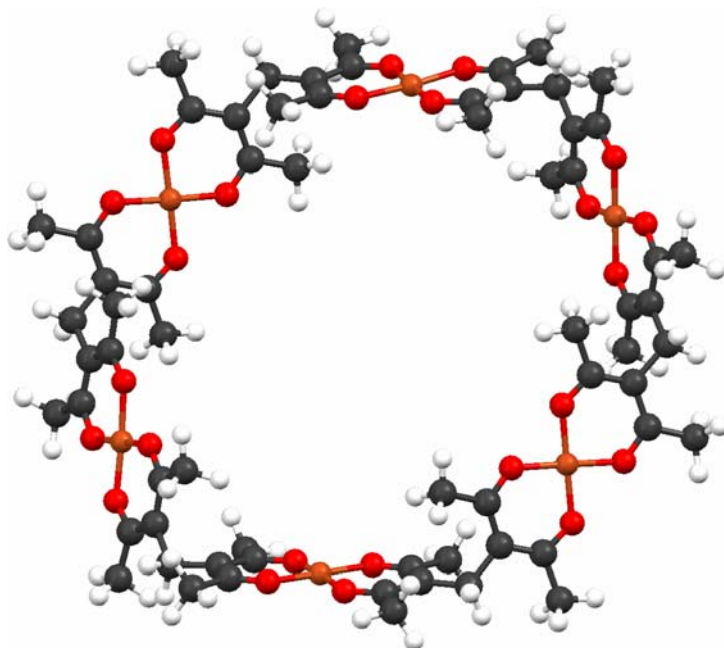


Figure 2.7. Ring-shaped hexanuclear Cu complex containing alternating  $\Delta$ - and  $\Lambda$ - C<sub>1</sub>BA<sup>2-</sup> bridging ligands.

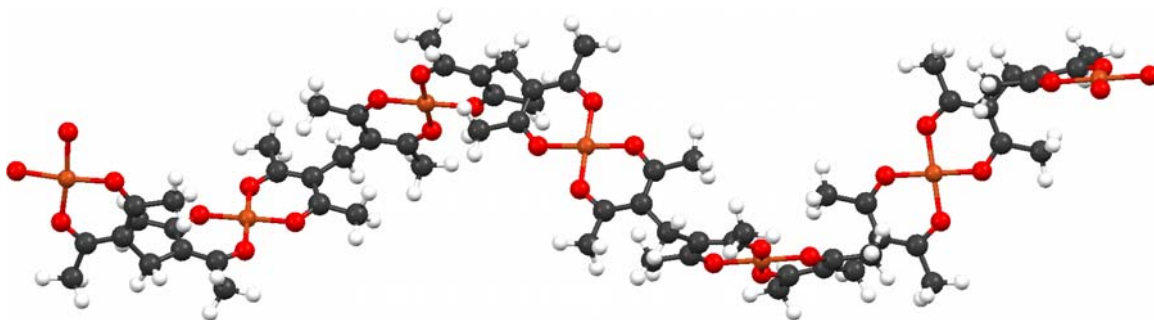


Figure 2.8. Helical hexanuclear Cu polymer containing all  $\Delta$ -C<sub>1</sub>BA<sup>2-</sup> bridging ligands.

Even though only a few conformations of a  $\text{Cu}_n(\text{C}_1\text{BA})_n$  chain can lead to ring formation, rings could still form in good yield if the enantiomers of individual  $\text{C}_1\text{BA}$  units can interconvert readily. To determine whether this is possible, we

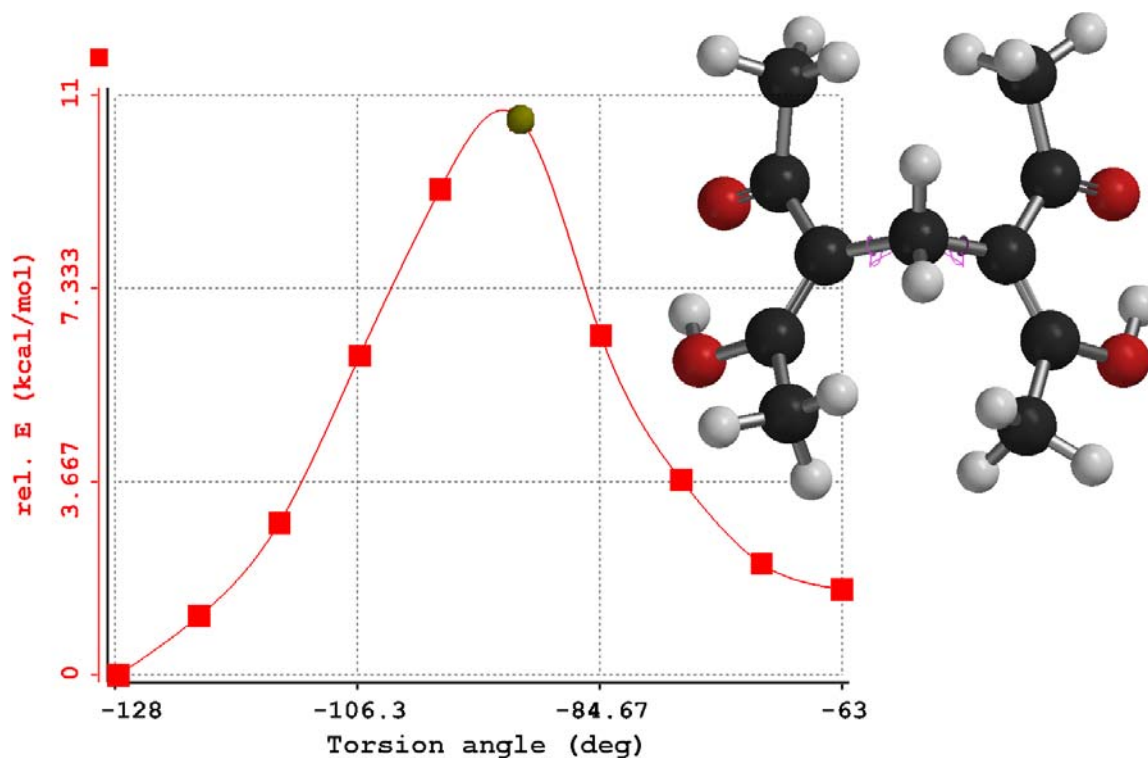


Figure 2.9: SPARTAN plot of conformational energy of the bis(enol) form of  $\text{C}_1\text{BAH}_2$  vs. central C-C-C-C torsion angle. Also shown is a ball-and-stick illustration of the molecule when this torsion angle is close to 90 deg, i.e. approximately in the highest-energy conformation required for interconversion of the two enantiomeric forms of the ligand.

modeled the enolic form of  $\text{C}_1\text{BAH}_2$  in SPARTAN<sup>2.15</sup> and determined that the interconversion energy barrier between its enantiomeric forms is relatively low, ~10.5 kcal/mol (Figure 2.9).

Thus, interconversion of the C<sub>1</sub>BA enantiomers may be relatively rapid. However, under our conditions, the interconversion may still not be fast enough to prevent formation of polymeric products.

## Chapter 3

### ***p*-Xylylenebis(acetylacetone) (*p*-XBAH<sub>2</sub>) and Its Metal Complexes**

#### **3.1. Introduction**

In our group's investigation of the chemistry of cofacial binuclear transition-metal complexes derived from bis( $\beta$ -diketone) ligands, we have searched for new types of bis( $\beta$ -diketones) to serve as linkers for our proposed molecular solids as well. Traditionally, alkylated  $\beta$ -diketones were prepared in a steel or glass bomb by the interaction of the sodium salt of a  $\beta$ -diketone and an alkyl halide.<sup>3.1-3.4</sup> A second procedure consisted of refluxing a mixture of the sodium salt of a  $\beta$ -diketone with excess alkyl halide in either a high boiling solvent such as nitrobenzene<sup>3.5</sup> or with no solvent at all.<sup>3.6-3.7</sup> In addition we've searched for ways to develop novel methods for the preparation of such bis( $\beta$ -diketones) as the previously known *p*-xylylenebis(acetylacetone) (*p*-XBAH<sub>2</sub>) which we synthesized by the method devised by Martin, et al.,<sup>3.8</sup> which consisted of interacting acetylacetone and a dihalide in a *t*-butanolic solution of potassium *t*-butoxide. In a prior work by our group, we attempted to prepare the Cu<sub>2</sub>(*p*-XBA)<sub>2</sub> dimer.<sup>3.9</sup> However all attempts to isolate the dimer and characterize it have proved to be unsuccessful.

#### **3.2. Experimental**

##### **3.2.1 Materials and Equipment**

Chemicals and solvents were reagent or spectrophotometric grade and

were used as received.  $^1\text{H}$  NMR spectra were recorded on a Bruker 250-MHz spectrometer. UV-Visible spectra were run on an AVIV model 14DS UV-VIS-IR spectrophotometer. IR spectra were run on a Bruker Tensor-27 infrared spectrophotometer.

### 3.2.2. Preparation of *p*-Xylylenebis(acetylacetone) (*p*-XBAH<sub>2</sub>)

The ligand *p*-xylylenebis(acetylacetone) (*p*-XBAH<sub>2</sub>), shown in Figure 3.1, was previously prepared in our laboratory by Yeager<sup>3,9</sup>, according to the method

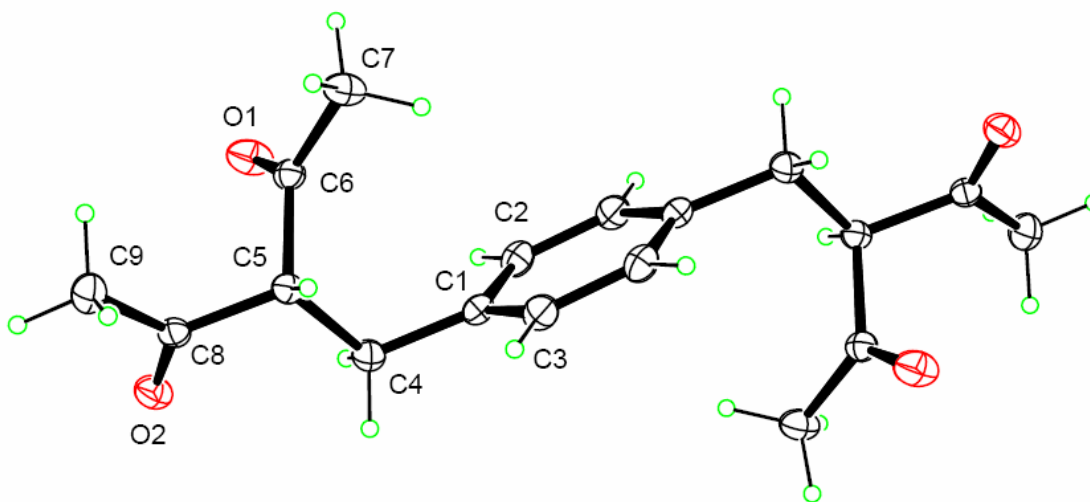
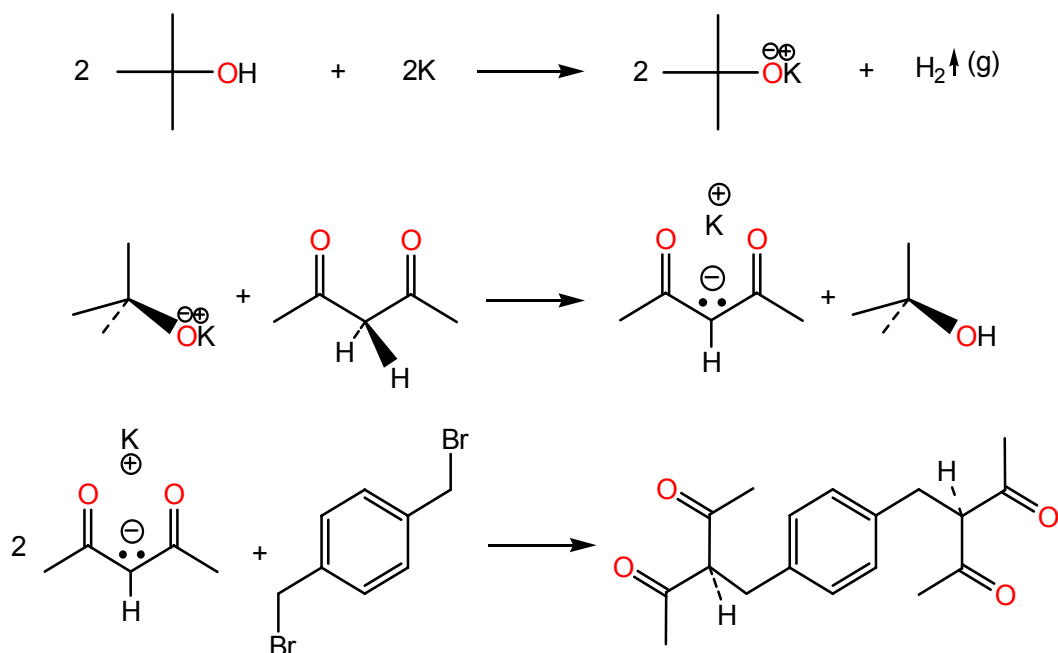


Figure 3.1. ORTEP diagram of *p*-XBAH<sub>2</sub>

to the method prescribed by Martin and Ferneli<sup>3,10</sup> (1959), who used it in their study as a component in the formation of organic and coordination polymers. We envisioned that this compound would act as a conformationally fixed, bridging ligand in the preparation of transition-metal coordinated molecular solid complexes. The established synthesis is shown in Scheme 3.1. The  $^1\text{H}$  NMR was consistent with previously reported spectrum. This compound was further



Scheme 3.1. Established synthetic scheme for *p*-XBAH<sub>2</sub>.

characterized by its melting point (109-110°C), IR (Figure 3.2) and x-ray structure (Figure 3.1). The x-ray crystal data for *p*-XBAH<sub>2</sub> is summarized in Table 3.1.

### 3.2.3. Attempted Preparation of Cu<sub>3</sub>(*p*-XBA)<sub>3</sub> Molecular Solids

A 5.013 g (20.1 mmole) portion of CuSO<sub>4</sub> • 5H<sub>2</sub>O was taken up in 25 mL of distilled water and introduced to a 500 mL separatory funnel. A 35 mL portion of conc. NH<sub>4</sub>OH was added to the funnel and the mixture was shaken until a white precipitate formed and dissolved. A 0.6065 g (2.01 mmole) portion of *p*-XBAH<sub>2</sub> was taken up in 150 mL of methylene chloride (CH<sub>2</sub>Cl<sub>2</sub>) and added to the mixture in the separatory funnel. After repeated agitation, the CH<sub>2</sub>Cl<sub>2</sub> layer was extracted. The aqueous layer was washed with 50 mL of CH<sub>2</sub>Cl<sub>2</sub> and the combined CH<sub>2</sub>Cl<sub>2</sub> layers were reduced in volume at low pressure on the roto-

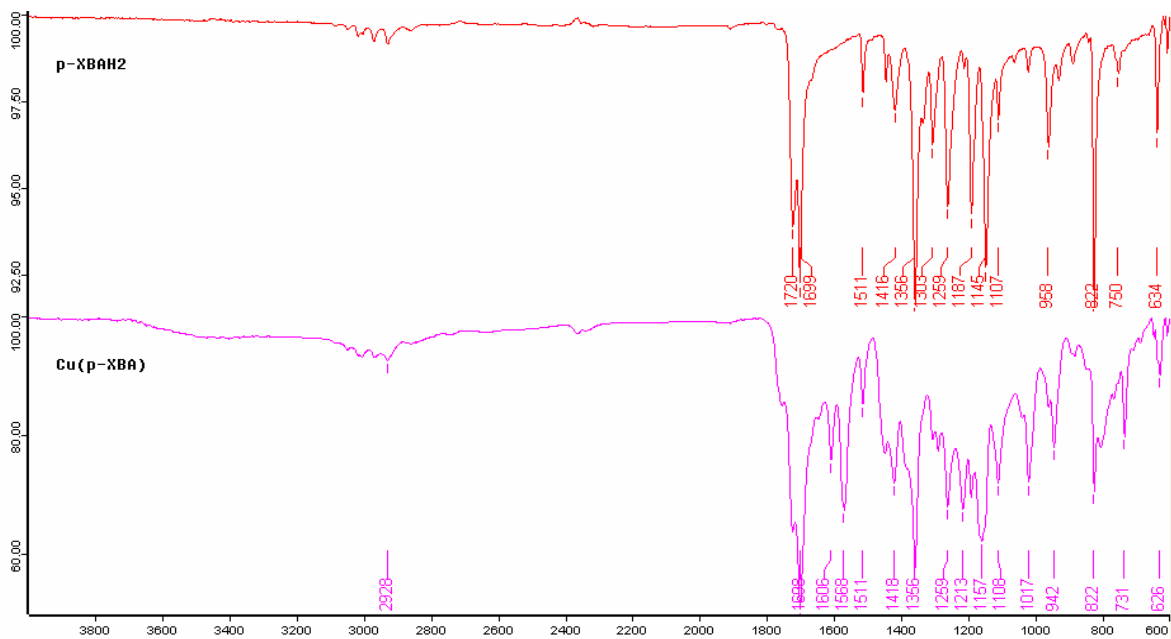


Figure 3.2. IR spectrum of  $p$ -XBAH<sub>2</sub> and Cu<sub>n</sub>( $p$ -XBA)<sub>n</sub>.

Table 3.1. Crystal data for  $p$ -XBAH<sub>2</sub>.

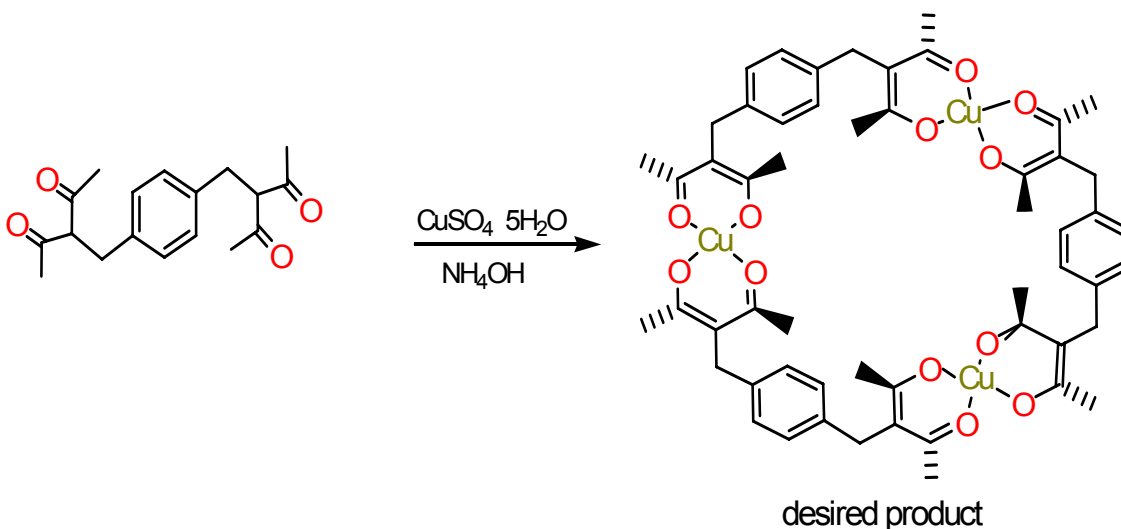
empirical formula	C18H22O4
fw	302.36
T (K)	100
cryst syst	monoclinic
space group	P21/c
a (Å)	13.796(6)
b (Å)	5.591(2)
c (Å)	10.819(4)
$\alpha$ (deg)	90
$\beta$ (deg)	107.890(15)
$\gamma$ (deg)	90
V (Å <sup>3</sup> )	794.2(5)
Z	2
d (calc'd) (Mg/m <sup>3</sup> )	1.264
R <sub>1</sub> (%)	4.5



evaporator to ~ 2 mL of a light blue-green organic solution. This solution was treated with anhydrous  $\text{Na}_2\text{SO}_2$ , filtered and allowed to air evaporate under the fume hood overnight. This yielded 0.467 g (0.421 mmole) ~63% yield of green precipitate. All attempts to grow X-ray quality crystals failed. The proposed synthetic pathway for preparing  $\text{Cu}_3(p\text{-XBA})_3$  is shown in Scheme 3.2.

### 3.2.4. Structural Analysis of $p\text{-XBAH}_2$

The  $p\text{-XBAH}_2$  crystallized with two distinct molecules ( $Z = 2$ ) in the unit cell. The structure was solved in the monoclinic system, in space group  $P2_1/c$ . Individual  $p\text{-XBAH}_2$  molecules in the crystal are centrosymmetric and are oriented in a trans-type configuration. If these molecules cannot easily rotate



Scheme 3.2. Proposed synthetic pathway for  $\text{Cu}_3(p\text{-XBA})_3$ .

and “trans”-type configuration is preferred, that may favor formation of polymers rather than rings. A view of  $p\text{-XBAH}_2$  along the  $c$  axis is shown in Figure 3.3.

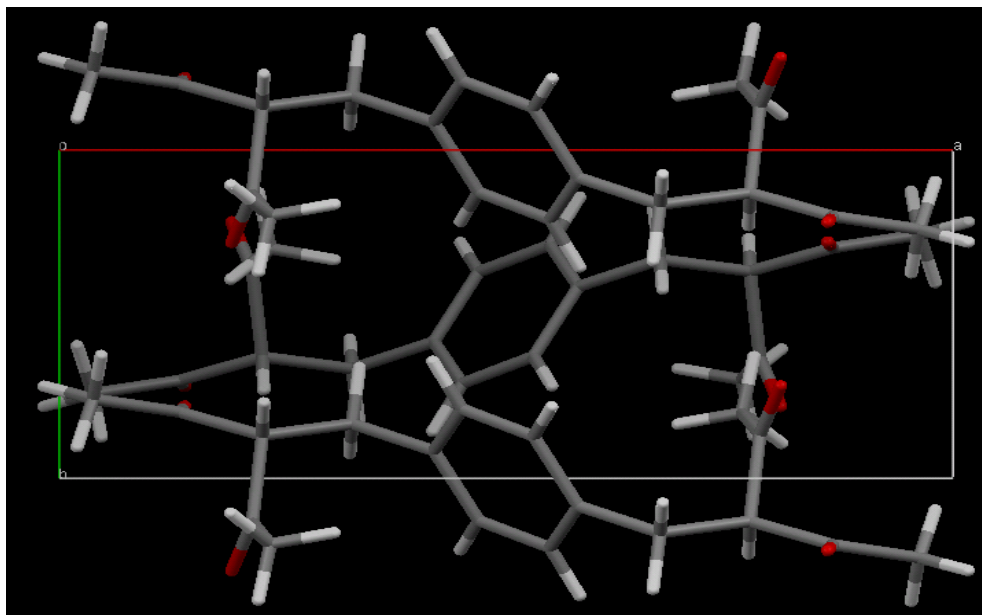


Figure 3.3. View of  $p\text{-XBAH}_2$  along the  $c$  axis.

### 3.3. Results and Discussion

It has been documented<sup>3,8</sup> that in the solid state some bis-( $\beta$ -diketones) of the type  $[(\text{RCO})(\text{R}'\text{CO})\text{-CH}_2\text{CHR}]$  exist to an appreciable extent in the keto form. This has been evidenced by the high intensity carbonyl absorption in the 1733-1709  $\text{cm}^{-1}$  region and the relatively low intensity enol-chelate absorption near 1550 - 1600  $\text{cm}^{-1}$ . Also, most of these bis-( $\beta$ -diketones) have hydroxyl stretching bands near 3389.8  $\text{cm}^{-1}$ . There has also been evidenced in some cases a shifting of the hydroxyl bands to where they become obscured by the C-H stretching vibration bands in the 2900 – 3000  $\text{cm}^{-1}$ . This is believed to be due to enolate formation.

The IR spectra for the  $p\text{-XBAH}_2$  ligand show two to three bands in the region 1500 -1600  $\text{cm}^{-1}$ , which are characteristic of the mixed modes of vibrations

arising due to the normal coordinates having contribution from  $\nu(\text{C}=\text{O})$  and  $\nu(\text{C}=\text{C})$  of the  $\beta$ -diketone groups.<sup>3,11</sup> The coordination of the carbonyl groups to the Cu center is evidenced by the absence of these bands between 1550 – 1600  $\text{cm}^{-1}$  in the  $\text{Cu}_2(p\text{-XBA})$  complex. Shown in Figure 3.4 are the proposed coordination polymer structures for  $\text{Cu}(p\text{-XBA})$ . I believe that the product we obtained in our experiment is at the least a mixture of structures II and III in an appreciable amount, (Fig. 3.4). This assumption is based on the presence of the low intensity broad stretching band observed between 3300  $\text{cm}^{-1}$  and 3500  $\text{cm}^{-1}$  in the IR spectrum depicted in Figure 3.2.

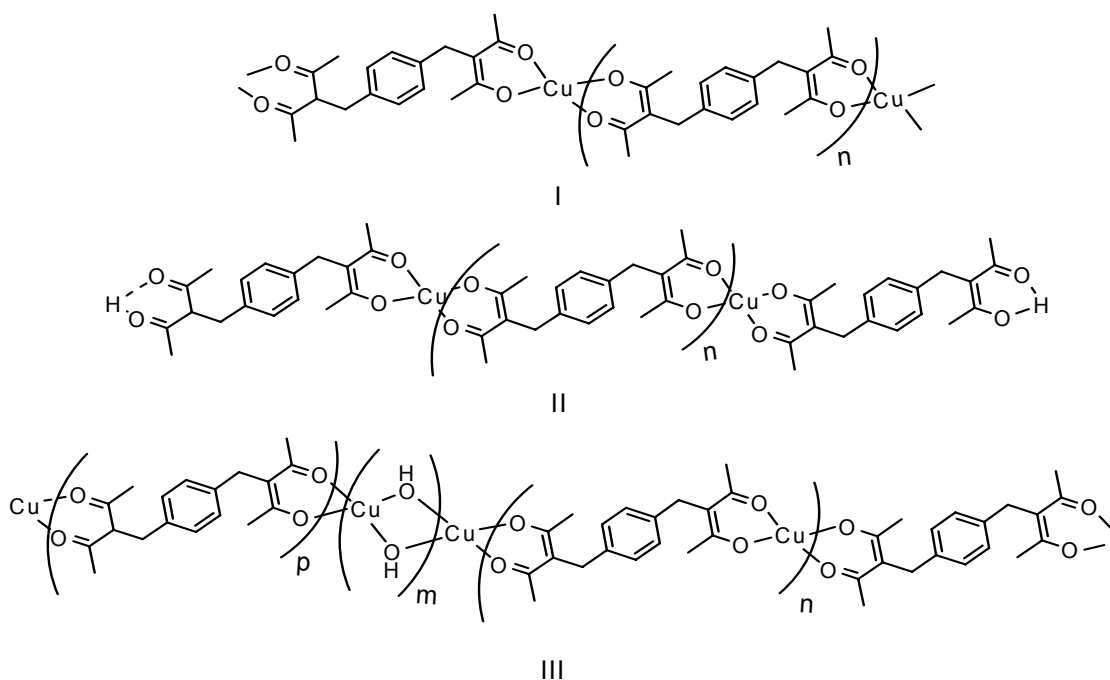


Figure 3.4. Proposed coordination polymer structures for  $\text{Cu}(p\text{-XBA})$ .

## Chapter 4

### $\text{Cu}_2(\text{NBA})_2 \cdot [\text{Substrate}]$ Studies

#### 4.1. Introduction

The use of chelating ligands in the synthesis of multimetal systems has been of both practical and fundamental interest. Numerous macrocyclic polynuclear metal complexes have been prepared in which metal atoms bind guest molecules. The complexing of two metal ions by the same macrocyclic ligand has also been the subject of a great deal of current interest. The general principle governing these structures allow for the study of (i) metal-metal interactions, (ii) insertion of substrates and their possible transformations. Furthermore, these types of structures are often found in biological systems such as metalloproteins, which often use binuclear metal centers to perform catalytic functions.<sup>4.1</sup> Our group has been exploring the use of cofacial binuclear bis( $\beta$ -diketone) complexes, such as  $\text{Cu}_2(\text{XBA})_2$  and  $\text{Cu}_2(\text{NBA})_2$ , for their ability to bind substrate molecules.<sup>4.2</sup> The copper atoms bound in this manner in proteins are commonly referred to as type-3 coppers.<sup>4.1</sup>

Our group's prior work has focused on the development of binuclear metal complexes derived from polydentate ligands, and their previous studies have shown that our larger complex  $\text{Cu}_2(\text{NBA})_2$  binds substrate molecules in an intramolecular fashion,<sup>4.3</sup> (Figure 4.1.) similar to those produced by several other flexible binucleating macrocycles.<sup>4.4-4.6</sup> In light of our group's success with binding nitrogenous bases to  $\text{Cu}_2(\text{NBA})_2$ , I undertook the task of exploring the

chemistry associated with the binding of sulfur-containing heterocyclic bases to our  $\text{Cu}_2(\text{NBA})_2$  and determine if the binding associated with the sulfur analogues would be more or less than those observed for the nitrogen counterparts. I attempted to bind the sulfur bases 1,4-dithiane and 2,5-dihydroxy-1,4-dithiane with  $\text{Cu}_2(\text{NBA})_2$ .

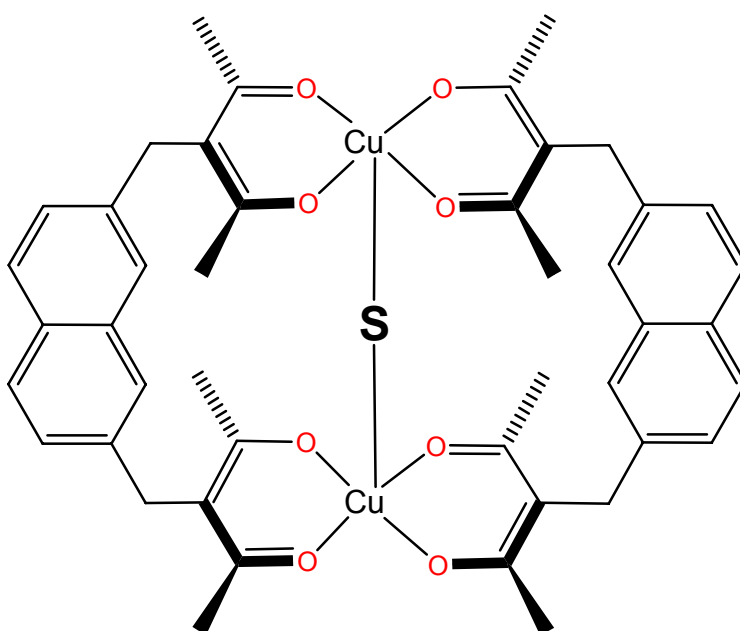


Figure 4.1. Intramolecular binding of generic substrate by  $\text{Cu}_2(\text{NBA})_2$ .

## 4.2. Experimental

### 4.2.1. Materials and procedures

Our  $\text{NBAH}_2$ , (2,7-naphthalenediylbis(methylene)bis(acetylacetonate)) ligand had previously been prepared by the general nucleophilic substitution method outlined by Martin, et. al.<sup>4.7</sup>  $\text{Cu}_2(\text{XBA})_2$  was prepared by previously published procedures,<sup>4.8-4.9</sup> and the 1,4-dithiane and 2,5-dihydroxy-1,4-dithiane were

obtained from the Aldrich Chemical Co. and used without further purification, unless stated otherwise.

#### **Preparation of $\text{Cu}_2(\text{NBA})_2 \cdot (1,4\text{-dithiane})$**

*Dilute.* A  $\text{CHCl}_3$  solution prepared from  $\text{Cu}_2(\text{NBA})_2$  (5.05 mM), which was initially olive-green in color, was combined with a 1,4-dithiane solution in  $\text{CHCl}_3$  (40.3 mM). This mixture was filtered and then layered with acetonitrile. After 24 hours the formation of olive green  $\text{Cu}_2(\text{NBA})_2$  crystals was evident and there were no signs of the formation of the 1,4-dithiane host guest adduct.

*More concentrated.* 1.016 M 1,4-dithiane in  $\text{CHCl}_3$  was prepared and combined with the initial  $\text{Cu}_2(\text{NBA})_2$  (5.05 mMolar) solution. After filtering and layering with acetonitrile, olive-green crystals of  $\text{Cu}_2(\text{NBA})_2$  were still evident after 24 hours, however, after 5 days larger olive-green crystals of  $\text{Cu}_2(\text{NBA})_2$  had formed along with tiny turquoise crystals of the  $\text{Cu}_2(\text{NBA})_2 \cdot (1,4\text{-dithiane})$  adduct (Figures 4.2 and 4.4).

#### **4.2.2. X-Ray analysis of $\text{Cu}_2(\text{NBA})_2 \cdot (1,4\text{-dithiane})$**

Diffraction data were collected at 120 K and refinement was carried out in the monoclinic space group for the unit cell ( $a = 7.7580(4)$ ,  $b = 28.9810(14)$ ,  $c = 9.6400(5)$  Å,  $\beta = 97.848(3)^\circ$ , MoK $\alpha$  source) and the structure solved in  $P2_1/c$  (Figure 4.2). In this space group, the unit cell contains two complete  $\text{Cu}_2(\text{NBA})_2 \cdot (1,4\text{-dithiane})$  units. The crystallographic data is summarized in Table 4.1.

Tabulated data in Table 4.2 gives a comparison of specific bond distances for  $\text{Cu}_2(\text{NBA})_2(\text{S})$  with  $\text{S} = 1,4\text{-dithiane}$ , dabco and 2,5-Me<sub>2</sub>pyz respectively.

These data when examined next to the Cu --- Cu distance (7.349 Å) of our empty Cu<sub>2</sub>(NBA)<sub>2</sub> host molecule indicate that as the size of the host molecule increases, the relative degree of skewing or puckering of the macrocyclic ring at the copper atoms increases, see Figure 4.5.

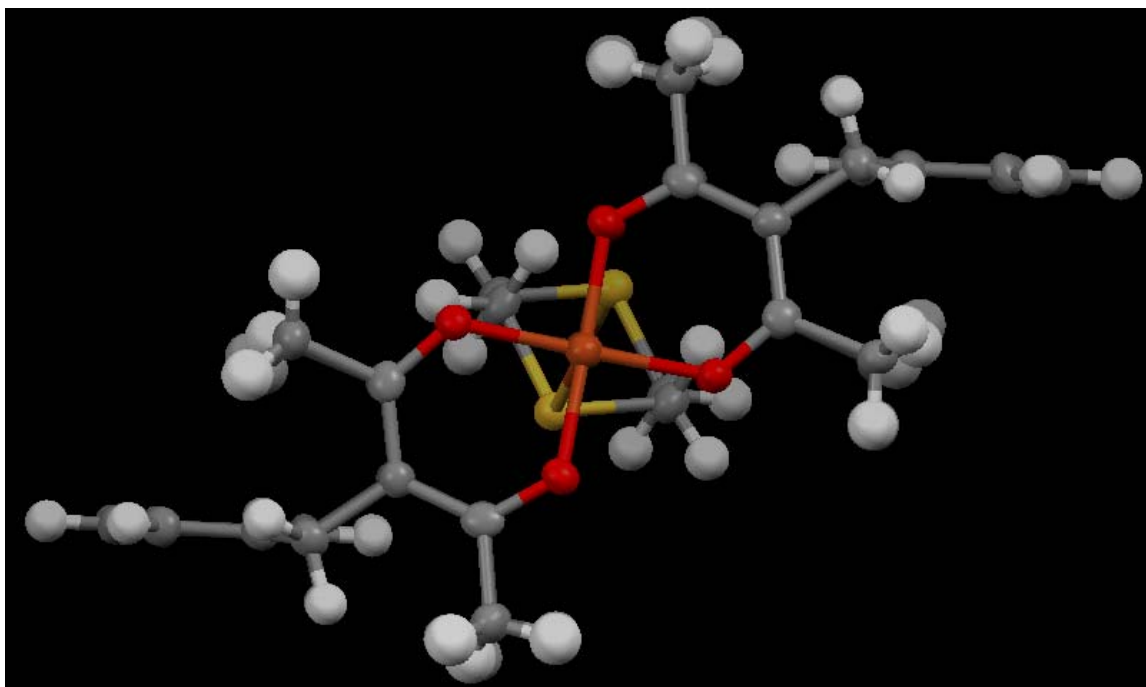


Figure 4.2. CCDC Mercury diagram of Cu<sub>2</sub>(NBA)<sub>2</sub> • (1,4-dithiane), top view.

Table 4.1. Crystal data for Cu<sub>2</sub>(NBA)<sub>2</sub> • (1,4-dithiane).

empirical formula	Cu <sub>2</sub> C <sub>48</sub> H <sub>52</sub> O <sub>8</sub> S <sub>2</sub>	$\alpha$ (deg)	90
fw	948.10	$\beta$ (deg)	97.848(3)
$T$ (K)	120	$\gamma$ (deg)	90
cryst syst	monoclinic	$V$ (Å <sup>3</sup> )	2147.10(19)
space group	$P2_1/c$	$Z$	2
$a$ (Å)	7.7580(4)	$d$ (calcd) (Mg/m <sup>3</sup> )	1.466
$b$ (Å)	28.9810(14)	$R_1$ (%)	3.8
$c$ (Å)	9.6400(5)		

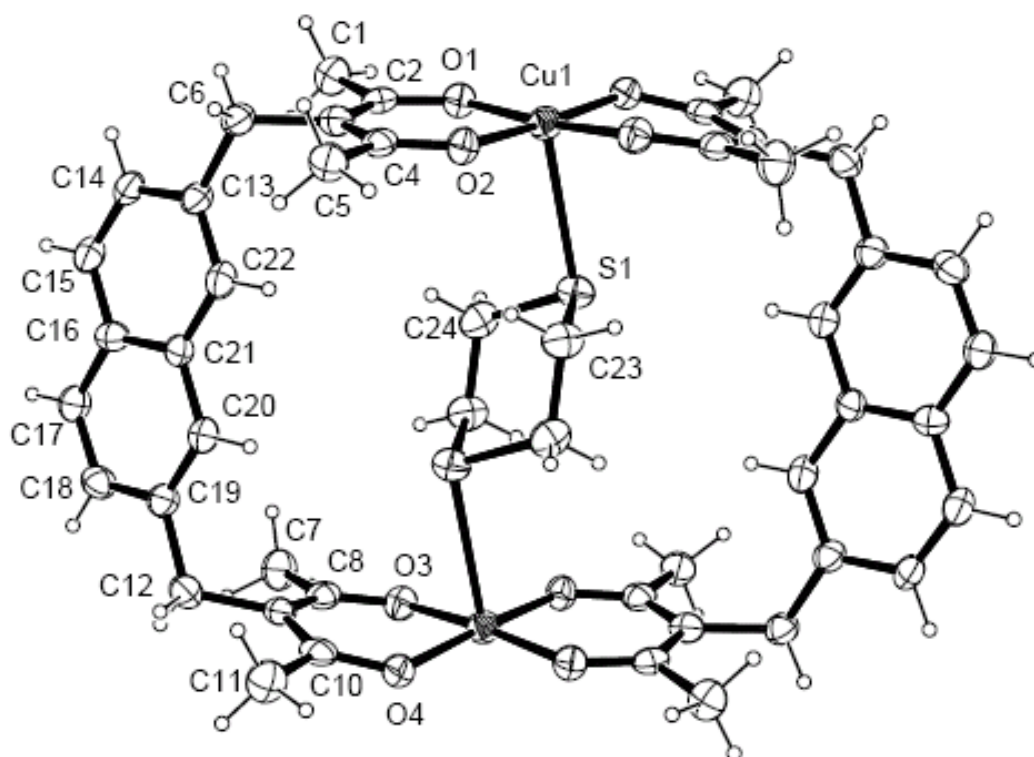


Figure 4.3. ORTEP diagram of  $\text{Cu}_2(\text{NBA})_2 \cdot (1,4\text{-dithiane})$ , side view, with ellipsoids at 50% probability level.

Figure 4.5 shows that the N atoms of the 2,5- $\text{Me}_2\text{pyz}$  and Dabco guests lie essentially in the same plane with the host Cu atoms, while the S atoms of the 1,4-dithiane guest do not. This is probably due to the molecular conformation (chair), and relatively larger size of the 1,4-dithiane substrate molecule.

Table 4.2. Selected bond distance comparisons.  
(G = 1,4-dithiane, 2,5- $\text{Me}_2\text{pyz}$  and dabco)

$\text{Cu}_2(\text{NBA})_2(\text{G})$	1,4-dithiane	2,5- $\text{Me}_2\text{pyz}$	dabco
Cu-----Cu (Å)	8.130	7.559	7.399
Cu-----S(N) (Å)	2.809	2.375	2.416
S-----S (N-----N) (Å)	3.451	2.808	2.590



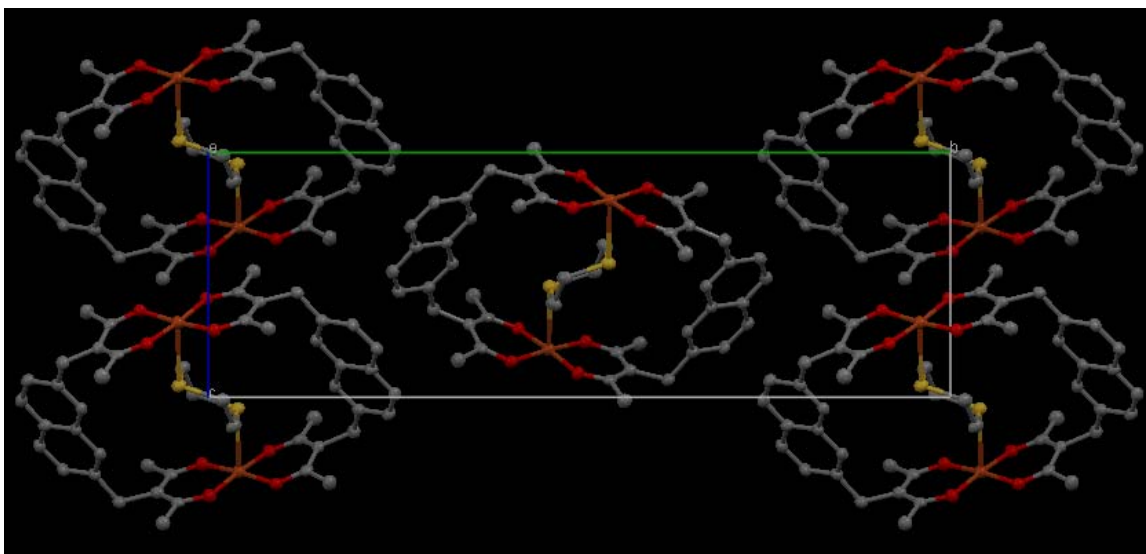


Figure 4.4. Crystal Packing diagram of  $\text{Cu}_2(\text{NBA})_2 \cdot (1,4\text{-dithiane})$ , view along a, showing the packing of adjacent molecules.

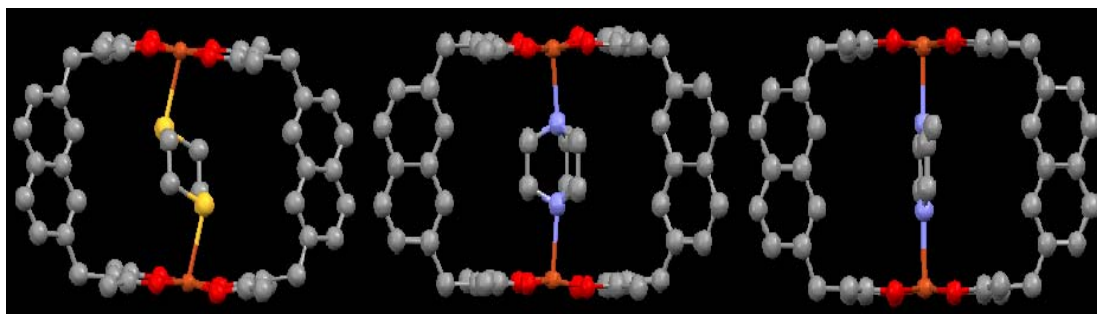


Figure 4.5. Comparative side views of  $\text{Cu}_2(\text{NBA})_2 \cdot (\text{S})$ , with  $\text{S} = 1,4\text{-dithiane}$ , dabco and 2,5-Me<sub>2</sub>pyz.

Also, Figure 4.6 shows that the naphthalene moieties are somewhat skewed and exist in parallel planes in the 1,4-dithiane and 2,5-Me<sub>2</sub>pyz adducts while the dabco adduct exhibits one naphthalene ring system horizontal, while the other is angled and is not parallel or in the same plane as the other. This twisting of the naphthalene rings could be affected by solution or crystal packing effects.

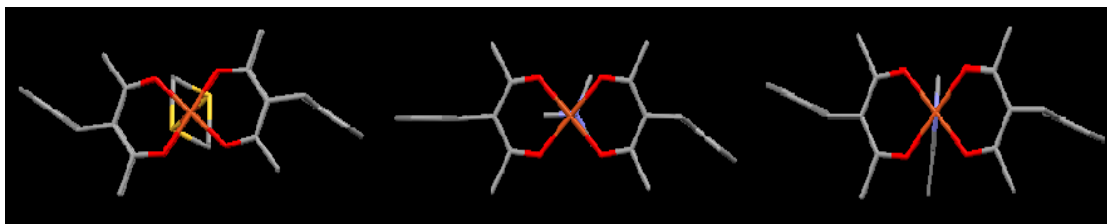


Figure 4.6. Comparative top views of  $\text{Cu}_2(\text{NBA})_2 \cdot (\text{S})$ , with  $\text{S} = 1,4\text{-dithiane}$ , dabco and  $2,5\text{-Me}_2\text{pyz}$  respectively.

We examined the  $\text{Cu}_2(\text{NBA})_2 \cdot (1,4\text{-dithiane})$  host-guest molecular complex using the Cambridge Crystallographic Data Centre's (CCDC) Mercury 1.4 software. This examination revealed that the coordinated (bis) $\beta$ -diketonate units within the complex deviate from coplanarity. The dihedral angle between the resultant planes is  $11.18^\circ$ , Figure 4.7. This relatively large deviation is probably caused by the unusually large 1,4-dithiane guest molecule.

### 4.3. Results and discussion

In this study I attempted to coordinate two dithiane guest molecules, 1,4-dithiane and 2,5-dihydroxy-1,4-dithiane with our  $\text{Cu}_2(\text{NBA})_2$  host. After preparing the  $\text{Cu}_2(\text{NBA})_2 \cdot (1,4\text{-dithiane})$  adduct, I attempted to determine its binding constant by examining its dilute methylene chloride ( $\text{CH}_2\text{Cl}_2$ ) and chloroform ( $\text{CHCl}_3$ ) solutions by UV-visible spectroscopy at room temperature.

The equilibrium constants (K) calculation was attempted by a graphical method outlined by Rose and Drago<sup>4,10</sup> in which Equation. 4.1 is solved simultaneously for varying concentrations of guest molecule. The spectral data for  $\text{Cu}_2(\text{NBA})_2 \cdot (1,4\text{-dithiane})$  proved to be inadequate for determining sufficient

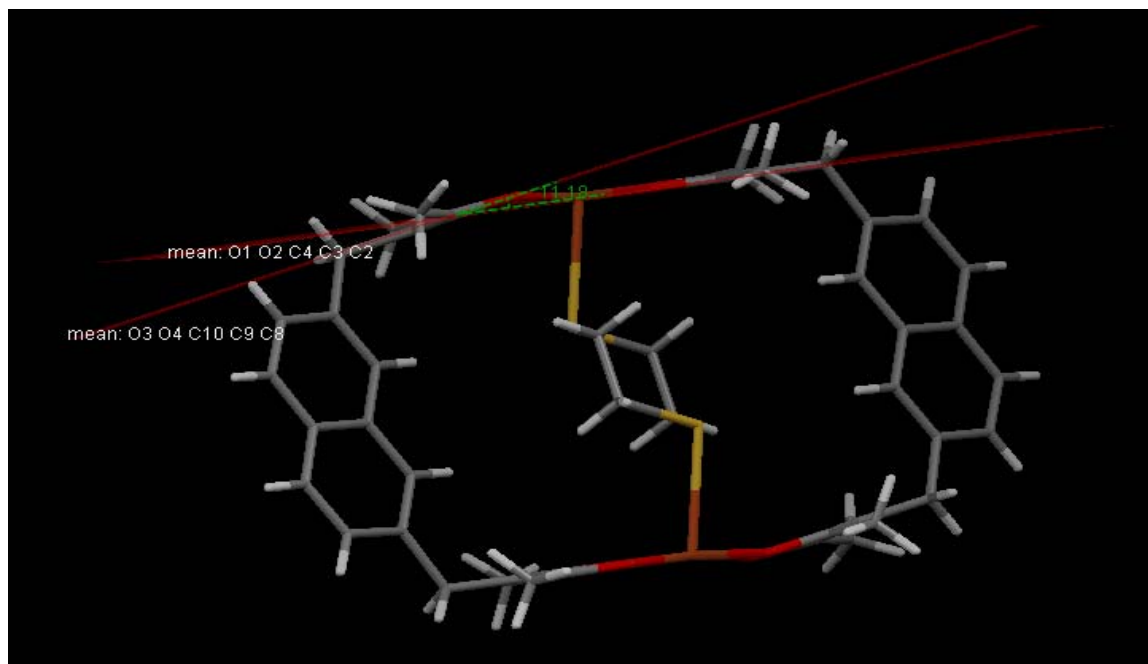


Figure 4.7. Stick figure view of  $\text{Cu}_2(\text{NBA})_2 \cdot (1,4\text{-dithiane})$  showing the deviation from co-planarity of the (bis) $\beta$ -diketonate units to be  $11.18^\circ$ .

binding constants, and we attribute this to an apparent low affinity of  $\text{Cu}_2(\text{NBA})_2$  for 1,4- dithiane. The spectral changes were too small, and this agrees with the premise that even with a large excess of 1,4-dithiane only a small fraction of the molecule contain guests, which is indicative that the equilibrium for the reaction is also very low.

$$\text{(Equation 4.1)} \quad K^{-1} = [\text{M}_0][\text{G}_0] \Delta\epsilon/\Delta A - ([\text{M}_0] + [\text{G}_0]) + \Delta A/\Delta\epsilon$$

Since the room temperature study did not allow for the successful determination of the binding constant for the  $\text{Cu}_2(\text{NBA})_2 \cdot (1,4\text{-dithiane})$  adduct, I attempted to introduce 2,5-dihydroxy-1,4-dithiane into our  $\text{Cu}_2(\text{NBA})_2$  ligand,

hoping that the presence of the hydroxyl groups would enhance binding to the host. However, all efforts to achieve this failed due to the insolubility of the 2,5-dihydroxy1,4-dithiane guest in either  $\text{CH}_2\text{Cl}_2$  or  $\text{CHCl}_3$ .

## Chapter 5

### $\text{Cu}_2(\text{XBDPr})_2$ and $\text{Cu}_2(\text{NBDPr})_2$ Studies

#### 5.1. Introduction

$\beta$ -diketone derivatives of acetylacetone have been used commonly as extractants in the solvate extraction of metals.<sup>5.7, 5.8</sup> Formerly, Koshimura<sup>5.9</sup> pointed out that in benzene at room temperature, the solubilities of  $\text{Cu}(\text{RCOCHCOR})_2$  increased substantially with increasing R, [For R =  $\text{CH}_3$  (2.5 mM), for R =  $\text{CH}_2\text{CH}_3$  (63 mM) and for R =  $\text{CH}_2\text{CH}_2\text{CH}_3$  (180 mM)], and that the molar volumes for the chelates were in direct proportionality to the additional carbon atoms in the molecule.

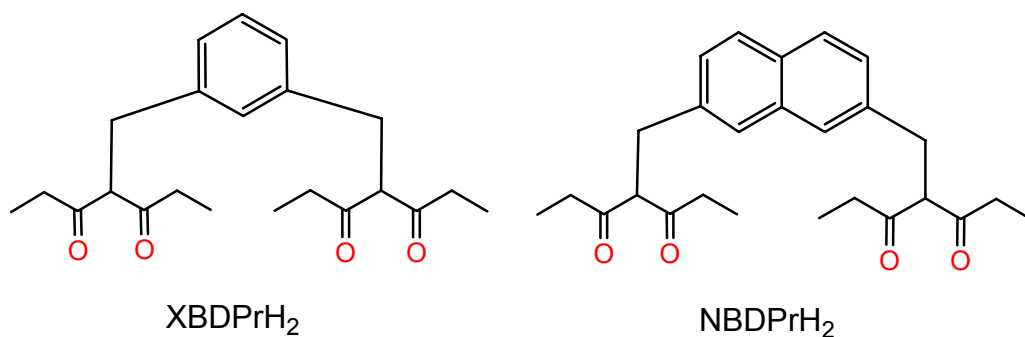


Figure 5.1. Structures of alkylated XBA and NBA ligands.

In previous work by our research group it was determined that  $\text{Cu}_2(\text{XBA})_2$  and  $\text{Cu}_2(\text{NBA})_2$  have low solubility in  $\text{CH}_2\text{Cl}_2$  and  $\text{CHCl}_3$ , and are almost insoluble in most other organic solvents. We undertook this segment of our work in order to examine the effect of substituents on the solubilities of our  $\beta$ -diketone copper chelates when the acetylacetone moiety has been alkyl-substituted. In so doing,

we undertook the synthetic challenge of preparing XBDPrH<sub>2</sub> and NBDPrH<sub>2</sub> (Figure 5.1), the alkylated derivatives of our XBAH<sub>2</sub> and NBAH<sub>2</sub> β-diketone ligands and their copper complexes as shown in Figure 5.2.

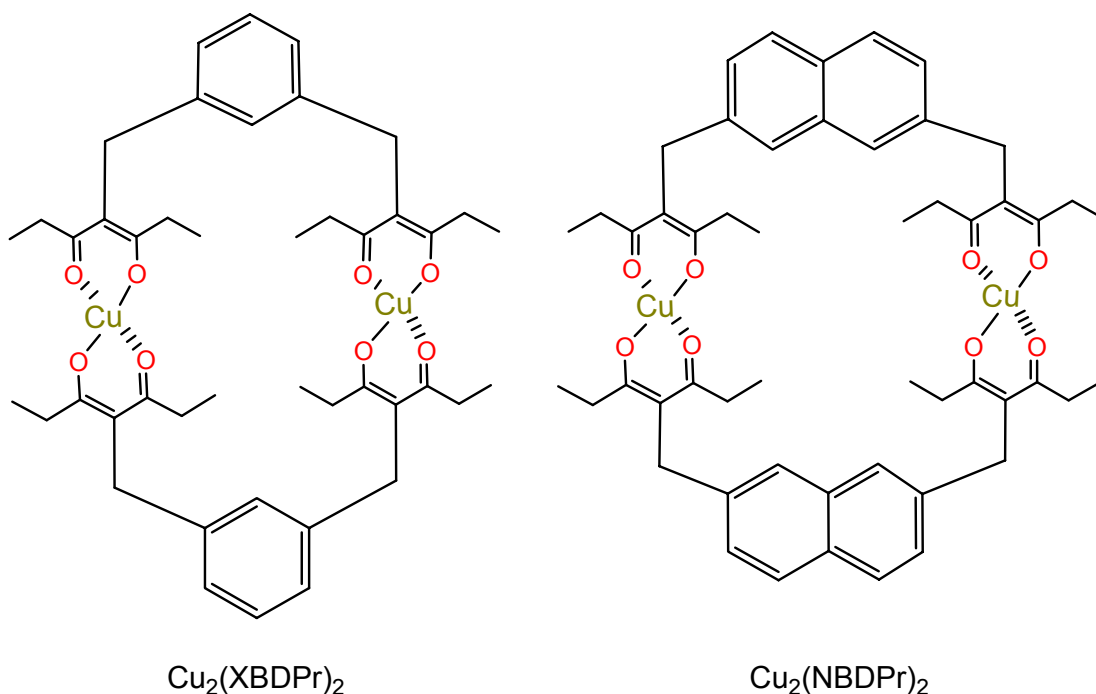


Figure 5.2. Structures of  $\text{Cu}_2(\text{XBDPr})_2$  and  $\text{Cu}_2(\text{NBDPr})_2$ .

The reaction of alkyl halides with the enolates<sup>5.1</sup> derived from β-diketones is a methodology that has been well established for forming C-C bonds. Fedorynski, et.al.,<sup>5.2</sup> showed that anhydrous sodium and potassium carbonates in the presence of catalytic amounts of tetraalkylammonium salts were strong enough bases for the generation and reaction of a variety of enolate carbanions. This methodology is usually a high yield chemoselective process. These findings had been earlier substantiated by work conducted by House,<sup>5.5</sup> who pointed out

that the most frequently observed difficulty that arises in the alkylation of  $\beta$ -dicarbonyl compounds is the concurrent formation of both C-alkylated and O-alkylated products and in some cases they form products from competing Claisen condensations,  $\beta$ -diketone cleavage, coupling of the enol salts of the starting materials and its monoalkylation product. However, Clark<sup>5.6</sup> later indicated that the problem of O-alkylated product formation could be minimized when hydrogen-bonding solvates were generated between tetraethylammonium fluoride and a number of  $\beta$ -dicarbonyl compounds. These reaction mixtures when introduced to alkyl iodides at room temperature could provide high yields of the mono-C-alkylated  $\beta$ -dicarbonyl products. Christoffers<sup>5.3</sup> showed that Ar-CH<sub>2</sub>-Br facile benzylation by alkyl-substituted<sup>5.4</sup>  $\beta$ -diketones of the type R<sub>2</sub>CCOCHR'COR", could be mediated by nBu<sub>4</sub>NF in THF-water. We have therefore, utilized a modification of Christoffers' chemistry, to attempt to prepare the desired ligands XBDPrH<sub>2</sub> and NBDPrH<sub>2</sub> and to subsequently synthesize their copper complexes. Upon initial inspection of Christoffers' chemistry we were led to believe that the synthesis would be straightforward and the products easily isolated.

## **5.2. Experimental**

### **5.2.1. Materials and Procedures**

The starting materials were all either commercially available or prepared according to the literature procedures, unless otherwise indicated. An aqueous solution of tetra-*n*-butylammonium fluoride (75 weight % solution in water) was

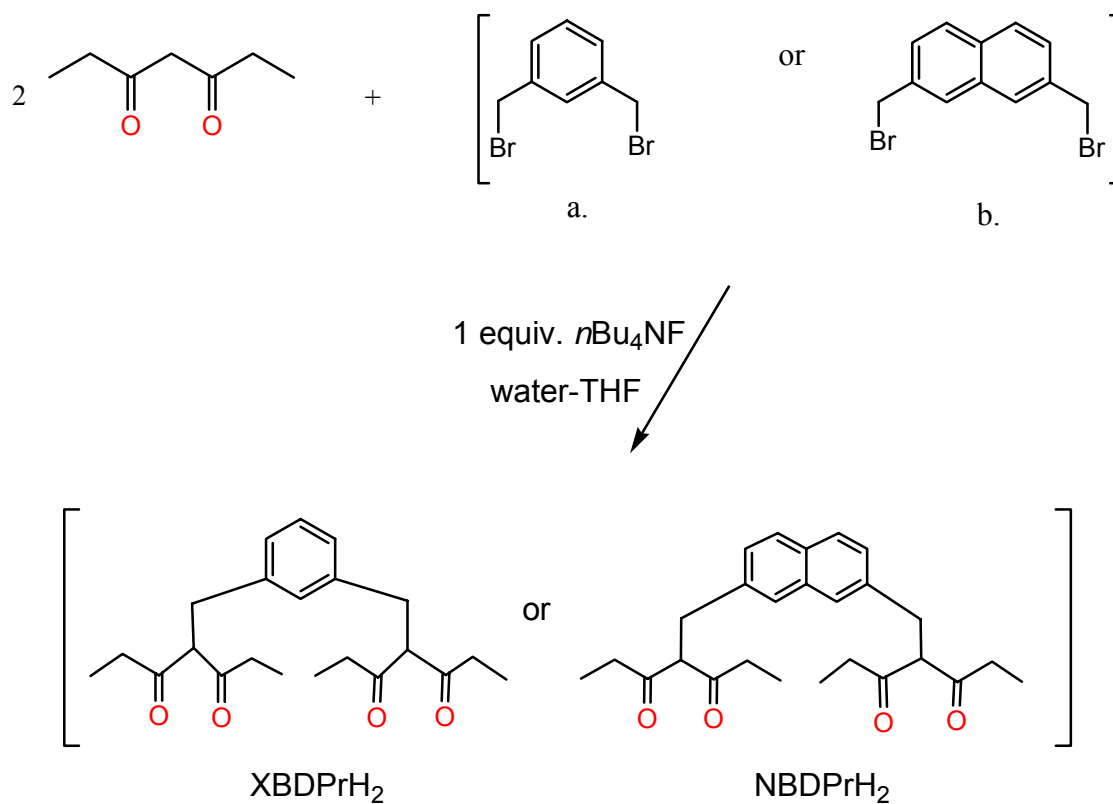
purchased from Sigma-Aldrich chemical company. The 3,5-heptanedione was purchased from Acros Organics chemical company. All chemicals and solvents were spectrophotometric or reagent grade and were used as received.  $^1\text{H}$  NMR spectra were recorded on a Bruker 250-MHz spectrometer. Microanalyses were performed by M-H-W Laboratories, of Phoenix, Arizona. The X-ray diffraction and crystal structure determinations were conducted on a Nonius Kappa CCD diffractometer at approximately 100 K.

**5.2.2. Preparation of 4,4'-(2,7-naphthalenediylbis(methylene))bis(dipropionyl methane) (NBDPrH<sub>2</sub>) and 4,4'-(1,3-xylenediylbis(methylene))bis(dipropionylmethane) (XBDPrH<sub>2</sub>).**

A solution of  $n\text{Bu}_4\text{NF}$  in water (75 weight % solution in water; 1.50 mL, 4.10 mmol) was added to a solution of the 3,5-heptanedione (0.56 mL, 4.10 mmol) in THF (1 mL). The mixture was stirred until homogeneous (~ 1 hour), and the aryl dibromide (a or b) (2.05 mmol) was added and this mixture was allowed to stir overnight at room temperature (Scheme 5.1). The literature cleanup and separation procedure using  $\text{SiO}_2$  as a filterant proved to be inadequate for separating the reaction components and removal of inorganic reaction materials. Therefore, the THF was removed at reduced pressure and the resulting reaction mixture was taken up in minimum  $\text{CH}_2\text{Cl}_2$  and repeatedly washed with distilled water to remove as much of the inorganic reaction material as possible and then dried over anhydrous  $\text{Na}_2\text{SO}_4$ , filtered, and the  $\text{CH}_2\text{Cl}_2$  solvent was removed at reduced pressure. These reactions generally produced 40 – 55 % of the crude product. In an attempt to purify the products, they were



each treated with  $[\text{Cu}(\text{NH}_3)_4]^{2+}$  and then with dilute HCl in order to extract the free ligand (Figures 5.3) before taking the  $^1\text{H}$  NMR spectra (Figures 5.4, 5.5, and Table 5.1).



Scheme 5.1

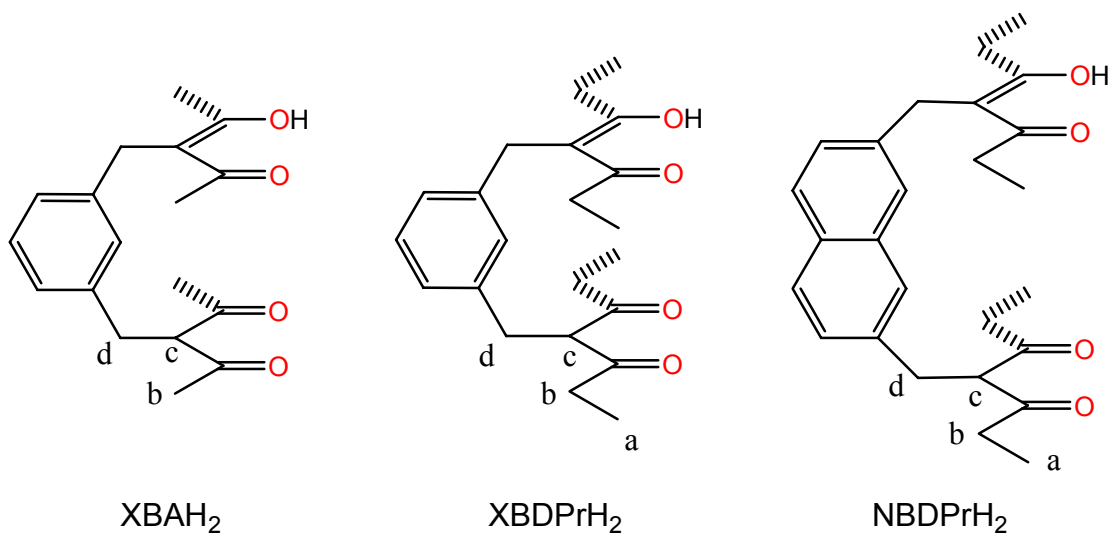


Figure 5.3. Structure of  $\text{XBAH}_2$ ,  $\text{XBdPrH}_2$  and  $\text{NBDPrH}_2$  ligands.

Table 5.1.  $^1\text{H}$  NMR shifts of (a)  $\text{XBAH}_2$ , (b)  $\text{XBdPrH}_2$  and (c)  $\text{NBDPrH}_2$ .

$^1\text{H}$	$\text{XBAH}_2(\text{k})$	$\text{XBAH}_2(\text{e})$
b	2.13s	2.19s
c	4.07t	
d, d'	3.18d	3.71s
O-H		16.9
Ar	7.06-7.3	

a.

$^1\text{H}$	$\text{XBdPrH}_2(\text{k})$	$\text{XBdPrH}_2(\text{e})$	$^1\text{H}$	$\text{NBDPrH}_2(\text{k})$	$\text{NBDPrH}_2(\text{e})$
a, a'	(1.1)	(1.1)	a, a'	(1.1)	
b	(2.5)	(2.2)	b	(2.3)	
c	4.08t		c	4.09	
d, d'	3.19	3.97	d, d'	3.29	3.33
O-H		16.9	O-H		17.0
Ar	6.91-7.3		Ar	7.2-7.8	

b.

c.

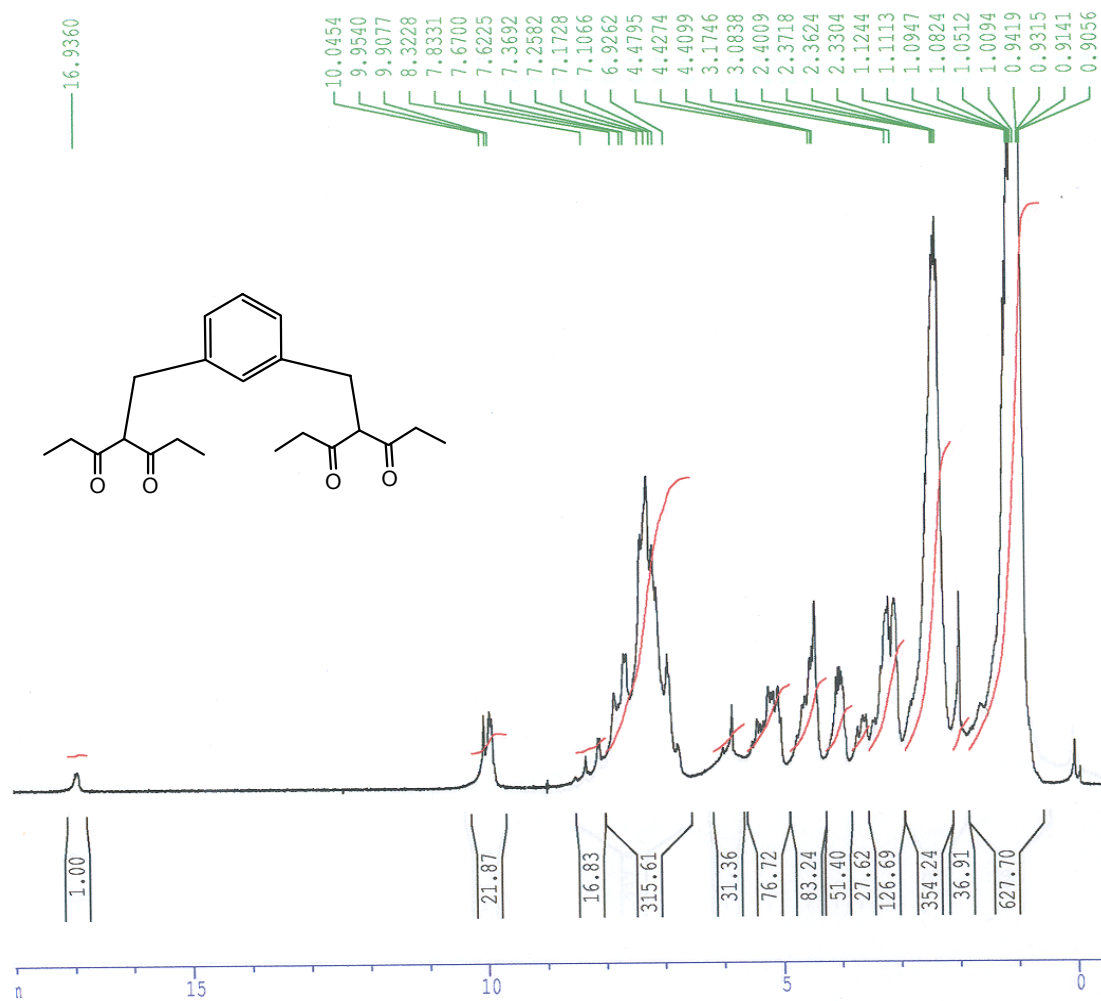


Figure 5.4. <sup>1</sup>H NMR spectrum of crude XBDPrH<sub>2</sub>.

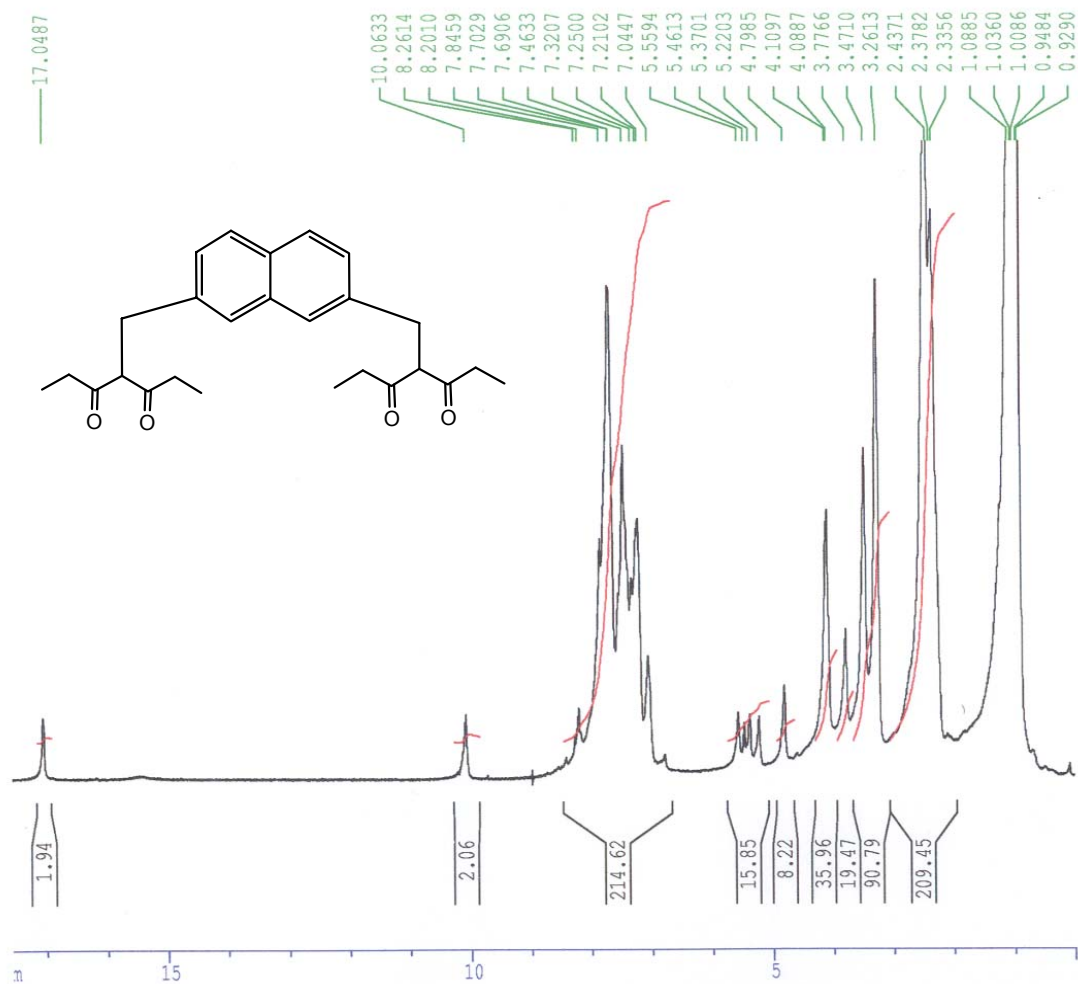


Figure 5.5. <sup>1</sup>H NMR spectrum of crude NBDPrH<sub>2</sub>.

### 5.2.3. Preparation of $\text{Cu}_2(\text{NBDPr})_2$ and Attempted Preparation of $\text{Cu}_2(\text{XBDPr})_2$

**$\text{Cu}_2(\text{NBDPr})_2$ :** An aqueous  $\text{CuSO}_4 \cdot 5\text{H}_2\text{O}$  solution (0.428 molar) was treated with  $\text{NH}_4\text{OH}$  (2.0 mL) to form a transparent deep blue aqueous solution, which was subsequently combined with a  $\text{CH}_2\text{Cl}_2$  solution of  $\text{NBDPrH}_2$ . The  $\text{CuSO}_4 \cdot 5\text{H}_2\text{O}$  to ligand molar ratio was 2:1 respectively. A green crystalline  $\text{Cu}_2(\text{NBDPr})_2$  solid formed at the aqueous–organic interface during the separatory funnel extraction sequence. This crystalline solid was utilized in the x-ray structure determination. Furthermore, the organic ( $\text{CH}_2\text{Cl}_2$ ) portion was extracted and dried over anhydrous  $\text{Na}_2\text{SO}_4$ . The  $\text{CH}_2\text{Cl}_2$  solvent was removed at reduced pressure and a grey powder  $\text{Cu}_2(\text{NBDPr})_2$  was evident. Elemental analysis: found (calculated) for  $\text{Cu}_2(\text{NBDPr})_2 \cdot \text{CH}_2\text{Cl}_2$ : C, 62.21 (62.10); H, 6.10 (6.10).

**$\text{Cu}_2(\text{XBDPr})_2$ :** An aqueous  $\text{CuSO}_4 \cdot 5\text{H}_2\text{O}$  solution (19.47 mmolar) was treated with  $\text{NH}_4\text{OH}$  (2.0 mL) to form a transparent deep blue aqueous solution, which was subsequently combined with a  $\text{CH}_2\text{Cl}_2$  solution (9.74 mmolar) of crude  $\text{XBDPrH}_2$ . The  $\text{CuSO}_4 \cdot 5\text{H}_2\text{O}$  to ligand molar ratio was 2:1 respectively. The organic ( $\text{CH}_2\text{Cl}_2$ ) portion was extracted, washed repeatedly with distilled water, dried over  $\text{Na}_2\text{SO}_4 \cdot \text{anhydrous}$ , filtered and the solvent ( $\text{CH}_2\text{Cl}_2$ ) was removed at reduced pressure. A mixture of blue-green and olive-green viscous to partially solid material, suspected of being both  $\text{Cu}(\text{3,5-heptanedionate})$  and  $\text{Cu}_2(\text{XBDPr})_2$  (3.18 g) was evident. All attempts to generate crystalline  $\text{Cu}_2(\text{XBDPr})_2$  sufficient for X-ray analysis failed. However, I was able to isolate a crude crystalline

material that revealed upon X-ray analysis, the structure for Cu(3,5-heptanedionate) (Figure 5.6).

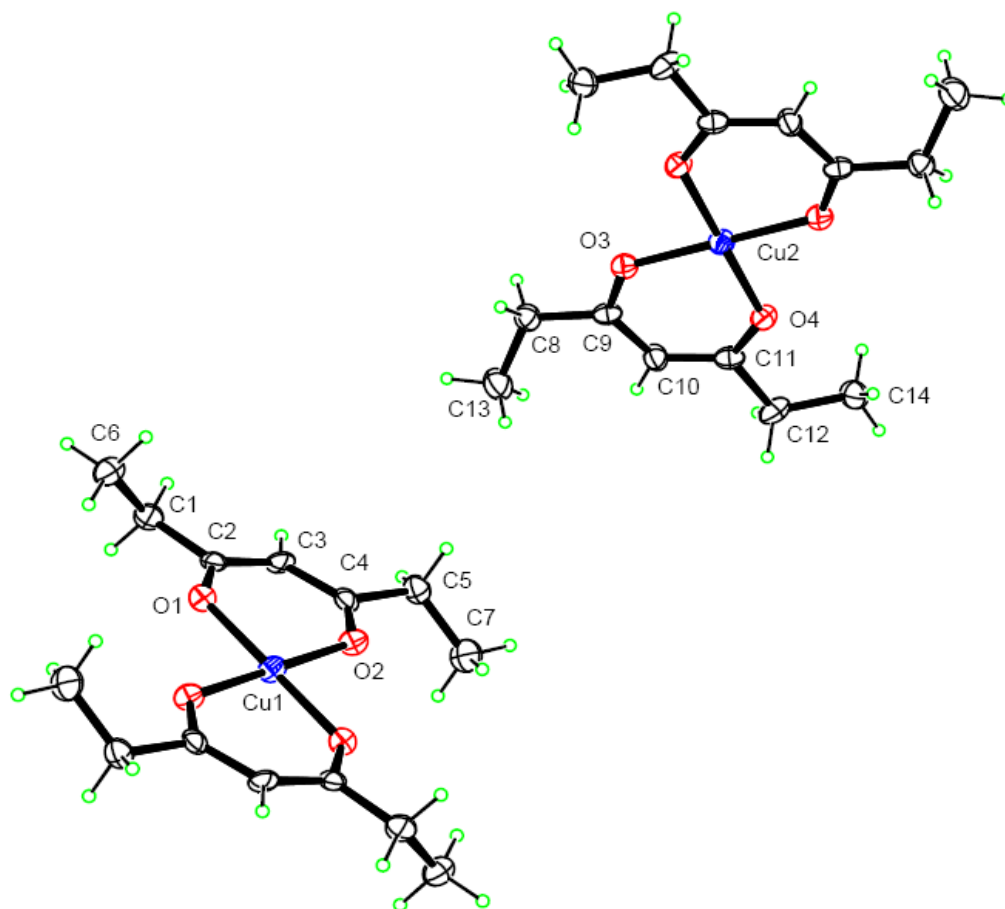


Figure 5.6. ORTEP diagram of Cu(3,5-heptanedionate).

#### 5.2.4. Structural Analysis of $\text{Cu}_2(\text{NBDPr})_2$

The elemental analysis of  $(\text{Cu}_2(\text{NBDPr})_2)$  the gray powder (C 62.21%, H 6.10%) was in line with the calculated values when we took into account the presence of 1 trapped solvent ( $\text{CH}_2\text{Cl}_2$ ) molecule. The crude X-ray structure of the  $\text{Cu}_2(\text{NBDPr})_2$  crystals (Figure 5.7) substantiated these findings by showing

the presence of 2 distinct molecules along with 2 trapped solvent molecules per unit cell. The crystal data is reported in Table 5.2.

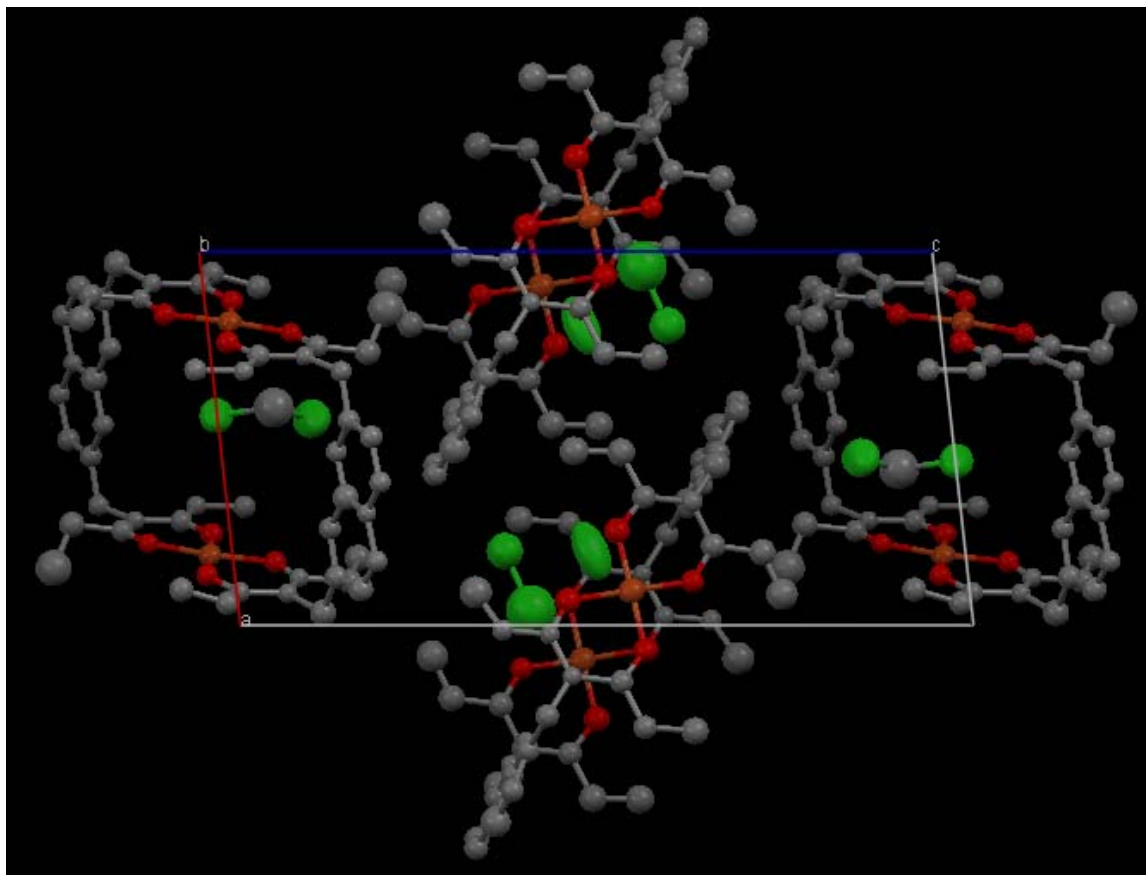


Figure 5.7. CCDC Mercury diagram of  $\text{Cu}_2(\text{NBDPr})_2$  with view along  $b$ .

Table 5.2. Crystal Data of  $\text{Cu}_2(\text{NBDPr})_2$ .

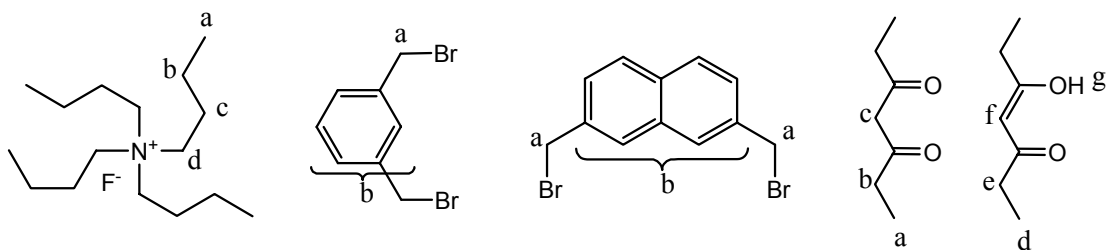
empirical formula	$\text{C}_{52}\text{H}_{60}\text{Cu}_2\text{O}_8 \cdot 2(\text{CH}_2\text{Cl}_2)$	$\alpha$ (deg)	84.761(3)
fw	1109.93	$\beta$ (deg)	83.255(3)
t(K)	110	$\gamma$ (deg)	84.734(3)
cryst. Syst.	Triclinic	$V$ ( $\text{\AA}^3$ )	2653.9(17)
space group	P-1	$Z$	2
$a$ ( $\text{\AA}$ )	11.153(3)	$d$ (calcd) ( $\text{Mg/m}^3$ )	1.389
$b$ ( $\text{\AA}$ )	11.089(4)	$R_1$ (%)	19.4
$c$ ( $\text{\AA}$ )	21.772(10)		

### 5.3. Results and Discussion

The reaction sequences of the XBDPrH<sub>2</sub> and NBDPrH<sub>2</sub> were both monitored by <sup>1</sup>H NMR and this revealed that the starting materials (3,5-heptanedione and tetra-n-butylammonium fluoride) concentration (Table 5.3) had diminished substantially by the end of the reaction, and further indicated that the desired ligands were present, in both the keto and enol forms, even though they were difficult to isolate. The <sup>1</sup>H NMR data are impure (Table 5.1, Figures 5.4 and 5.5) of NBDPrH<sub>2</sub> and XBDPrH<sub>2</sub>, but the presence of the c, d peaks along with the shifted enol peaks indicate that the desired ligands are present. Peaks a and b are not conclusive, because they could also be indicative of 3,5-heptanedione (Table 5.3).

Table 5.3. Tabulated <sup>1</sup>H NMR data of starting materials.

<sup>1</sup> H	nBu <sub>4</sub> NF	α, α'-Br <sub>2</sub> - <i>m</i> -Xylene	2,7-(bis)MeBrNaphth	3,5-heptanedione
a	0.65-0.70	2.18(s)	4.65	0.99-1.02
b	1.1-1.3	7.3-7.4	7.5-7.8	2.4-2.5( <i>q</i> )
c	1.70( <i>m</i> )			3.5( <i>s</i> )
d	2.49( <i>t</i> )			0.99-1.02
e				2.20-2.29( <i>q</i> )
f				5.44( <i>s</i> )
g				15.4





The attempts to prepare  $\text{Cu}_2(\text{NBDPr})_2$  and  $\text{Cu}_2(\text{XBDPr})_2$  crystals suitable for X-ray analysis were carried out by layering dichloromethane ( $\text{CH}_2\text{Cl}_2$ ) solutions of the respective copper complexes with hexane, acetone and acetonitrile. The hexane experiments with  $\text{Cu}_2(\text{NBDPr})_2$  afforded crude crystals, but they were not as good as those that formed during the initial synthesis. Therefore, the crystal used in the X-ray analysis (Figure 5.7) was one of those isolated during the initial synthesis. Also, the  $\text{Cu}_2(\text{XBDPr})_2$  experiments to produce X-ray quality crystals failed. Furthermore, the solubility data for  $\text{Cu}_2(\text{NBDPr})_2$  indicate that it is less soluble in  $\text{CH}_2\text{Cl}_2$  and  $\text{CHCl}_3$  than  $\text{Cu}_2(\text{NBA})_2$  and insoluble in acetonitrile, benzene and THF.

## Chapter 6

### Summary and Conclusions

Molecular manufacturing methodologies that aim to create solid materials containing chemical functionalities that are spatially organized by covalent or noncovalent interactions may lead to materials that are useful for applications such as separations, chemical sensing, and catalysis. While these methodologies may be conceptually straightforward, they can be difficult to accomplish experimentally. Here we have reported our efforts to design coordination specific transition metal (copper) complexes that could be utilized for, (a) host-guest binding studies and (b) the formation of well defined porous molecular solids.

In our preparation of 3,5-diacetyl-2,6-heptanedione ( $C_1BAH_2$ ), we utilized a modification of Knoevenagel's 1898 condensation reaction<sup>6.1</sup> of acetylacetone and formalin. In so doing we were also able to isolate the crystalline form of a second alkylation product of this reaction (3,5,5-triacetyl-tetrahydropyran-2-ol) that had been prepared previously by Aarna.<sup>6.2</sup>

The diketone groups of  $C_1BAH_2$  (with their propensity to rotate about a central methylene bridge) orient themselves in an anti fashion and seem to be best suited for the formation of linear polymeric coordination structures. This is evidenced by its X-ray crystal structure, the copper complex's elemental analysis and mass spectrum correlations. Therefore, this ligand was determined to be unsuitable for the preparation of our proposed cyclic molecular solids. However,

replacing the methylene bridge of  $C_1BAH_2$  with a double bond to form (Z)-3,6-diacetyloct-4-ene-2,7-dione (Figure 6.1) could conceivably produce a more structurally rigid diketone. This could conceptually generate a conformation for the diketo groups that would allow for the preparation of a well defined cyclic supramolecular molecular solid.

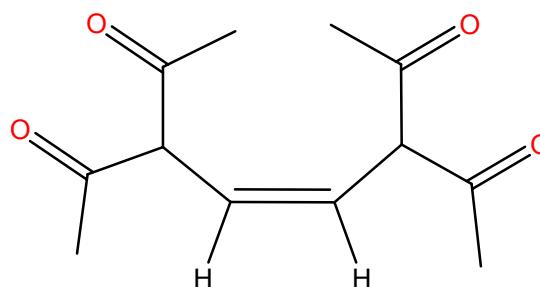


Figure 6.1. (Z)-3,6-diacetyloct-4-ene-2,7-dione.

The X-ray structure of  $p\text{-XBAH}_2$  shows that the diketone moieties are oriented approximately trans (or anti) to each other. If the ligand has a preference for this conformation in its metal complexes, this could explain our difficulties in isolating well behaved molecular products. However, as with the  $C_1BAH_2$  this ligand has

also shown promise for being a good precursor for the formation of metal coordination polymers. Other members of the group have begun to explore other (Figure 6.2a) (bis) $\beta$ -diketonates as

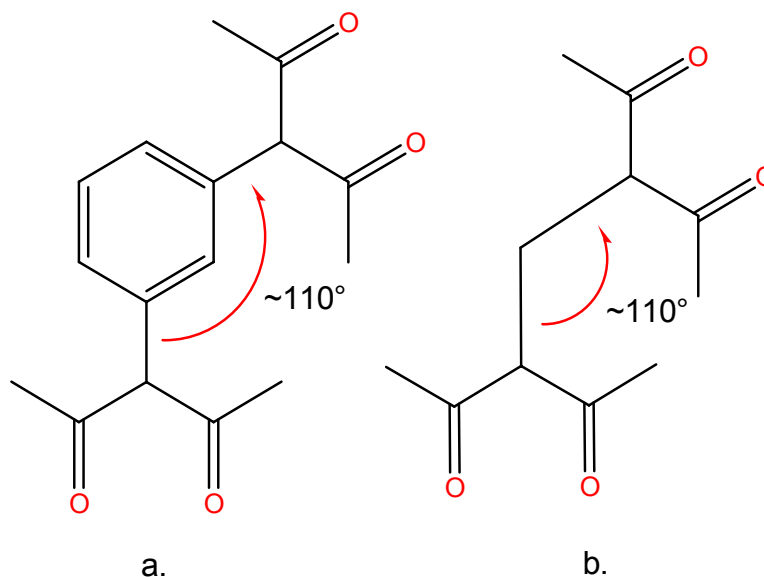


Figure 6.2. Possible (bis) $\beta$ -diketonate precursor compared to  $C_1BAH_2$ .

possible precursors for the preparation of our envisioned molecular solids.

The room temperature study to determine binding constants of the  $\text{Cu}_2(\text{NBA})_2$  complex with select heterocyclic sulfur guests proved to be unfruitful. We initiated this segment of our work by coordinating 1,4-dithiane with our  $\text{Cu}_2(\text{NBA})_2$ . By layering a  $\text{CHCl}_3$  solution of  $\text{Cu}_2(\text{NBA})_2$  and 1,4-dithiane with acetonitrile, small turquoise crystals of  $\text{Cu}_2(\text{NBA})_2 \cdot (1,4\text{-dithiane})$  were obtained, which were suitable for x-ray structure determination. Additionally, attempts to incorporate 2,5-dihydroxy-1,4-dithiane into our  $\text{Cu}_2(\text{NBA})_2$  ligand failed due to the insolubility of this guest in  $\text{CH}_2\text{Cl}_2$  and  $\text{CHCl}_3$ .

Subsequently, all attempts to determine equilibrium binding constants for  $\text{Cu}_2(\text{NBA})_2 \cdot (1,4\text{-dithiane})$  failed, and is attributed to the low affinity of  $\text{Cu}_2(\text{NBA})_2$  for the heterocyclic sulfur compound. We then reviewed the low temperature binding constant calculations that had previously been determined by our group for  $\text{Cu}_2(\text{NBA})_2 \cdot (\mathbf{N})$ , (where  $\mathbf{N}$  = dabco, pyrazine, 2-Mepyz, and 2-NH<sub>2</sub>pyz) and observed that a general increase in the equilibrium binding constants ( $\text{K/mol}^{-1}$ ) occurred throughout each series as the temperature was decreased. These observations indicate that measuring low temperature visible spectra of the  $\text{Cu}_2(\text{NBA})_2 \cdot (1,4\text{-dithiane})$  adduct could lead to the generation of the desired equilibrium binding constant data.

In light of the solubility characteristics that had previously been observed with  $\text{Cu}_2(\text{NBA})_2$ , those that were evaluated during the dithiane experiments and the other selected sulfur analogue, I decided to extend the aliphatic chains of our

betadiketone moieties by alkylating them. I had hoped that the extended aliphatic chain would increase the solubility of the  $\text{Cu}_2(\text{NBDPr})_2$  metal complex. However, the qualitative solubility data that I observed with ethyl groups replacing the methyls gave opposite findings from what I had anticipated. The solubility of the  $\text{Cu}_2(\text{NBDPr})_2$  metal complex was appreciably less in  $\text{CH}_2\text{Cl}_2$ ,  $\text{CHCl}_3$ , acetonitrile, benzene and THF than those observed for  $\text{Cu}_2(\text{NBA})_2$ .

## References

- 1.1 Arunasalam, V-C.; Baxter, I.; Drake, S. R.; Hursthouse, M. B.; Malik, K. M. A.; Otway, D. J. *Inorg. Chem.* **1995**, 34, 5295.
- 1.2 Drake, S. R.; Hursthouse, M. B.; Malik, K. M. A.; Miller, S. A. S.; Otway, D. J. *Inorg. Chem.* **1993**, 32, 4464.
- 1.3 Drake, S. R.; Hursthouse, M. B.; Malik, K. M. A.; Otway, D. J. *J. Chem. Soc., Dalton Trans.* **1993**, (19), 2883.
- 1.4 Huang, L.; Turnipseed, S. B.; Haltiwanger, R. C.; Barkley, R. M.; Sievers, R. E. *Inorg. Chem.* **1994**, 33, 798.
- 1.5 Drake, S. R.; Miller, S.; Williams, D. J. *Inorg. Chem.* **1993**, 32(15), 3233.
- 1.6 Thornton, D. A. *Coord. Chem. Rev.* **1990**, 104, 173.
- 1.7 Englert, U.; Kaser, M.; Salzer, A. *Inorg. Chem.* **1995**, 34, 6231.
- 1.8 Togni, A. *Organometallics.* **1990**, 9, 3106.
- 1.9 Danishefsky, S. *Chemtracts: Org. Chem.* **1989**, 2, 273.
- 1.10 Schurig, V. *Chromatographia.* **1980**, 13, 263.
- 1.11 Cotton, F. A.; Wilkinson, G.; Murillo, C. A.; Bochmann, M. *Advanced Inorganic Chemistry*, 6<sup>th</sup> Ed. Wiley: New York, **1999**; pp 480.
- 1.12 Grillo, V. A.; Seddon, E. J.; Grant, C. M.; Arom, G.; Bollinger, J. C.; Folting, K.; Christou, G. *Chem. Commun.* **1997**, (16), 1561.
- 1.13 Maverick, A. W.; Klavetter, F. *Inorg. Chem.* **1984**, 23, 4129.
- 1.14 Maverick, A. W.; Buchkingham, S. C.; Yao, Q.; Bradbury, J. R.; Stanley, G. G. *J. Am. Chem. Soc.* **1986**, 108, 7430.
- 1.15 Maverick, A. W.; Martone, D. P.; Bradbury, J. R.; Nelson, J. E. *Polyhedron.* **1989**, 8, 1549.
- 1.16 Maverick, A. W.; Ivie, M. L.; Waggenspack, J. H.; Fronczek, F. R. *Inorg. Chem.* **1990**, 29, 2403.
- 1.17 Fronczek, F. R.; Ivie, M. L.; Maverick, A. W. *Acta. Crystallogr., Sect. C*,

- 1990**, C46, 2057.
- 1.18 Kumar, R.; Fronczek, F. R.; Maverick, A. W.; Lai, W. G.; Griffin, G. *Chem. Mater.* **1992**, 4, 577.
- 1.19 Borgharkar, N. S.; Griffin, G. L.; Fan, H.; Maverick, A. W. *J. Electrochem. Soc.* **1999**, 146, 1041.
- 1.20 He, Xiaohui.; Yao, Yingzheng.; Luo, Xiang.; Zhang, Junkai.; Liu, Yunhai.; Zhang, Ling.; Wu, Qing. *Organometallics* **2003**, 22, 4952.
- 1.21 Bradbury, J. R.; Hampton, J. L.; Martone, D. P.; Maverick, A. W. *Inorg. Chem.* **1989**, 28, 2392.
- 1.22 Oh, J. S.; Bailar, J. C. Jr. *J. Inorg. Nucl. Chem.* **1962**, 24, 1225.
- 1.23 Bullen, G. J.; Mason, R.; Pauling, P. *Inorg. Chem.* **1965**, 4, 456.
- 2.1 Knoevenagel, E. *Ann.* **1894**, 25, 1223
- 2.2 Knoevenagel, E.; Ruschhaupt W. *Chem. Ber.* **1898**, 31, 1025.
- 2.3 Knoevenagel, E. *Chem. Ber.* **1903**, 36, 2136.
- 2.4 Wilson, B. D. *J. Org. Chem.* **1963**, 28, 314.
- 2.5 O'Loane, J. K.; Combs, C. M.; Griffith, R. L. *J. Org. Chem.* **1964**, 29, 1730.
- 2.6 Martin, D. F.; Fernelius, W. C. *J. Am. Chem. Soc.* **1959**, 81, 1509.
- 2.7 Aarna, A.; Koosel, A.; Kiisler, K. *Finnish Chemical Letters.* **1975**, (3-4), 102-4.
- 2.8 Rogers, M. T.; Burdett, J.L. *Can. J. Chem.* **1965**, 43, 1516.
- 2.9 Meany, J. E. *J. Phys. Chem.* **1969**, 10, 3421.
- 2.10 Spencer, J. N.; Holmbe, E. S.; Kirshenbaum, M. R.; Firth, D. W.; Pinto, P. B. *Can. J. Chem.* **1982**, 60, 1178.
- 2.11 Silverstein, R. M.; Bassler, G. C. *Spectrophotometric Identification of Organic Compounds*, 2ed.; Wiley: New York, **1967**; p.159.
- 2.12 Yoffee, S. T.; Popov, E. M.; Yatsuro, K.V.; Tulikova, E. M.; Kabachnik, M.

- I. *Tetrahedron*. **1962**, 18, 923.
- 2.13 Kennedy, W. A.; McMurry, T. B. H. *J. Chem. Soc. [Sec. C. Organic]*. **1969**, (6), 879-82.
- 2.14 Oh, J. S.; Bailar, J. C. Jr. *J. Inorg. Nucl. Chem.* **1962**, 24, 1225.
- 2.15 Burton, S.; Maverick, A. W.; Stanley, G. G. unpublished work.
- 3.1 Adkins, H.; Kutz, W.; Coffman, D. D. *J. Am. Chem. Soc.* **1930**, 52, 3213.
- 3.2 Morgan, G. T.; Thomason, R. W. *J. Chem. Soc.* **1924**, 754.
- 3.3 Morgan, G. T. *J. Chem. Soc.* **1925**, 2611.
- 3.4 Holtzclaw, H. F. Jr.; Johnson, K. W. R.; Hengeveld, F. W. *J. Am. Chem. Soc.* **1952**, 74, 3776.
- 3.5 Holtzclaw, H. F. Jr.; Collman, J. P. *J. Am. Chem. Soc.* **1957**, 79, 3318.
- 3.6 Morgan, G. T.; Drew, H. K. *J. Chem. Soc.* **1924**, 731.
- 3.7 Holtzclaw, H. F. Jr.; Carlson, A. H.; Collman, J. P. *J. Am. Chem. Soc.* **1956**, 78, 1838.
- 3.8 Martin, D. F.; Shamma, M.; Fernelius, W. C. *J. Am. Chem. Soc.* **1958**, 80, 5851.
- 3.9 Yeager, M. A.; Maverick, A. W. *unpublished work*.
- 3.10 Martin, D. F.; Fernelius, W. C.; Shamma, M. *J. Am. Chem. Soc.* **1959**, 81, 130.
- 3.11 Dawber, J. G.; Crane, M. M. *J. Chem. Ed.* **1967**, 44(3), 150.
- 4.1 Agnus, Y.; Louis, R.; Weiss, R. *J. Am. Chem. Soc.* **1979**, 101, 3381.
- 4.2 Maverick, A. W.; Klavetter, F. *Inorg. Chem.* **1984**, 23, 4129.
- 4.3 Maverick, A. W.; Buckingham, S. C.; Bradbury, J. R.; Yao, Q.; Stanley, G. G. *J. Am. Chem. Soc.* **1986**, 108, 7430.



- 4.4 Hoshino, N.; Jircitano, A.; Busch, D. H. *Inorg. Chem.* **1988**, 27, 2292.
- 4.5 Coughlin, P. K.; Lippard, S. J. *Inorg. Chem.* **1984**, 23, 1446.
- 4.6 Drew, M. G. B.; McCann, M.; Nelson, S. M. *J. Chem. Soc., Chem. Commun.* **1979**, 481.
- 4.7 Martin, D. F.; Fernelius, W. C.; Shamma, M. *J. Am. Chem. Soc.* **1959**, 81, 130.
- 4.8 Maverick, A. W.; Klavetter, F. *Inorg. Chem.* **1984**, 23, 4129.
- 4.9 Maverick, A. W.; Bradbury, J. R.; Martone, D. P.; Hampton, J. L.; Nelson, J. E. *Polyhedron*. **1989**, 8, 1549.
- 4.10 Rose, N. J.; Drago, R. S. *J. Am. Chem. Soc.* **1959**, 81, 6138.
- 5.1 Abel, R. D. *J. Chem. Soc.* **1912**, 101, 989.
- 5.2 Fedorynski, M.; Wojciechowski, K.; Matacz, Z.; Makosza, M. *J. Org. Chem.* **1978**, 43, 4682.
- 5.3 Christoffers, J. *Synthetic Communications*, **1999**, 29(1), 117-122.
- 5.4 Koshimura, H. *Analytic Chimica Acta*, **1973**, 67, 331-340.
- 5.5 House, H. O. 'Modern Synthetic Reactions'. 2<sup>nd</sup> edn., Benjamin, Menlo Park, **1972**.
- 5.6 Clark, J. H.; Miller, J. M. *J. Chem. Soc., Chem. Commun.* **1977**, 64.
- 5.7 Stary, J. 'The Solvent Extraction of Metal Chelates'. Pergamon Press. Oxford, **1964**.
- 5.8 Marcus, Y.; Kertes, A. S. 'Ion Exchange and Solvent Extraction of Metal Complexes'. Wiley, New York, **1969**.
- 5.9 Koshimura, H. *J. Inorg. Nucl. Chem.*, **1976**, 38(9), 1705-1712.
- 6.1 Knoevenagel, E.; Ruschhaupt, W. *Chem. Ber.* **1898**, 31, 1025.
- 6.2 Aarna, A.; Koosel, A.; Kiisler, K. *Finnish Chemical Letters*. **1975**, (3-4), 102-4.

## Appendix Crystal Data in CIF Format

### C<sub>1</sub>BAH<sub>2</sub>

_audit_creation_method	SHELXL-97
_chemical_name_systematic	'3,5-diacetyl-heptane-2,6-dione'
_chemical_name_common	'methylenediacetylacetone,
_chemical_melting_point	'313.5-314.0'
_chemical_compound_source	'local laboratory'
_chemical_formula_moiety	'C11 H16 O4'
_chemical_formula_sum	'C11 H16 O4'
_chemical_formula_weight	212.24
loop_	
_atom_type_symbol	
_atom_type_description	
_atom_type_scatter_dispersion_real	
_atom_type_scatter_dispersion_imag	
_atom_type_scatter_source	
'C' 'C' 0.0033 0.0016	'International Tables Vol C Tables 4.2.6.8 and 6.1.1.4'
'H' 'H' 0.0000 0.0000	'International Tables Vol C Tables 4.2.6.8 and 6.1.1.4'
'O' 'O' 0.0106 0.0060	'International Tables Vol C Tables 4.2.6.8 and 6.1.1.4'
_symmetry_space_group_name_H-M	
	'P 21 21 21'
_symmetry_cell_setting	'Orthorhombic'
loop_	
_symmetry_equiv_pos_as_xyz	
	'x, y, z'
	'-x+1/2, -y, z+1/2'
	'x+1/2, -y+1/2, -z'
	'-x, y+1/2, -z+1/2'
_cell_length_a	
	7.810(2)
_cell_length_b	8.611(2)
_cell_length_c	17.431(4)
_cell_angle_alpha	90
_cell_angle_beta	90
_cell_angle_gamma	90
_cell_volume	1172.3(5)
_cell_formula_units_Z	4
_cell_measurement_temperature	100
_cell_measurement_reflns_used	2556

_cell_measurement_theta_min	2.5
_cell_measurement_theta_max	33.7
_exptl_crystal_description	fragment
_exptl_crystal_colour	colorless
_exptl_crystal_size_max	0.47
_exptl_crystal_size_mid	0.43
_exptl_crystal_size_min	0.40
_exptl_crystal_density_meas	?
_exptl_crystal_density_diffn	1.203
_exptl_crystal_density_method	'not measured'
_exptl_crystal_F_000456	
_exptl_absorpt_coefficient_mu	0.091
_exptl_absorpt_correction_type	none
_exptl_absorpt_correction_T_min	?
_exptl_absorpt_correction_T_max	?
_exptl_absorpt_process_details	?
_exptl_special_details	?
_diffn_ambient_temperature	100
_diffn_radiation_wavelength	0.71073
_diffn_radiation_type	MoK $\alpha$
_diffn_radiation_source	'fine-focus sealed tube'
_diffn_radiation_monochromator	graphite
_diffn_measurement_device	'KappaCCD (with Oxford Cryostream)'
_diffn_measurement_method	'\w scans with \k offsets'
_diffn_detector_area_resol_mean	?
_diffn_standards_number	0
_diffn_standards_interval_count	?
_diffn_standards_interval_time	?
_diffn_standards_decay_	%<2
_diffn_reflns_number	15692
_diffn_reflns_av_R_equivalents	0.016
_diffn_reflns_av_signal/netl	0.0257
_diffn_reflns_limit_h_min	-11
_diffn_reflns_limit_h_max	11
_diffn_reflns_limit_k_min	-13
_diffn_reflns_limit_k_max	13
_diffn_reflns_limit_l_min	-27
_diffn_reflns_limit_l_max	27
_diffn_reflns_theta_min	2.8
_diffn_reflns_theta_max	33.7
_reflns_number_total	2647
_reflns_number_gt	2352
_reflns_threshold_expression	$I > 2\sigma(I)$
_computing_data_collection	'COLLECT (Nonius, 2000)'

_computing_cell_refinement	'HKL Scalepack (Otwinowski & Minor 1997)'
_computing_data_reduction	'HKL Denzo and Scalepack (Otwinowski & Minor 1997)'
_computing_structure_solution	'SIR97 (Altomare et al., 1999)'
_computing_structure_refinement	'SHELXL-97 (Sheldrick, 1997)'
_computing_molecular_graphics	'ORTEP-3 for Windows (Farrugia, 1997)'
_computing_publication_material	'SHELXL-97 (Sheldrick, 1997)'
_refine_special_details	

;

Refinement of  $F^2$  against ALL reflections. The weighted R-factor wR and goodness of fit S are based on  $F^2$ , conventional R-factors R are based on F, with F set to zero for negative  $F^2$ . The threshold expression of  $F^2 > 2\sigma(F^2)$  is used only for calculating R-factors(gt) etc. and is not relevant to the choice of reflections for refinement. R-factors based on  $F^2$  are statistically about twice as large as those based on F, and R-factors based on ALL data will be even larger.

;

_refine_ls_structure_factor_coef	Fsqd
_refine_ls_matrix_type	full
_refine_ls_weighting_scheme	calc
_refine_ls_weighting_details	
	'calc w=1/[ $s^2(F_o^2)+(0.0668P)^2+0.1309P$ ] where $P=(F_o^2+2F_c^2)/3$ '
_atom_sites_solution_	direct
_atom_sites_solution_secondary	difmap
_atom_sites_solution_hydrogens	geom
_refine_ls_hydrogen_treatment	constr
_refine_ls_extinction_method	none
_refine_ls_extinction_coef	?
_refine_ls_abs_structure_details	?
_refine_ls_abs_structure_Flack	?
_refine_ls_number_reflns	2647
_refine_ls_number_parameters	140
_refine_ls_number_restraints	0
_refine_ls_R_factor_all	0.048
_refine_ls_R_factor_gt	0.041
_refine_ls_wR_factor_ref	0.113
_refine_ls_wR_factor_gt	0.107
_refine_ls_goodness_of_fit_ref	1.041
_refine_ls_restrained_S_all	1.041
_refine_ls_shift/su_max	0.006
_refine_ls_shift/su_mean	0.000

```

loop_
  _atom_site_label
  _atom_site_type_symbol
  _atom_site_fract_x
  _atom_site_fract_y
  _atom_site_fract_z
  _atom_site_U_iso_or_equiv
  _atom_site_adp_type
  _atom_site_occupancy
  _atom_site_symmetry_multiplicity
  _atom_site_calc_flag
  _atom_site_refinement_flags
  _atom_site_disorder_assembly
  _atom_site_disorder_group
O1 O 0.05730(14) 0.48942(13) 0.67423(5) 0.0284(2) Uani 1 1 d . . .
O2 O -0.06423(14) 0.21860(16) 0.54715(7) 0.0388(3) Uani 1 1 d . . .
O3 O 0.52584(15) 0.07629(14) 0.65558(6) 0.0346(3) Uani 1 1 d . . .
O4 O 0.45874(17) 0.10347(15) 0.84527(6) 0.0383(3) Uani 1 1 d . . .
C1 C 0.1592(2) 0.53906(18) 0.54771(8) 0.0296(3) Uani 1 1 d . . .
H1A H 0.0884 0.6328 0.5508 0.044 Uiso 1 1 calc R . .
H1B H 0.1286 0.4802 0.5016 0.044 Uiso 1 1 calc R . .
H1C H 0.2803 0.5686 0.5452 0.044 Uiso 1 1 calc R . .
C2 C 0.12923(16) 0.44037(15) 0.61741(7) 0.0212(2) Uani 1 1 d . . .
C3 C 0.19679(15) 0.27436(14) 0.61312(6) 0.0184(2) Uani 1 1 d . . .
H3 H 0.3141 0.2768 0.5901 0.022 Uiso 1 1 calc R . .
C4 C 0.08071(18) 0.17786(17) 0.56105(7) 0.0246(2) Uani 1 1 d . . .
C5 C 0.1554(2) 0.03050(19) 0.52954(9) 0.0366(3) Uani 1 1 d . . .
H5A H 0.0644 -0.0469 0.5234 0.055 Uiso 1 1 calc R . .
H5B H 0.2423 -0.0092 0.5650 0.055 Uiso 1 1 calc R . .
H5C H 0.2082 0.0514 0.4796 0.055 Uiso 1 1 calc R . .
C6 C 0.20811(15) 0.19736(15) 0.69250(6) 0.0195(2) Uani 1 1 d . . .
H6A H 0.1052 0.2245 0.7228 0.023 Uiso 1 1 calc R . .
H6B H 0.2105 0.0831 0.6863 0.023 Uiso 1 1 calc R . .
C7 C 0.69870(18) 0.2565(2) 0.72430(11) 0.0348(3) Uani 1 1 d . . .
H7A H 0.7860 0.1755 0.7298 0.052 Uiso 1 1 calc R . .
H7B H 0.6838 0.3103 0.7734 0.052 Uiso 1 1 calc R . .
H7C H 0.7351 0.3310 0.6851 0.052 Uiso 1 1 calc R . .
C8 C 0.53220(16) 0.18388(16) 0.70076(7) 0.0231(2) Uani 1 1 d . . .
C9 C 0.36884(15) 0.24996(14) 0.73593(6) 0.0182(2) Uani 1 1 d . . .
H9 H 0.3751 0.3659 0.7337 0.022 Uiso 1 1 calc R . .
C10 C 0.36087(17) 0.20085(16) 0.82022(7) 0.0236(2) Uani 1 1 d . . .
C11 C 0.22526(19) 0.27536(18) 0.86857(7) 0.0294(3) Uani 1 1 d . . .
H11A H 0.2417 0.2456 0.9223 0.044 Uiso 1 1 calc R . .
H11B H 0.1122 0.2407 0.8512 0.044 Uiso 1 1 calc R . .

```

H11C H 0.2332 0.3885 0.8638 0.044 Uiso 1 1 calc R . .

loop\_

\_atom\_site\_aniso\_label  
\_atom\_site\_aniso\_U\_11  
\_atom\_site\_aniso\_U\_22  
\_atom\_site\_aniso\_U\_33  
\_atom\_site\_aniso\_U\_23  
\_atom\_site\_aniso\_U\_13  
\_atom\_site\_aniso\_U\_12

O1 0.0318(5) 0.0291(5) 0.0243(4) -0.0015(4) 0.0051(4) 0.0065(4)  
O2 0.0300(5) 0.0493(7) 0.0371(6) -0.0062(5) -0.0138(5) 0.0006(5)  
O3 0.0336(5) 0.0348(6) 0.0354(5) -0.0080(5) -0.0005(4) 0.0123(5)  
O4 0.0445(7) 0.0436(6) 0.0269(5) 0.0120(4) -0.0062(5) 0.0058(6)  
C1 0.0315(6) 0.0299(6) 0.0275(6) 0.0104(5) 0.0050(5) 0.0059(5)  
C2 0.0197(5) 0.0237(5) 0.0201(4) 0.0018(4) -0.0005(4) 0.0015(4)  
C3 0.0182(5) 0.0219(5) 0.0152(4) -0.0002(4) -0.0008(4) 0.0000(4)  
C4 0.0287(6) 0.0280(6) 0.0169(4) -0.0007(4) -0.0027(4) -0.0038(5)  
C5 0.0404(8) 0.0341(7) 0.0353(7) -0.0142(6) -0.0031(6) -0.0033(7)  
C6 0.0203(5) 0.0220(5) 0.0163(4) 0.0018(4) -0.0024(4) -0.0024(4)  
C7 0.0203(6) 0.0335(7) 0.0506(9) 0.0075(7) -0.0019(6) -0.0010(6)  
C8 0.0211(5) 0.0231(5) 0.0250(5) 0.0053(4) -0.0009(4) 0.0033(5)  
C9 0.0197(4) 0.0184(4) 0.0165(4) 0.0012(4) -0.0014(4) -0.0011(4)  
C10 0.0283(6) 0.0249(5) 0.0175(4) 0.0018(4) -0.0043(4) -0.0066(5)  
C11 0.0338(7) 0.0348(7) 0.0198(5) -0.0036(5) 0.0050(5) -0.0117(6)

\_geom\_special\_details

;

All esds (except the esd in the dihedral angle between two l.s. planes) are estimated using the full covariance matrix. The cell esds are taken into account individually in the estimation of esds in distances, angles and torsion angles; correlations between esds in cell parameters are only used when they are defined by crystal symmetry. An approximate (isotropic) treatment of cell esds is used for estimating esds involving l.s. planes.

;

loop\_

\_geom\_bond\_atom\_site\_label\_1  
\_geom\_bond\_atom\_site\_label\_2  
\_geom\_bond\_distance  
\_geom\_bond\_site\_symmetry\_2  
\_geom\_bond\_publ\_flag

O1 C2 1.2145(15) . ?

O2 C4 1.2097(18) . ?

O3 C8 1.2169(18) . ?  
 O4 C10 1.2158(17) . ?  
 C1 C2 1.5011(18) . ?  
 C1 H1A 0.9800 . ?  
 C1 H1B 0.9800 . ?  
 C1 H1C 0.9800 . ?  
 C2 C3 1.5256(17) . ?  
 C3 C4 1.5284(17) . ?  
 C3 C6 1.5370(16) . ?  
 C3 H3 1.0000 . ?  
 C4 C5 1.501(2) . ?  
 C5 H5A 0.9800 . ?  
 C5 H5B 0.9800 . ?  
 C5 H5C 0.9800 . ?  
 C6 C9 1.5343(16) . ?  
 C6 H6A 0.9900 . ?  
 C6 H6B 0.9900 . ?  
 C7 C8 1.500(2) . ?  
 C7 H7A 0.9800 . ?  
 C7 H7B 0.9800 . ?  
 C7 H7C 0.9800 . ?  
 C8 C9 1.5256(18) . ?  
 C9 C10 1.5301(17) . ?  
 C9 H9 1.0000 . ?  
 C10 C11 1.498(2) . ?  
 C11 H11A 0.9800 . ?  
 C11 H11B 0.9800 . ?  
 C11 H11C 0.9800 . ?

loop\_  
 \_geom\_angle\_atom\_site\_label\_1  
 \_geom\_angle\_atom\_site\_label\_2  
 \_geom\_angle\_atom\_site\_label\_3  
 \_geom\_angle  
 \_geom\_angle\_site\_symmetry\_1  
 \_geom\_angle\_site\_symmetry\_3  
 \_geom\_angle\_publ\_flag  
 C2 C1 H1A 109.5 . . ?  
 C2 C1 H1B 109.5 . . ?  
 H1A C1 H1B 109.5 . . ?  
 C2 C1 H1C 109.5 . . ?  
 H1A C1 H1C 109.5 . . ?  
 H1B C1 H1C 109.5 . . ?  
 O1 C2 C1 122.37(12) . . ?

O1 C2 C3 121.72(11) . . ?  
 C1 C2 C3 115.90(10) . . ?  
 C2 C3 C4 109.48(10) . . ?  
 C2 C3 C6 112.33(10) . . ?  
 C4 C3 C6 109.52(10) . . ?  
 C2 C3 H3 108.5 . . ?  
 C4 C3 H3 108.5 . . ?  
 C6 C3 H3 108.5 . . ?  
 O2 C4 C5 122.38(14) . . ?  
 O2 C4 C3 121.09(13) . . ?  
 C5 C4 C3 116.53(12) . . ?  
 C4 C5 H5A 109.5 . . ?  
 C4 C5 H5B 109.5 . . ?  
 H5A C5 H5B 109.5 . . ?  
 C4 C5 H5C 109.5 . . ?  
 H5A C5 H5C 109.5 . . ?  
 H5B C5 H5C 109.5 . . ?  
 C9 C6 C3 111.34(9) . . ?  
 C9 C6 H6A 109.4 . . ?  
 C3 C6 H6A 109.4 . . ?  
 C9 C6 H6B 109.4 . . ?  
 C3 C6 H6B 109.4 . . ?  
 H6A C6 H6B 108.0 . . ?  
 C8 C7 H7A 109.5 . . ?  
 C8 C7 H7B 109.5 . . ?  
 H7A C7 H7B 109.5 . . ?  
 C8 C7 H7C 109.5 . . ?  
 H7A C7 H7C 109.5 . . ?  
 H7B C7 H7C 109.5 . . ?  
 O3 C8 C7 121.98(13) . . ?  
 O3 C8 C9 120.65(12) . . ?  
 C7 C8 C9 117.37(12) . . ?  
 C8 C9 C10 108.47(10) . . ?  
 C8 C9 C6 112.08(10) . . ?  
 C10 C9 C6 111.04(10) . . ?  
 C8 C9 H9 108.4 . . ?  
 C10 C9 H9 108.4 . . ?  
 C6 C9 H9 108.4 . . ?  
 O4 C10 C11 122.55(12) . . ?  
 O4 C10 C9 120.66(12) . . ?  
 C11 C10 C9 116.78(11) . . ?  
 C10 C11 H11A 109.5 . . ?  
 C10 C11 H11B 109.5 . . ?  
 H11A C11 H11B 109.5 . . ?



C10 C11 H11C 109.5 . . ?  
H11A C11 H11C 109.5 . . ?  
H11B C11 H11C 109.5 . . ?

loop\_  
\_geom\_torsion\_atom\_site\_label\_1  
\_geom\_torsion\_atom\_site\_label\_2  
\_geom\_torsion\_atom\_site\_label\_3  
\_geom\_torsion\_atom\_site\_label\_4  
\_geom\_torsion  
\_geom\_torsion\_site\_symmetry\_1  
\_geom\_torsion\_site\_symmetry\_2  
\_geom\_torsion\_site\_symmetry\_3  
\_geom\_torsion\_site\_symmetry\_4  
\_geom\_torsion\_publ\_flag  
O1 C2 C3 C4 106.19(14) . . . . ?  
C1 C2 C3 C4 -74.56(13) . . . . ?  
O1 C2 C3 C6 -15.71(16) . . . . ?  
C1 C2 C3 C6 163.54(11) . . . . ?  
C2 C3 C4 O2 -20.20(17) . . . . ?  
C6 C3 C4 O2 103.37(14) . . . . ?  
C2 C3 C4 C5 160.62(12) . . . . ?  
C6 C3 C4 C5 -75.80(14) . . . . ?  
C2 C3 C6 C9 -79.56(12) . . . . ?  
C4 C3 C6 C9 158.56(10) . . . . ?  
O3 C8 C9 C10 107.67(13) . . . . ?  
C7 C8 C9 C10 -72.17(14) . . . . ?  
O3 C8 C9 C6 -15.27(16) . . . . ?  
C7 C8 C9 C6 164.88(12) . . . . ?  
C3 C6 C9 C8 -70.39(13) . . . . ?  
C3 C6 C9 C10 168.12(10) . . . . ?  
C8 C9 C10 O4 -11.25(17) . . . . ?  
C6 C9 C10 O4 112.32(14) . . . . ?  
C8 C9 C10 C11 170.22(11) . . . . ?  
C6 C9 C10 C11 -66.21(14) . . . . ?

_diffraction_measured_fraction_theta_max	0.993
_diffraction_reflns_theta_full	33.7
_diffraction_measured_fraction_theta_full	0.993
_refinement_diff_density_max	0.29
_refinement_diff_density_min	-0.18
_refinement_diff_density_rms	0.047
# END OF CIF	

## 2-Methyl-3,5,5-Triacetyltetrahydropyran-2-ol

_audit_creation_method	SHELXL-97
_chemical_name_systematic	2-methyl-3,5,5-triacetyltetrahydropyran-2-ol
_chemical_name_common	?
_chemical_melting_point	not measured
_chemical_compound_source	'local laboratory'
_chemical_formula_moiety	'C <sub>12</sub> H <sub>18</sub> O <sub>5</sub> '
_chemical_formula_sum	'C <sub>12</sub> H <sub>18</sub> O <sub>5</sub> '
_chemical_formula_weight	242.26

loop\_

_atom_type_symbol	
_atom_type_description	
_atom_type_scatter_dispersion_real	
_atom_type_scatter_dispersion_imag	
_atom_type_scatter_source	
'C' 'C' 0.0033 0.0016	'International Tables Vol C Tables 4.2.6.8 and 6.1.1.4'
'H' 'H' 0.0000 0.0000	'International Tables Vol C Tables 4.2.6.8 and 6.1.1.4'
'O' 'O' 0.0106 0.0060	'International Tables Vol C Tables 4.2.6.8 and 6.1.1.4'

_symmetry_space_group_name_H-M	'P n'
_symmetry_cell_setting	'Monoclinic'

loop\_

_symmetry_equiv_pos_as_xyz	
	'x, y, z'
	'x+1/2, -y, z+1/2'

_cell_length_a	7.5981(4)
_cell_length_b	8.8133(5)
_cell_length_c	9.1692(4)
_cell_angle_alpha	90
_cell_angle_beta	91.260(4)
_cell_angle_gamma	90
_cell_volume	613.86(5)
_cell_formula_units_Z	2
_cell_measurement_temperature	120
_cell_measurement_reflns_used	1738
_cell_measurement_theta_min	2.5
_cell_measurement_theta_max	30.0

_exptl_crystal_description	lath
_exptl_crystal_colour	colorless

_exptl_crystal_size_max	0.46
_exptl_crystal_size_mid	0.07
_exptl_crystal_size_min	0.05
_exptl_crystal_density_meas.	?
_exptl_crystal_density_diffn	1.311
_exptl_crystal_density_method	'not measured'
_exptl_crystal_F_000	260
_exptl_absorpt_coefficient_mu	0.102
_exptl_absorpt_correction_type	none
_exptl_absorpt_correction_T_min	?
_exptl_absorpt_correction_T_max	?
_exptl_absorpt_process_details	?
_exptl_special_details	?
_diffn_ambient_temperature	120
_diffn_radiation_wavelength	0.71073
_diffn_radiation_type	MoK $\alpha$
_diffn_radiation_source	'fine-focus sealed tube'
_diffn_radiation_monochromator	graphite
_diffn_measurement_device	'KappaCCD (with Oxford Cryostream)'
_diffn_measurement_method	'\w scans with \k offsets'
_diffn_detector_area_resol_mean	?
_diffn_standards_number	0
_diffn_standards_interval_count	?
_diffn_standards_interval_time	?
_diffn_standards_decay_%	none
_diffn_reflns_number	6461
_diffn_reflns_av_R_equivalents	0.024
_diffn_reflns_av_signal/netI	0.0427
_diffn_reflns_limit_h_min	-10
_diffn_reflns_limit_h_max	10
_diffn_reflns_limit_k_min	-12
_diffn_reflns_limit_k_max	9
_diffn_reflns_limit_l_min	-12
_diffn_reflns_limit_l_max	12
_diffn_reflns_theta_min	3.2
_diffn_reflns_theta_max	30.0
_reflns_number_total	1796
_reflns_number_gt	1588
_reflns_threshold_expression	I>2\sigma(I)
_computing_data_collection	'COLLECT (Nonius, 2000)'
_computing_data_reduction	'Denzo and Scalepak (Otwinowski & Minor, 1997)'

```

_computing_cell_refinement 'Denzo and Scalepak (Otwinowski & Minor, 1997)'
_computing_structure_solution 'SIR97 (Altomare et al., 1999)'
_computing_structure_refinement 'SHELXL-97 (Sheldrick, 1997)'
_computing_molecular_graphics 'ORTEP-3 (Farrugia, 1997)'
_computing_publication_material 'SHELXL-97 (Sheldrick, 1997)'

```

```
_refine_special_details
```

```
;
```

Refinement of  $F^2$  against ALL reflections. The weighted R-factor  $wR$  and goodness of fit  $S$  are based on  $F^2$ , conventional R-factors  $R$  are based on  $F$ , with  $F$  set to zero for negative  $F^2$ . The threshold expression of  $F^2 > 2\sigma(F^2)$  is used only for calculating R-factors(gt) etc. and is not relevant to the choice of reflections for refinement. R-factors based on  $F^2$  are statistically about twice as large as those based on  $F$ , and R-factors based on ALL data will be even larger.

```

_refine_ls_structure_factor_coef      Fsqd
_refine_ls_matrix_type                full
_refine_ls_weighting_scheme           calc
_refine_ls_weighting_details
    'calc w=1/[\s^2*(Fo^2)+(0.0424P)^2+0.2367P] where P=(Fo^2+2Fc^2)/3'
_atom_sites_solution_primary          direct
_atom_sites_solution_secondary        difmap
_atom_sites_solution_hydrogens        geom
_refine_ls_hydrogen_treatment         mixed
_refine_ls_extinction_method          none
_refine_ls_extinction_coef            ?
_refine_ls_abs_structure_details      ?
_refine_ls_abs_structure_Flack        ?
_refine_ls_number_reflns              1796
_refine_ls_number_parameters          159
_refine_ls_number_restraints          2
_refine_ls_R_factor_all               0.058
_refine_ls_R_factor_gt               0.046
_refine_ls_wR_factor_ref              0.106
_refine_ls_wR_factor_gt              0.099
_refine_ls_goodness_of_fit_ref        1.074
_refine_ls_restrained_S_all           1.073
_refine_ls_shift/su_max               0.000
_refine_ls_shift/su_mean              0.000

```

```
loop_
```

```
_atom_site_label
```

```
_atom_site_type_symbol
```

\_atom\_site\_fract\_x  
 \_atom\_site\_fract\_y  
 \_atom\_site\_fract\_z  
 \_atom\_site\_U\_iso\_or\_equiv  
 \_atom\_site\_adp\_type  
 \_atom\_site\_occupancy  
 \_atom\_site\_symmetry\_multiplicity  
 \_atom\_site\_calc\_flag  
 \_atom\_site\_refinement\_flags  
 \_atom\_site\_disorder\_assembly  
 \_atom\_site\_disorder\_group  
 O1 O 0.1656(2) 0.2610(2) 0.24547(19) 0.0205(4) Uani 1 1 d . . .  
 O2 O 0.3818(2) 0.1034(2) 0.14888(19) 0.0211(4) Uani 1 1 d . . .  
 H2 H 0.3066 0.0561 0.0981 0.032 Uiso 1 1 calc R . .  
 O3 O 0.6059(3) 0.0523(3) 0.5097(3) 0.0368(5) Uani 1 1 d . . .  
 O4 O 0.3071(3) 0.5370(3) 0.5145(2) 0.0338(5) Uani 1 1 d . . .  
 O5 O 0.3491(3) 0.6508(3) 0.0520(2) 0.0379(5) Uani 1 1 d . . .  
 C1 C 0.3040(3) 0.1551(3) 0.2779(3) 0.0186(5) Uani 1 1 d . . .  
 C2 C 0.4495(3) 0.2361(3) 0.3707(2) 0.0163(4) Uani 1 1 d . . .  
 H2A H 0.3980 0.2597 0.4675 0.020 Uiso 1 1 calc R . .  
 C3 C 0.5066(3) 0.3870(3) 0.3041(3) 0.0176(5) Uani 1 1 d . . .  
 H3A H 0.5786 0.3668 0.2176 0.021 Uiso 1 1 calc R . .  
 H3B H 0.5807 0.4431 0.3761 0.021 Uiso 1 1 calc R . .  
 C4 C 0.3477(3) 0.4854(3) 0.2588(3) 0.0178(5) Uani 1 1 d . . .  
 C5 C 0.2215(3) 0.3897(3) 0.1647(3) 0.0200(5) Uani 1 1 d . . .  
 H5A H 0.1180 0.4514 0.1348 0.024 Uiso 1 1 calc R . .  
 H5B H 0.2814 0.3559 0.0756 0.024 Uiso 1 1 calc R . .  
 C6 C 0.2164(3) 0.0275(3) 0.3598(3) 0.0267(6) Uani 1 1 d . . .  
 H6A H 0.1299 -0.0228 0.2954 0.040 Uiso 1 1 calc R . .  
 H6B H 0.1571 0.0688 0.4449 0.040 Uiso 1 1 calc R . .  
 H6C H 0.3057 -0.0462 0.3921 0.040 Uiso 1 1 calc R . .  
 C7 C 0.6035(3) 0.1282(3) 0.3987(3) 0.0224(5) Uani 1 1 d . . .  
 C8 C 0.7479(4) 0.1169(3) 0.2907(3) 0.0279(6) Uani 1 1 d . . .  
 H8A H 0.8311 0.2007 0.3063 0.042 Uiso 1 1 calc R . .  
 H8B H 0.6975 0.1228 0.1916 0.042 Uiso 1 1 calc R . .  
 H8C H 0.8096 0.0200 0.3036 0.042 Uiso 1 1 calc R . .  
 C9 C 0.2494(3) 0.5486(3) 0.3917(3) 0.0218(5) Uani 1 1 d . . .  
 C10 C 0.0762(4) 0.6266(3) 0.3594(3) 0.0298(6) Uani 1 1 d . . .  
 H10A H -0.0185 0.5511 0.3565 0.045 Uiso 1 1 calc R . .  
 H10B H 0.0813 0.6782 0.2649 0.045 Uiso 1 1 calc R . .  
 H10C H 0.0533 0.7012 0.4360 0.045 Uiso 1 1 calc R . .  
 C11 C 0.4126(3) 0.6231(3) 0.1709(3) 0.0214(5) Uani 1 1 d . . .  
 C12 C 0.5579(4) 0.7183(3) 0.2368(4) 0.0331(6) Uani 1 1 d . . .  
 H12A H 0.6715 0.6693 0.2201 0.050 Uiso 1 1 calc R . .

H12B H 0.5405 0.7286 0.3419 0.050 Uiso 1 1 calc R . .  
H12C H 0.5566 0.8189 0.1914 0.050 Uiso 1 1 calc R . .

loop\_

\_atom\_site\_aniso\_label  
\_atom\_site\_aniso\_U\_11  
\_atom\_site\_aniso\_U\_22  
\_atom\_site\_aniso\_U\_33  
\_atom\_site\_aniso\_U\_23  
\_atom\_site\_aniso\_U\_13  
\_atom\_site\_aniso\_U\_12

O1 0.0143(8) 0.0194(9) 0.0276(9) 0.0027(7) -0.0032(7) 0.0005(7)  
O2 0.0183(8) 0.0215(9) 0.0234(8) -0.0068(7) -0.0040(7) -0.0019(7)  
O3 0.0276(10) 0.0362(12) 0.0462(12) 0.0207(10) -0.0100(9) 0.0012(9)  
O4 0.0340(11) 0.0405(12) 0.0267(10) -0.0064(9) -0.0020(8) 0.0043(10)  
O5 0.0432(13) 0.0379(12) 0.0321(10) 0.0165(9) -0.0105(9) -0.0081(10)  
C1 0.0142(10) 0.0175(12) 0.0239(12) 0.0010(9) -0.0019(9) -0.0006(9)  
C2 0.0152(11) 0.0155(11) 0.0181(11) 0.0000(9) -0.0032(8) 0.0003(9)  
C3 0.0177(10) 0.0150(11) 0.0200(11) 0.0019(9) -0.0021(9) -0.0010(9)  
C4 0.0172(10) 0.0164(11) 0.0198(11) 0.0001(9) -0.0021(8) 0.0010(9)  
C5 0.0173(10) 0.0192(12) 0.0232(11) 0.0023(9) -0.0048(9) 0.0006(10)  
C6 0.0193(12) 0.0227(13) 0.0381(15) 0.0054(11) 0.0002(10) -0.0044(10)  
C7 0.0194(11) 0.0163(11) 0.0311(13) -0.0007(10) -0.0089(10) -0.0029(9)  
C8 0.0175(11) 0.0250(13) 0.0410(16) -0.0078(12) -0.0031(11) 0.0047(10)  
C9 0.0231(12) 0.0182(12) 0.0241(12) -0.0003(9) 0.0032(9) -0.0040(10)  
C10 0.0234(13) 0.0282(14) 0.0379(15) 0.0000(12) 0.0046(11) 0.0039(11)  
C11 0.0238(12) 0.0165(11) 0.0239(12) 0.0023(10) 0.0013(9) 0.0014(10)  
C12 0.0338(14) 0.0238(14) 0.0415(16) 0.0062(13) -0.0026(12) -0.0044(12)

\_geom\_special\_details

All esds (except the esd in the dihedral angle between two l.s. planes) are estimated using the full covariance matrix. The cell esds are taken into account individually in the estimation of esds in distances, angles and torsion angles; correlations between esds in cell parameters are only used when they are defined by crystal symmetry. An approximate (isotropic) treatment of cell esds is used for estimating esds involving l.s. planes.

loop\_

\_geom\_bond\_atom\_site\_label\_1  
\_geom\_bond\_atom\_site\_label\_2  
\_geom\_bond\_distance  
\_geom\_bond\_site\_symmetry\_2  
\_geom\_bond\_publ\_flag

O1 C5 1.424(3) . ?  
 O1 C1 1.432(3) . ?  
 O2 C1 1.410(3) . ?  
 O2 H2 0.8400 . ?  
 O3 C7 1.217(3) . ?  
 O4 C9 1.204(3) . ?  
 O5 C11 1.207(3) . ?  
 C1 C6 1.515(4) . ?  
 C1 C2 1.554(3) . ?  
 C2 C7 1.525(3) . ?  
 C2 C3 1.530(3) . ?  
 C2 H2A 1.0000 . ?  
 C3 C4 1.536(3) . ?  
 C3 H3A 0.9900 . ?  
 C3 H3B 0.9900 . ?  
 C4 C5 1.529(3) . ?  
 C4 C11 1.543(3) . ?  
 C4 C9 1.547(4) . ?  
 C5 H5A 0.9900 . ?  
 C5 H5B 0.9900 . ?  
 C6 H6A 0.9800 . ?  
 C6 H6B 0.9800 . ?  
 C6 H6C 0.9800 . ?  
 C7 C8 1.498(4) . ?  
 C8 H8A 0.9800 . ?  
 C8 H8B 0.9800 . ?  
 C8 H8C 0.9800 . ?  
 C9 C10 1.508(4) . ?  
 C10 H10A 0.9800 . ?  
 C10 H10B 0.9800 . ?  
 C10 H10C 0.9800 . ?  
 C11 C12 1.503(4) . ?  
 C12 H12A 0.9800 . ?  
 C12 H12B 0.9800 . ?  
 C12 H12C 0.9800 . ?

loop\_  
 \_geom\_angle\_atom\_site\_label\_1  
 \_geom\_angle\_atom\_site\_label\_2  
 \_geom\_angle\_atom\_site\_label\_3  
 \_geom\_angle  
 \_geom\_angle\_site\_symmetry\_1  
 \_geom\_angle\_site\_symmetry\_3  
 \_geom\_angle\_publ\_flag

C5 O1 C1 113.62(18) . . ?  
 C1 O2 H2 109.5 . . ?  
 O2 C1 O1 110.82(19) . . ?  
 O2 C1 C6 111.9(2) . . ?  
 O1 C1 C6 105.0(2) . . ?  
 O2 C1 C2 107.56(19) . . ?  
 O1 C1 C2 108.98(19) . . ?  
 C6 C1 C2 112.6(2) . . ?  
 C7 C2 C3 112.73(19) . . ?  
 C7 C2 C1 109.87(19) . . ?  
 C3 C2 C1 112.65(18) . . ?  
 C7 C2 H2A 107.1 . . ?  
 C3 C2 H2A 107.1 . . ?  
 C1 C2 H2A 107.1 . . ?  
 C2 C3 C4 111.76(19) . . ?  
 C2 C3 H3A 109.3 . . ?  
 C4 C3 H3A 109.3 . . ?  
 C2 C3 H3B 109.3 . . ?  
 C4 C3 H3B 109.3 . . ?  
 H3A C3 H3B 107.9 . . ?  
 C5 C4 C3 108.7(2) . . ?  
 C5 C4 C11 110.1(2) . . ?  
 C3 C4 C11 109.1(2) . . ?  
 C5 C4 C9 109.6(2) . . ?  
 C3 C4 C9 112.36(19) . . ?  
 C11 C4 C9 107.1(2) . . ?  
 O1 C5 C4 109.7(2) . . ?  
 O1 C5 H5A 109.7 . . ?  
 C4 C5 H5A 109.7 . . ?  
 O1 C5 H5B 109.7 . . ?  
 C4 C5 H5B 109.7 . . ?  
 H5A C5 H5B 108.2 . . ?  
 C1 C6 H6A 109.5 . . ?  
 C1 C6 H6B 109.5 . . ?  
 H6A C6 H6B 109.5 . . ?  
 C1 C6 H6C 109.5 . . ?  
 H6A C6 H6C 109.5 . . ?  
 H6B C6 H6C 109.5 . . ?  
 O3 C7 C8 121.2(2) . . ?  
 O3 C7 C2 118.8(2) . . ?  
 C8 C7 C2 120.0(2) . . ?  
 C7 C8 H8A 109.5 . . ?  
 C7 C8 H8B 109.5 . . ?  
 H8A C8 H8B 109.5 . . ?



C7 C8 H8C 109.5 . . ?  
 H8A C8 H8C 109.5 . . ?  
 H8B C8 H8C 109.5 . . ?  
 O4 C9 C10 121.4(2) . . ?  
 O4 C9 C4 122.3(2) . . ?  
 C10 C9 C4 116.4(2) . . ?  
 C9 C10 H10A 109.5 . . ?  
 C9 C10 H10B 109.5 . . ?  
 H10A C10 H10B 109.5 . . ?  
 C9 C10 H10C 109.5 . . ?  
 H10A C10 H10C 109.5 . . ?  
 H10B C10 H10C 109.5 . . ?  
 O5 C11 C12 121.7(2) . . ?  
 O5 C11 C4 120.3(2) . . ?  
 C12 C11 C4 118.0(2) . . ?  
 C11 C12 H12A 109.5 . . ?  
 C11 C12 H12B 109.5 . . ?  
 H12A C12 H12B 109.5 . . ?  
 C11 C12 H12C 109.5 . . ?  
 H12A C12 H12C 109.5 . . ?  
 H12B C12 H12C 109.5 . . ?

loop\_  
 \_geom\_torsion\_atom\_site\_label\_1  
 \_geom\_torsion\_atom\_site\_label\_2  
 \_geom\_torsion\_atom\_site\_label\_3  
 \_geom\_torsion\_atom\_site\_label\_4  
 \_geom\_torsion  
 \_geom\_torsion\_site\_symmetry\_1  
 \_geom\_torsion\_site\_symmetry\_2  
 \_geom\_torsion\_site\_symmetry\_3  
 \_geom\_torsion\_site\_symmetry\_4  
 \_geom\_torsion\_publ\_flag  
 C5 O1 C1 O2 -57.8(3) . . . . ?  
 C5 O1 C1 C6 -178.7(2) . . . . ?  
 C5 O1 C1 C2 60.4(2) . . . . ?  
 O2 C1 C2 C7 -56.4(2) . . . . ?  
 O1 C1 C2 C7 -176.58(19) . . . . ?  
 C6 C1 C2 C7 67.4(3) . . . . ?  
 O2 C1 C2 C3 70.2(2) . . . . ?  
 O1 C1 C2 C3 -50.0(2) . . . . ?  
 C6 C1 C2 C3 -166.0(2) . . . . ?  
 C7 C2 C3 C4 172.71(19) . . . . ?  
 C1 C2 C3 C4 47.7(3) . . . . ?

C2 C3 C4 C5 -51.1(3) . . . . ?  
 C2 C3 C4 C11 -171.08(19) . . . . ?  
 C2 C3 C4 C9 70.4(3) . . . . ?  
 C1 O1 C5 C4 -66.7(2) . . . . ?  
 C3 C4 C5 O1 59.2(2) . . . . ?  
 C11 C4 C5 O1 178.63(19) . . . . ?  
 C9 C4 C5 O1 -63.9(2) . . . . ?  
 C3 C2 C7 O3 140.7(2) . . . . ?  
 C1 C2 C7 O3 -92.7(3) . . . . ?  
 C3 C2 C7 C8 -39.3(3) . . . . ?  
 C1 C2 C7 C8 87.2(3) . . . . ?  
 C5 C4 C9 O4 130.1(3) . . . . ?  
 C3 C4 C9 O4 9.1(3) . . . . ?  
 C11 C4 C9 O4 -110.6(3) . . . . ?  
 C5 C4 C9 C10 -50.1(3) . . . . ?  
 C3 C4 C9 C10 -171.0(2) . . . . ?  
 C11 C4 C9 C10 69.2(3) . . . . ?  
 C5 C4 C11 O5 7.7(3) . . . . ?  
 C3 C4 C11 O5 126.8(3) . . . . ?  
 C9 C4 C11 O5 -111.4(3) . . . . ?  
 C5 C4 C11 C12 -171.2(2) . . . . ?  
 C3 C4 C11 C12 -52.0(3) . . . . ?  
 C9 C4 C11 C12 69.8(3) . . . . ?

loop\_

\_geom\_hbond\_atom\_site\_label\_D  
 \_geom\_hbond\_atom\_site\_label\_H  
 \_geom\_hbond\_atom\_site\_label\_A  
 \_geom\_hbond\_distance\_DH  
 \_geom\_hbond\_distance\_HA  
 \_geom\_hbond\_distance\_DA  
 \_geom\_hbond\_angle\_DHA

\_geom\_hbond\_site\_symmetry\_A    O2 H2 O3   0.84 1.96 2.791(3) 170.1 2\_454

_diffraction_measured_fraction_theta_max	0.996
_diffraction_reflns_theta_full	30.0
_diffraction_measured_fraction_theta_full	0.996
_refinement_diff_density_max	0.45
_refinement_diff_density_min	-0.20
_refinement_diff_density_rms	0.051
# END OF CIF	

***p*-xylylenebis(3-(2,4-pentanedione))  
(*p*-XBAH<sub>2</sub>)**

_audit_creation_method	SHELXL-97
_chemical_name_systematic	1,4-bis-(2,2-diacetyethyl)-benzene
_chemical_name_common	<i>p</i> -xylylenebis(3-(2,4-pentanedione))
_chemical_melting_point	not measured
_chemical_compound_source	'local laboratory'
_chemical_formula_moiety	'C18 H22 O4'
_chemical_formula_sum	'C18 H22 O4'
_chemical_formula_weight	302.36
loop_	
_atom_type_symbol	
_atom_type_description	
_atom_type_scatter_dispersion_real	
_atom_type_scatter_dispersion_imag	
_atom_type_scatter_source	
'C' 'C' 0.0033 0.0016	'International Tables Vol C Tables 4.2.6.8 and 6.1.1.4'
'H' 'H' 0.0000 0.0000	'International Tables Vol C Tables 4.2.6.8 and 6.1.1.4'
'O' 'O' 0.0106 0.0060	'International Tables Vol C Tables 4.2.6.8 and 6.1.1.4'
_symmetry_space_group_name_H-M	'P 21/c'
_symmetry_cell_setting	'Monoclinic'
loop_	
_symmetry_equiv_pos_as_xyz	
	'x, y, z'
	'-x, y+1/2, -z+1/2'
	'-x, -y, -z'
	'x, -y-1/2, z-1/2'
_cell_length_a	13.796(6)
_cell_length_b	5.591(2)
_cell_length_c	10.819(4)
_cell_angle_alpha	90
_cell_angle_beta	107.890(15)
_cell_angle_gamma	90
_cell_volume	794.2(5)
_cell_formula_units_Z	2
_cell_measurement_temperature	100
_cell_measurement_reflns_used	2079
_cell_measurement_theta_min	2.5
_cell_measurement_theta_max	30.0
_exptl_crystal_description	lath

_exptl_crystal_colour	colorless
_exptl_crystal_size_max	0.47
_exptl_crystal_size_mid	0.22
_exptl_crystal_size_min	0.05
_exptl_crystal_density_meas	?
_exptl_crystal_density_diffn	1.264
_exptl_crystal_density_method	'not measured'
_exptl_crystal_F_000	324
_exptl_absorpt_coefficient_mu	0.088
_exptl_absorpt_correction_type	none
_exptl_absorpt_correction_T_min	?
_exptl_absorpt_correction_T_max	?
_exptl_absorpt_process_details	?
_exptl_special_details	?
_diffn_ambient_temperature	100
_diffn_radiation_wavelength	0.71073
_diffn_radiation_type	MoK $\alpha$
_diffn_radiation_source	'fine-focus sealed tube'
_diffn_radiation_monochromator	graphite
_diffn_measurement_device	'KappaCCD (with Oxford Cryostream)'
_diffn_measurement_method	'\w scans with \k offsets'
_diffn_detector_area_resol_mean	?
_diffn_standards_number	0
_diffn_standards_interval_count	?
_diffn_standards_interval_time	?
_diffn_standards_decay_%	<2
_diffn_reflns_number	7329
_diffn_reflns_av_R_equivalents	0.027
_diffn_reflns_av_sigmal/netl	0.0452
_diffn_reflns_limit_h_min	-19
_diffn_reflns_limit_h_max	19
_diffn_reflns_limit_k_min	-7
_diffn_reflns_limit_k_max	7
_diffn_reflns_limit_l_min	-15
_diffn_reflns_limit_l_max	15
_diffn_reflns_theta_min	3.1
_diffn_reflns_theta_max	30.0
_reflns_number_total	2298
_reflns_number_gt	1718
_reflns_threshold_expression	l>2\sigma(l)
_computing_data_collection	'COLLECT (Nonius, 2000)'
_computing_data_reduction	'Denzo and Scalepak (Otwinowski & Minor, 1997)'

_computing_cell_refinement	'Denzo and Scalepak (Otwinowski & Minor, 1997)'
_computing_structure_solution	'SIR97 (Altomare et al., 1999)'
_computing_structure_refinement	'SHELXL-97 (Sheldrick, 1997)'
_computing_molecular_graphics	'ORTEP-3 (Farrugia, 1997)'
_computing_publication_material	'SHELXL-97 (Sheldrick, 1997)'

\_refine\_special\_details

Refinement of  $F^2$  against ALL reflections. The weighted R-factor wR and goodness of fit S are based on  $F^2$ , conventional R-factors R are based on F, with F set to zero for negative  $F^2$ . The threshold expression of  $F^2 > 2\sigma(F^2)$  is used only for calculating R-factors(gt) etc. and is not relevant to the choice of reflections for refinement. R-factors based on  $F^2$  are statistically about twice as large as those based on F, and R-factors based on ALL data will be even larger.

_refine_ls_structure_factor_coef	Fsqd
_refine_ls_matrix_type	full
_refine_ls_weighting_scheme	calc
_refine_ls_weighting_details	'calc w=1/[\sigma^2(Fo^2)+(0.0514P)^2+0.2199P] where P=(Fo^2+2Fc^2)/3'
_atom_sites_solution_primary	direct
_atom_sites_solution_secondary	difmap
_atom_sites_solution_hydrogens	geom
_refine_ls_hydrogen_treatment	constr
_refine_ls_extinction_method	none
_refine_ls_extinction_coef	?
_refine_ls_number_reflns	2298
_refine_ls_number_parameters	102
_refine_ls_number_restraints	0
_refine_ls_R_factor_all	0.065
_refine_ls_R_factor_gt	0.045
_refine_ls_wR_factor_ref	0.118
_refine_ls_wR_factor_gt	0.109
_refine_ls_goodness_of_fit_ref	1.045
_refine_ls_restrained_S_all	1.045
_refine_ls_shift/su_max	0.005
_refine_ls_shift/su_mean	0.000

loop\_

_atom_site_label
_atom_site_type_symbol
_atom_site_fract_x
_atom_site_fract_y

\_atom\_site\_fract\_z  
 \_atom\_site\_U\_iso\_or\_equiv  
 \_atom\_site\_adp\_type  
 \_atom\_site\_occupancy  
 \_atom\_site\_symmetry\_multiplicity  
 \_atom\_site\_calc\_flag  
 \_atom\_site\_refinement\_flags  
 \_atom\_site\_disorder\_assembly  
 \_atom\_site\_disorder\_group  
 O1 O 0.19301(8) 0.21842(15) 0.49780(9) 0.0268(2) Uani 1 1 d . . .  
 O2 O 0.14022(7) 0.72009(15) 0.62567(9) 0.0220(2) Uani 1 1 d . . .  
 C1 C 0.41895(9) 0.5841(2) 0.54249(12) 0.0180(3) Uani 1 1 d . . .  
 C2 C 0.46931(9) 0.3716(2) 0.59078(12) 0.0203(3) Uani 1 1 d . . .  
 H2 H 0.4489 0.2820 0.6532 0.024 Uiso 1 1 calc R . .  
 C3 C 0.45102(9) 0.7111(2) 0.45111(12) 0.0203(3) Uani 1 1 d . . .  
 H3 H 0.4179 0.8565 0.4169 0.024 Uiso 1 1 calc R . .  
 C4 C 0.32777(9) 0.6664(2) 0.58101(12) 0.0197(3) Uani 1 1 d . . .  
 H4A H 0.3358 0.8380 0.6047 0.024 Uiso 1 1 calc R . .  
 H4B H 0.3249 0.5758 0.6584 0.024 Uiso 1 1 calc R . .  
 C5 C 0.22725(9) 0.6304(2) 0.47058(11) 0.0156(2) Uani 1 1 d . . .  
 H5 H 0.2287 0.7302 0.3945 0.019 Uiso 1 1 calc R . .  
 C6 C 0.21604(9) 0.3657(2) 0.42961(11) 0.0163(2) Uani 1 1 d . . .  
 C7 C 0.23631(11) 0.3002(2) 0.30613(13) 0.0231(3) Uani 1 1 d . . .  
 H7A H 0.2228 0.1293 0.2888 0.035 Uiso 1 1 calc R . .  
 H7B H 0.3076 0.3344 0.3140 0.035 Uiso 1 1 calc R . .  
 H7C H 0.1918 0.3938 0.2344 0.035 Uiso 1 1 calc R . .  
 C8 C 0.13498(9) 0.70188(19) 0.51202(12) 0.0166(2) Uani 1 1 d . . .  
 C9 C 0.03783(10) 0.7417(2) 0.40415(13) 0.0239(3) Uani 1 1 d . . .  
 H9A H -0.0169 0.7806 0.4409 0.036 Uiso 1 1 calc R . .  
 H9B H 0.0200 0.5961 0.3516 0.036 Uiso 1 1 calc R . .  
 H9C H 0.0469 0.8743 0.3495 0.036 Uiso 1 1 calc R . .

loop\_

\_atom\_site\_aniso\_label  
 \_atom\_site\_aniso\_U\_11  
 \_atom\_site\_aniso\_U\_22  
 \_atom\_site\_aniso\_U\_33  
 \_atom\_site\_aniso\_U\_23  
 \_atom\_site\_aniso\_U\_13  
 \_atom\_site\_aniso\_U\_12  
 O1 0.0427(6) 0.0175(4) 0.0254(5) 0.0010(3) 0.0180(4) -0.0027(4)  
 O2 0.0263(5) 0.0207(4) 0.0212(5) -0.0019(3) 0.0106(4) 0.0001(4)  
 C1 0.0146(6) 0.0196(5) 0.0181(6) -0.0035(4) 0.0025(4) -0.0026(4)  
 C2 0.0187(6) 0.0219(6) 0.0195(6) 0.0022(5) 0.0050(5) -0.0036(5)

C3 0.0186(6) 0.0175(5) 0.0229(6) 0.0013(5) 0.0038(5) 0.0002(4)  
 C4 0.0183(6) 0.0227(6) 0.0178(6) -0.0044(5) 0.0051(5) -0.0004(5)  
 C5 0.0176(6) 0.0145(5) 0.0152(6) -0.0002(4) 0.0058(4) -0.0002(4)  
 C6 0.0155(6) 0.0159(5) 0.0160(6) -0.0005(4) 0.0026(4) 0.0008(4)  
 C7 0.0319(7) 0.0194(6) 0.0194(6) -0.0030(5) 0.0102(5) -0.0019(5)  
 C8 0.0184(6) 0.0119(5) 0.0206(6) -0.0007(4) 0.0074(5) -0.0009(4)  
 C9 0.0185(6) 0.0271(6) 0.0252(7) -0.0010(5) 0.0052(5) 0.0007(5)

#### \_geom\_special\_details

All esds (except the esd in the dihedral angle between two l.s. planes) are estimated using the full covariance matrix. The cell esds are taken into account individually in the estimation of esds in distances, angles and torsion angles; correlations between esds in cell parameters are only used when they are defined by crystal symmetry. An approximate (isotropic) treatment of cell esds is used for estimating esds involving l.s. planes.

loop\_  
 \_geom\_bond\_atom\_site\_label\_1  
 \_geom\_bond\_atom\_site\_label\_2  
 \_geom\_bond\_distance  
 \_geom\_bond\_site\_symmetry\_2  
 \_geom\_bond\_publ\_flag  
 O1 C6 1.2112(15) . ?  
 O2 C8 1.2136(15) . ?  
 C1 C2 1.3946(18) . ?  
 C1 C3 1.3948(17) . ?  
 C1 C4 1.5133(17) . ?  
 C2 C3 1.3905(18) 3\_666 ?  
 C2 H2 0.9500 . ?  
 C3 C2 1.3904(18) 3\_666 ?  
 C3 H3 0.9500 . ?  
 C4 C5 1.5405(18) . ?  
 C4 H4A 0.9900 . ?  
 C4 H4B 0.9900 . ?  
 C5 C8 1.5270(17) . ?  
 C5 C6 1.5394(16) . ?  
 C5 H5 1.0000 . ?  
 C6 C7 1.4922(18) . ?  
 C7 H7A 0.9800 . ?  
 C7 H7B 0.9800 . ?  
 C7 H7C 0.9800 . ?  
 C8 C9 1.4989(18) . ?  
 C9 H9A 0.9800 . ?

C9 H9B 0.9800 . ?

C9 H9C 0.9800 . ?

loop\_

\_geom\_angle\_atom\_site\_label\_1

\_geom\_angle\_atom\_site\_label\_2

\_geom\_angle\_atom\_site\_label\_3

\_geom\_angle

\_geom\_angle\_site\_symmetry\_1

\_geom\_angle\_site\_symmetry\_3

\_geom\_angle\_publ\_flag

C2 C1 C3 117.98(11) . . ?

C2 C1 C4 121.10(11) . . ?

C3 C1 C4 120.79(11) . . ?

C3 C2 C1 120.93(11) 3\_666 . ?

C3 C2 H2 119.5 3\_666 . ?

C1 C2 H2 119.5 . . ?

C2 C3 C1 121.09(11) 3\_666 . ?

C2 C3 H3 119.5 3\_666 . ?

C1 C3 H3 119.5 . . ?

C1 C4 C5 111.91(10) . . ?

C1 C4 H4A 109.2 . . ?

C5 C4 H4A 109.2 . . ?

C1 C4 H4B 109.2 . . ?

C5 C4 H4B 109.2 . . ?

H4A C4 H4B 107.9 . . ?

C8 C5 C6 108.48(10) . . ?

C8 C5 C4 111.79(10) . . ?

C6 C5 C4 109.62(9) . . ?

C8 C5 H5 109.0 . . ?

C6 C5 H5 109.0 . . ?

C4 C5 H5 109.0 . . ?

O1 C6 C7 122.34(11) . . ?

O1 C6 C5 120.02(11) . . ?

C7 C6 C5 117.64(10) . . ?

C6 C7 H7A 109.5 . . ?

C6 C7 H7B 109.5 . . ?

H7A C7 H7B 109.5 . . ?

C6 C7 H7C 109.5 . . ?

H7A C7 H7C 109.5 . . ?

H7B C7 H7C 109.5 . . ?

O2 C8 C9 122.49(11) . . ?

O2 C8 C5 121.59(11) . . ?

C9 C8 C5 115.90(11) . . ?



C8 C9 H9A 109.5 . . ?  
 C8 C9 H9B 109.5 . . ?  
 H9A C9 H9B 109.5 . . ?  
 C8 C9 H9C 109.5 . . ?  
 H9A C9 H9C 109.5 . . ?  
 H9B C9 H9C 109.5 . . ?

loop\_

\_geom\_torsion\_atom\_site\_label\_1  
 \_geom\_torsion\_atom\_site\_label\_2  
 \_geom\_torsion\_atom\_site\_label\_3  
 \_geom\_torsion\_atom\_site\_label\_4  
 \_geom\_torsion  
 \_geom\_torsion\_site\_symmetry\_1  
 \_geom\_torsion\_site\_symmetry\_2  
 \_geom\_torsion\_site\_symmetry\_3  
 \_geom\_torsion\_site\_symmetry\_4  
 \_geom\_torsion\_publ\_flag  
 C3 C1 C2 C3 -0.1(2) . . . 3\_666 ?  
 C4 C1 C2 C3 175.91(11) . . . 3\_666 ?  
 C2 C1 C3 C2 0.1(2) . . . 3\_666 ?  
 C4 C1 C3 C2 -175.92(11) . . . 3\_666 ?  
 C2 C1 C4 C5 -105.53(13) . . . . ?  
 C3 C1 C4 C5 70.33(15) . . . . ?  
 C1 C4 C5 C8 177.13(10) . . . . ?  
 C1 C4 C5 C6 56.80(13) . . . . ?  
 C8 C5 C6 O1 -47.21(15) . . . . ?  
 C4 C5 C6 O1 75.11(15) . . . . ?  
 C8 C5 C6 C7 133.89(11) . . . . ?  
 C4 C5 C6 C7 -103.80(12) . . . . ?  
 C6 C5 C8 O2 102.57(12) . . . . ?  
 C4 C5 C8 O2 -18.42(15) . . . . ?  
 C6 C5 C8 C9 -75.98(12) . . . . ?  
 C4 C5 C8 C9 163.02(10) . . . . ?

_diffn_measured_fraction_theta_max	0.997
_diffn_reflns_theta_full	30.0
_diffn_measured_fraction_theta_full	0.997
_refine_diff_density_max	0.30
_refine_diff_density_min	-0.24
_refine_diff_density_rms	0.049
# END OF CIF	

# **Cu<sub>2</sub>(NBA)<sub>2</sub> · (1,4-dithiane)**

_audit_creation_method	SHELXL-97
_chemical_name_systematic	?
_chemical_name_common	Cu <sub>2</sub> (NBA) <sub>2</sub> · (1,4-dithiane)
_chemical_melting_point	'not measured'
_chemical_compound_source	local laboratory
_chemical_formula_moiety	'C <sub>48</sub> H <sub>52</sub> Cu <sub>2</sub> O <sub>8</sub> S <sub>2</sub> '
_chemical_formula_sum	'C <sub>48</sub> H <sub>52</sub> Cu <sub>2</sub> O <sub>8</sub> S <sub>2</sub> '
_chemical_formula_weight	948.10

loop_	
_atom_type_symbol	
_atom_type_description	
_atom_type_scatter_dispersion_real	
_atom_type_scatter_dispersion_imag	
_atom_type_scatter_source	
'C' 'C' 0.0033 0.0016	'International Tables Vol C Tables 4.2.6.8 and 6.1.1.4'
'H' 'H' 0.0000 0.0000	'International Tables Vol C Tables 4.2.6.8 and 6.1.1.4'
'O' 'O' 0.0106 0.0060	'International Tables Vol C Tables 4.2.6.8 and 6.1.1.4'
'Cu' 'Cu' 0.3201 1.2651	'International Tables Vol C Tables 4.2.6.8 and 6.1.1.4'
'S' 'S' 0.1246 0.1234	'International Tables Vol C Tables 4.2.6.8 and 6.1.1.4'

_symmetry_space_group_name_H-M	'P 21/c
_symmetry_cell_setting	'Monoclinic'

loop_	
_symmetry_equiv_pos_as_xyz	
	'x, y, z'
	'-x, y+1/2, -z+1/2'
	'-x, -y, -z'
	'x, -y-1/2, z-1/2'

_cell_length_a	7.7580(4)
_cell_length_b	28.9810(14)
_cell_length_c	9.6400(5)
_cell_angle_alpha	90
_cell_angle_beta	97.848(3)
_cell_angle_gamma	90
_cell_volume	2147.10(19)
_cell_formula_units_Z	2
_cell_measurement_temperature	120
_cell_measurement_reflns_used	29394
_cell_measurement_theta_min	2.5

_cell_measurement_theta_max	25.0
_exptl_crystal_description	prism
_exptl_crystal_colour	turquoise
_exptl_crystal_size_max	0.15
_exptl_crystal_size_mid	0.08
_exptl_crystal_size_min	0.07
_exptl_crystal_density_meas	?
_exptl_crystal_density_diffn	1.466
_exptl_crystal_density_method	'not measured'
_exptl_crystal_F_000	988
_exptl_absorpt_coefficient_mu	1.143
_exptl_absorpt_correction_type	'multi-scan'
_exptl_absorpt_correction_T_min	0.778
_exptl_absorpt_correction_T_max	0.924
_exptl_absorpt_process_details	'HKL Scalepack (Otwinowski & Minor 1997)'
_exptl_special_details	?
_diffn_ambient_temperature	120
_diffn_radiation_wavelength	0.71073
_diffn_radiation_type	MoK $\alpha$
_diffn_radiation_source	'fine-focus sealed tube'
_diffn_radiation_monochromator	graphite
_diffn_measurement_device_type	'KappaCCD (with Oxford Cryostream)'
_diffn_measurement_method	'\w scans with \k offsets'
_diffn_detector_area_resol_mean	?
_diffn_standards_number	?
_diffn_standards_interval_count	?
_diffn_standards_interval_time	?
_diffn_standards_decay_%	?
_diffn_reflns_number	29394
_diffn_reflns_av_R_equivalents	0.049
_diffn_reflns_av_sigmaI/netI	0.103
_diffn_reflns_limit_h_min	-9
_diffn_reflns_limit_h_max	8
_diffn_reflns_limit_k_min	-33
_diffn_reflns_limit_k_max	32
_diffn_reflns_limit_l_min	-11
_diffn_reflns_limit_l_max	11
_diffn_reflns_theta_min	2.6
_diffn_reflns_theta_max	25.0
_reflns_number_total	3418
_reflns_number_gt	1999

<code>_reflns_threshold_expression</code>	<code>&gt;2sigma(I)</code>
<code>_computing_data_collection</code>	<code>'KappaCCD'</code>
<code>_computing_cell_refinement</code>	<code>'HKL Scalepack (Otwinowski &amp; Minor 1997)'</code>
<code>_computing_data_reduction</code>	<code>'HKL Denzo and Scalepack (Otwinowski &amp; Minor 1997)'</code>
<code>_computing_structure_solution</code>	<code>'SIR92 (Altomare et al., 1994)'</code>
<code>_computing_structure_refinement</code>	<code>'SHELXL-97 (Sheldrick, 1997)'</code>
<code>_computing_molecular_graphics</code>	<code>?</code>
<code>_computing_publication_material</code>	<code>'SHELXL-97 (Sheldrick, 1997)'</code>

#### `_refine_special_details`

Refinement of  $F^2$  against ALL reflections. The weighted R-factor  $wR$  and goodness of fit  $S$  are based on  $F^2$ , conventional R-factors  $R$  are based on  $F$ , with  $F$  set to zero for negative  $F^2$ . The threshold expression of  $F^2 > 2\sigma(F^2)$  is used only for calculating R-factors(gt) etc. and is not relevant to the choice of reflections for refinement. R-factors based on  $F^2$  are statistically about twice as large as those based on  $F$ , and R-factors based on ALL data will be even larger.

<code>_refine_ls_structure_factor_coef</code>	<code>Fsqd</code>
<code>_refine_ls_matrix_type</code>	<code>full</code>
<code>_refine_ls_weighting_scheme</code>	<code>calc</code>
<code>_refine_ls_weighting_details</code>	<code>'calc w=1/[s^2(Fo^2)+(0.0358P)^2]' where P=(Fo^2+2Fc^2)/3'</code>
<code>_atom_sites_solution_primary</code>	<code>direct</code>
<code>_atom_sites_solution_secondary</code>	<code>difmap</code>
<code>_atom_sites_solution_hydrogens</code>	<code>geom</code>
<code>_refine_ls_hydrogen_treatment</code>	<code>constr</code>
<code>_refine_ls_extinction_method</code>	<code>none</code>
<code>_refine_ls_extinction_coef</code>	<code>?</code>
<code>_refine_ls_number_reflns</code>	<code>3418</code>
<code>_refine_ls_number_parameters</code>	<code>275</code>
<code>_refine_ls_number_restraints</code>	<code>0</code>
<code>_refine_ls_R_factor_all</code>	<code>0.082</code>
<code>_refine_ls_R_factor_gt</code>	<code>0.038</code>
<code>_refine_ls_wR_factor_ref</code>	<code>0.086</code>
<code>_refine_ls_wR_factor_gt</code>	<code>0.078</code>
<code>_refine_ls_goodness_of_fit_ref</code>	<code>0.883</code>
<code>_refine_ls_restrained_S_all</code>	<code>0.883</code>
<code>_refine_ls_shift/su_max</code>	<code>0.001</code>
<code>_refine_ls_shift/su_mean</code>	<code>0.000</code>

```

loop_
  _atom_site_label
  _atom_site_type_symbol
  _atom_site_fract_x
  _atom_site_fract_y
  _atom_site_fract_z
  _atom_site_U_iso_or_equiv
  _atom_site_adp_type
  _atom_site_occupancy
  _atom_site_symmetry_multiplicity
  _atom_site_calc_flag
  _atom_site_refinement_flags
  _atom_site_disorder_assembly
  _atom_site_disorder_group
Cu1 Cu 0.88337(6) 0.458966(15) 0.80517(5) 0.02939(16) Uani 1 1 d . . .
S1 S 0.66505(12) 0.46085(3) 0.54758(10) 0.0331(3) Uani 1 1 d . . .
O1 O 1.0347(3) 0.50850(8) 0.7737(2) 0.0290(6) Uani 1 1 d . . .
O2 O 0.7427(3) 0.49798(8) 0.9033(2) 0.0291(6) Uani 1 1 d . . .
O3 O 0.2550(3) 0.59178(8) 0.1455(2) 0.0300(6) Uani 1 1 d . . .
O4 O -0.0323(3) 0.58236(8) 0.2801(2) 0.0291(6) Uani 1 1 d . . .
C1 C 1.1720(4) 0.58089(13) 0.7810(4) 0.0356(10) Uani 1 1 d . . .
H1A H 1.2465 0.5895 0.8676 0.053 Uiso 1 1 calc R . .
H1B H 1.1232 0.6088 0.7336 0.053 Uiso 1 1 calc R . .
H1C H 1.2411 0.5642 0.7194 0.053 Uiso 1 1 calc R . .
C2 C 1.0269(5) 0.55050(12) 0.8153(4) 0.0289(9) Uani 1 1 d . . .
C3 C 0.8971(4) 0.56851(12) 0.8897(4) 0.0280(9) Uani 1 1 d . . .
C4 C 0.7629(4) 0.54102(13) 0.9297(4) 0.0285(9) Uani 1 1 d . . .
C5 C 0.6320(4) 0.56102(12) 1.0147(4) 0.0340(10) Uani 1 1 d . . .
H5A H 0.5341 0.5396 1.0141 0.051 Uiso 1 1 calc R . .
H5B H 0.5897 0.5906 0.9740 0.051 Uiso 1 1 calc R . .
H5C H 0.6871 0.5659 1.1112 0.051 Uiso 1 1 calc R . .
C6 C 0.9059(4) 0.61985(11) 0.9282(4) 0.0293(9) Uani 1 1 d . . .
H6A H 0.8458 0.6243 1.0114 0.035 Uiso 1 1 calc R . .
H6B H 1.0296 0.6282 0.9556 0.035 Uiso 1 1 calc R . .
C7 C 0.3945(5) 0.66348(12) 0.1506(4) 0.0393(10) Uani 1 1 d . . .
H7A H 0.5020 0.6625 0.2171 0.059 Uiso 1 1 calc R . .
H7B H 0.3499 0.6951 0.1435 0.059 Uiso 1 1 calc R . .
H7C H 0.4187 0.6531 0.0585 0.059 Uiso 1 1 calc R . .
C8 C 0.2612(4) 0.63233(13) 0.2010(4) 0.0296(9) Uani 1 1 d . . .
C9 C 0.1539(4) 0.64831(12) 0.2977(4) 0.0257(9) Uani 1 1 d . . .
C10 C 0.0089(4) 0.62301(13) 0.3266(4) 0.0294(9) Uani 1 1 d . . .
C11 C -0.1178(5) 0.64297(13) 0.4144(4) 0.0398(10) Uani 1 1 d . . .
H11A H -0.2097 0.6204 0.4234 0.060 Uiso 1 1 calc R . .
H11B H -0.1695 0.6710 0.3699 0.060 Uiso 1 1 calc R . .

```

H11C H -0.0570 0.6505 0.5076 0.060 Uiso 1 1 calc R . .  
 C12 C 0.1908(4) 0.69621(12) 0.3596(4) 0.0317(9) Uani 1 1 d . . .  
 H12A H 0.1820 0.7187 0.2817 0.038 Uiso 1 1 calc R . .  
 H12B H 0.0985 0.7039 0.4173 0.038 Uiso 1 1 calc R . .  
 C13 C 0.8278(4) 0.65323(12) 0.8151(4) 0.0282(9) Uani 1 1 d . . .  
 C14 C 0.9166(5) 0.69515(11) 0.7956(4) 0.0317(9) Uani 1 1 d . . .  
 H14 H 1.0252 0.7011 0.8511 0.038 Uiso 1 1 calc R . .  
 C15 C 0.8490(5) 0.72711(12) 0.6989(4) 0.0324(9) Uani 1 1 d . . .  
 H15 H 0.9119 0.7547 0.6881 0.039 Uiso 1 1 calc R . .  
 C16 C 0.6881(4) 0.71991(12) 0.6148(4) 0.0285(9) Uani 1 1 d . . .  
 C17 C 0.6175(4) 0.75160(12) 0.5128(4) 0.0305(9) Uani 1 1 d . . .  
 H17 H 0.6788 0.7793 0.4998 0.037 Uiso 1 1 calc R . .  
 C18 C 0.4621(5) 0.74330(12) 0.4318(4) 0.0323(9) Uani 1 1 d . . .  
 H18 H 0.4176 0.7652 0.3626 0.039 Uiso 1 1 calc R . .  
 C19 C 0.3664(4) 0.70273(12) 0.4493(4) 0.0288(9) Uani 1 1 d . . .  
 C20 C 0.4350(4) 0.67094(12) 0.5462(4) 0.0285(9) Uani 1 1 d . . .  
 H20 H 0.3729 0.6432 0.5565 0.034 Uiso 1 1 calc R . .  
 C21 C 0.5968(4) 0.67833(12) 0.6320(4) 0.0271(9) Uani 1 1 d . . .  
 C22 C 0.6716(4) 0.64566(12) 0.7320(4) 0.0303(9) Uani 1 1 d . . .  
 H22 H 0.6117 0.6175 0.7420 0.036 Uiso 1 1 calc R . .  
 C23 C 0.4616(5) 0.46546(13) 0.6187(4) 0.0360(10) Uani 1 1 d . . .  
 H23A H 0.4343 0.4351 0.6577 0.043 Uiso 1 1 calc R . .  
 H23B H 0.4763 0.4879 0.6968 0.043 Uiso 1 1 calc R . .  
 C24 C 0.6918(5) 0.51949(12) 0.4876(4) 0.0369(10) Uani 1 1 d . . .  
 H24A H 0.7030 0.5407 0.5688 0.044 Uiso 1 1 calc R . .  
 H24B H 0.8002 0.5215 0.4444 0.044 Uiso 1 1 calc R . .

loop\_

\_atom\_site\_aniso\_label  
 \_atom\_site\_aniso\_U\_11  
 \_atom\_site\_aniso\_U\_22  
 \_atom\_site\_aniso\_U\_33  
 \_atom\_site\_aniso\_U\_23  
 \_atom\_site\_aniso\_U\_13  
 \_atom\_site\_aniso\_U\_12  
 Cu1 0.0288(3) 0.0309(3) 0.0285(3) -0.0009(2) 0.00385(19) -0.0002(2)  
 S1 0.0315(6) 0.0372(6) 0.0301(6) 0.0026(5) 0.0023(4) 0.0030(5)  
 O1 0.0273(14) 0.0293(15) 0.0310(16) -0.0013(12) 0.0069(11) -0.0012(11)  
 O2 0.0309(15) 0.0271(15) 0.0299(16) -0.0040(13) 0.0066(12) -0.0005(11)  
 O3 0.0332(15) 0.0310(15) 0.0260(16) -0.0006(12) 0.0053(12) -0.0016(12)  
 O4 0.0316(14) 0.0269(14) 0.0281(15) -0.0017(13) 0.0008(12) 0.0012(12)  
 C1 0.036(2) 0.038(2) 0.034(2) -0.004(2) 0.0103(19) -0.0012(19)  
 C2 0.026(2) 0.036(2) 0.022(2) 0.0004(19) -0.0056(17) 0.0000(18)  
 C3 0.025(2) 0.033(2) 0.025(2) -0.0008(19) 0.0019(17) 0.0034(18)

C4 0.030(2) 0.034(2) 0.019(2) -0.001(2) -0.0028(16) 0.003(2)  
 C5 0.030(2) 0.036(2) 0.036(2) -0.001(2) 0.0068(19) 0.0006(18)  
 C6 0.030(2) 0.031(2) 0.026(2) -0.0024(19) 0.0003(17) -0.0019(17)  
 C7 0.044(3) 0.034(2) 0.041(3) 0.001(2) 0.011(2) -0.0044(19)  
 C8 0.031(2) 0.033(2) 0.023(2) 0.0065(19) -0.0048(18) -0.0018(18)  
 C9 0.022(2) 0.026(2) 0.027(2) 0.0027(18) -0.0013(17) 0.0017(17)  
 C10 0.030(2) 0.038(2) 0.018(2) 0.0033(19) -0.0032(17) 0.0090(19)  
 C11 0.037(2) 0.041(2) 0.043(3) -0.002(2) 0.010(2) -0.004(2)  
 C12 0.032(2) 0.029(2) 0.034(2) 0.0004(19) 0.0032(18) 0.0052(17)  
 C13 0.030(2) 0.030(2) 0.025(2) -0.0041(19) 0.0009(18) -0.0011(18)  
 C14 0.036(2) 0.026(2) 0.031(2) -0.005(2) -0.0021(19) -0.0062(19)  
 C15 0.038(2) 0.027(2) 0.032(2) -0.005(2) 0.0036(19) -0.0063(18)  
 C16 0.027(2) 0.032(2) 0.025(2) 0.0009(19) 0.0014(18) 0.0016(19)  
 C17 0.031(2) 0.027(2) 0.034(2) 0.001(2) 0.0080(19) -0.0059(18)  
 C18 0.036(2) 0.031(2) 0.029(2) 0.0053(19) 0.0024(19) 0.0044(19)  
 C19 0.030(2) 0.030(2) 0.026(2) -0.0034(19) 0.0029(18) 0.0016(18)  
 C20 0.031(2) 0.024(2) 0.030(2) -0.0018(19) 0.0058(19) -0.0033(17)  
 C21 0.031(2) 0.024(2) 0.025(2) -0.0039(18) 0.0016(18) 0.0025(17)  
 C22 0.038(2) 0.024(2) 0.029(2) -0.0019(19) 0.0058(19) -0.0057(18)  
 C23 0.033(2) 0.043(2) 0.032(2) 0.008(2) 0.0045(18) -0.005(2)  
 C24 0.035(2) 0.043(2) 0.033(2) 0.001(2) 0.0058(19) -0.0076(19)

\_geom\_special\_details

;

All esds (except the esd in the dihedral angle between two l.s. planes)  
 are estimated using the full covariance matrix. The cell esds are taken  
 into account individually in the estimation of esds in distances, angles  
 and torsion angles; correlations between esds in cell parameters are only  
 used when they are defined by crystal symmetry. An approximate (isotropic)  
 treatment of cell esds is used for estimating esds involving l.s. planes.

;

loop\_

\_geom\_bond\_atom\_site\_label\_1

\_geom\_bond\_atom\_site\_label\_2

\_geom\_bond\_distance

\_geom\_bond\_site\_symmetry\_2

\_geom\_bond\_publ\_flag

Cu1 O1 1.905(2) . ?

Cu1 O2 1.910(2) . ?

Cu1 O3 1.918(2) 3\_666 ?

Cu1 O4 1.925(2) 3\_666 ?

Cu1 S1 2.8088(10) . ?

S1 C23 1.809(4) . ?

S1 C24 1.816(4) . ?  
 O1 C2 1.286(4) . ?  
 O2 C4 1.278(4) . ?  
 O3 C8 1.289(4) . ?  
 O3 Cu1 1.918(2) 3\_666 ?  
 O4 C10 1.285(4) . ?  
 O4 Cu1 1.925(2) 3\_666 ?  
 C1 C2 1.502(5) . ?  
 C1 H1A 0.9800 . ?  
 C1 H1B 0.9800 . ?  
 C1 H1C 0.9800 . ?  
 C2 C3 1.413(5) . ?  
 C3 C4 1.406(5) . ?  
 C3 C6 1.533(5) . ?  
 C4 C5 1.505(4) . ?  
 C5 H5A 0.9800 . ?  
 C5 H5B 0.9800 . ?  
 C5 H5C 0.9800 . ?  
 C6 C13 1.520(5) . ?  
 C6 H6A 0.9900 . ?  
 C6 H6B 0.9900 . ?  
 C7 C8 1.502(5) . ?  
 C7 H7A 0.9800 . ?  
 C7 H7B 0.9800 . ?  
 C7 H7C 0.9800 . ?  
 C8 C9 1.410(5) . ?  
 C9 C10 1.402(5) . ?  
 C9 C12 1.523(5) . ?  
 C10 C11 1.499(5) . ?  
 C11 H11A 0.9800 . ?  
 C11 H11B 0.9800 . ?  
 C11 H11C 0.9800 . ?  
 C12 C19 1.522(5) . ?  
 C12 H12A 0.9900 . ?  
 C12 H12B 0.9900 . ?  
 C13 C22 1.376(5) . ?  
 C13 C14 1.422(5) . ?  
 C14 C15 1.367(5) . ?  
 C14 H14 0.9500 . ?  
 C15 C16 1.408(5) . ?  
 C15 H15 0.9500 . ?  
 C16 C17 1.401(5) . ?  
 C16 C21 1.419(5) . ?  
 C17 C18 1.365(5) . ?



C17 H17 0.9500 . ?  
 C18 C19 1.413(5) . ?  
 C18 H18 0.9500 . ?  
 C19 C20 1.367(5) . ?  
 C20 C21 1.422(5) . ?  
 C20 H20 0.9500 . ?  
 C21 C22 1.418(5) . ?  
 C22 H22 0.9500 . ?  
 C23 C24 1.525(5) 3\_666 ?  
 C23 H23A 0.9900 . ?  
 C23 H23B 0.9900 . ?  
 C24 C23 1.525(5) 3\_666 ?  
 C24 H24A 0.9900 . ?  
 C24 H24B 0.9900 . ?

loop\_  
 \_geom\_angle\_atom\_site\_label\_1  
 \_geom\_angle\_atom\_site\_label\_2  
 \_geom\_angle\_atom\_site\_label\_3  
 \_geom\_angle  
 \_geom\_angle\_site\_symmetry\_1  
 \_geom\_angle\_site\_symmetry\_3  
 \_geom\_angle\_publ\_flag  
 O1 Cu1 O2 92.23(10) . . ?  
 O1 Cu1 O3 174.31(10) . 3\_666 ?  
 O2 Cu1 O3 87.38(10) . 3\_666 ?  
 O1 Cu1 O4 88.97(10) . 3\_666 ?  
 O2 Cu1 O4 175.62(10) . 3\_666 ?  
 O3 Cu1 O4 91.01(10) 3\_666 3\_666 ?  
 O1 Cu1 S1 98.91(8) . . ?  
 O2 Cu1 S1 96.32(7) . . ?  
 O3 Cu1 S1 86.77(7) 3\_666 . ?  
 O4 Cu1 S1 87.66(7) 3\_666 . ?  
 C23 S1 C24 101.26(17) . . ?  
 C23 S1 Cu1 96.79(13) . . ?  
 C24 S1 Cu1 102.62(13) . . ?  
 C2 O1 Cu1 127.4(2) . . ?  
 C4 O2 Cu1 127.8(2) . . ?  
 C8 O3 Cu1 126.0(2) . 3\_666 ?  
 C10 O4 Cu1 125.7(2) . 3\_666 ?  
 C2 C1 H1A 109.5 . . ?  
 C2 C1 H1B 109.5 . . ?  
 H1A C1 H1B 109.5 . . ?  
 C2 C1 H1C 109.5 . . ?

H1A C1 H1C 109.5 . . ?  
 H1B C1 H1C 109.5 . . ?  
 O1 C2 C3 125.1(3) . . ?  
 O1 C2 C1 114.7(3) . . ?  
 C3 C2 C1 120.2(3) . . ?  
 C4 C3 C2 122.4(3) . . ?  
 C4 C3 C6 119.6(3) . . ?  
 C2 C3 C6 118.0(3) . . ?  
 O2 C4 C3 125.0(3) . . ?  
 O2 C4 C5 114.2(3) . . ?  
 C3 C4 C5 120.7(3) . . ?  
 C4 C5 H5A 109.5 . . ?  
 C4 C5 H5B 109.5 . . ?  
 H5A C5 H5B 109.5 . . ?  
 C4 C5 H5C 109.5 . . ?  
 H5A C5 H5C 109.5 . . ?  
 H5B C5 H5C 109.5 . . ?  
 C13 C6 C3 116.3(3) . . ?  
 C13 C6 H6A 108.2 . . ?  
 C3 C6 H6A 108.2 . . ?  
 C13 C6 H6B 108.2 . . ?  
 C3 C6 H6B 108.2 . . ?  
 H6A C6 H6B 107.4 . . ?  
 C8 C7 H7A 109.5 . . ?  
 C8 C7 H7B 109.5 . . ?  
 H7A C7 H7B 109.5 . . ?  
 C8 C7 H7C 109.5 . . ?  
 H7A C7 H7C 109.5 . . ?  
 H7B C7 H7C 109.5 . . ?  
 O3 C8 C9 125.5(3) . . ?  
 O3 C8 C7 113.7(3) . . ?  
 C9 C8 C7 120.7(3) . . ?  
 C10 C9 C8 121.4(3) . . ?  
 C10 C9 C12 120.8(3) . . ?  
 C8 C9 C12 117.5(3) . . ?  
 O4 C10 C9 125.4(3) . . ?  
 O4 C10 C11 113.5(3) . . ?  
 C9 C10 C11 121.1(3) . . ?  
 C10 C11 H11A 109.5 . . ?  
 C10 C11 H11B 109.5 . . ?  
 H11A C11 H11B 109.5 . . ?  
 C10 C11 H11C 109.5 . . ?  
 H11A C11 H11C 109.5 . . ?  
 H11B C11 H11C 109.5 . . ?

C19 C12 C9 116.2(3) . . ?  
 C19 C12 H12A 108.2 . . ?  
 C9 C12 H12A 108.2 . . ?  
 C19 C12 H12B 108.2 . . ?  
 C9 C12 H12B 108.2 . . ?  
 H12A C12 H12B 107.4 . . ?  
 C22 C13 C14 117.6(3) . . ?  
 C22 C13 C6 123.3(3) . . ?  
 C14 C13 C6 119.1(3) . . ?  
 C15 C14 C13 121.4(3) . . ?  
 C15 C14 H14 119.3 . . ?  
 C13 C14 H14 119.3 . . ?  
 C14 C15 C16 121.3(3) . . ?  
 C14 C15 H15 119.4 . . ?  
 C16 C15 H15 119.4 . . ?  
 C17 C16 C15 122.5(3) . . ?  
 C17 C16 C21 119.0(3) . . ?  
 C15 C16 C21 118.4(3) . . ?  
 C18 C17 C16 121.0(3) . . ?  
 C18 C17 H17 119.5 . . ?  
 C16 C17 H17 119.5 . . ?  
 C17 C18 C19 121.1(3) . . ?  
 C17 C18 H18 119.5 . . ?  
 C19 C18 H18 119.5 . . ?  
 C20 C19 C18 118.7(3) . . ?  
 C20 C19 C12 122.6(3) . . ?  
 C18 C19 C12 118.7(3) . . ?  
 C19 C20 C21 121.8(3) . . ?  
 C19 C20 H20 119.1 . . ?  
 C21 C20 H20 119.1 . . ?  
 C22 C21 C16 118.8(3) . . ?  
 C22 C21 C20 122.8(3) . . ?  
 C16 C21 C20 118.4(3) . . ?  
 C13 C22 C21 122.4(3) . . ?  
 C13 C22 H22 118.8 . . ?  
 C21 C22 H22 118.8 . . ?  
 C24 C23 S1 114.1(3) 3\_666 . ?  
 C24 C23 H23A 108.7 3\_666 . ?  
 S1 C23 H23A 108.7 . . ?  
 C24 C23 H23B 108.7 3\_666 . ?  
 S1 C23 H23B 108.7 . . ?  
 H23A C23 H23B 107.6 . . ?  
 C23 C24 S1 111.7(3) 3\_666 . ?  
 C23 C24 H24A 109.3 3\_666 . ?

S1 C24 H24A 109.3 . . ?  
 C23 C24 H24B 109.3 3\_666 . ?  
 S1 C24 H24B 109.3 . . ?  
 H24A C24 H24B 107.9 . . ?

loop\_  
 \_geom\_torsion\_atom\_site\_label\_1  
 \_geom\_torsion\_atom\_site\_label\_2  
 \_geom\_torsion\_atom\_site\_label\_3  
 \_geom\_torsion\_atom\_site\_label\_4  
 \_geom\_torsion  
 \_geom\_torsion\_site\_symmetry\_1  
 \_geom\_torsion\_site\_symmetry\_2  
 \_geom\_torsion\_site\_symmetry\_3  
 \_geom\_torsion\_site\_symmetry\_4  
 \_geom\_torsion\_publ\_flag  
 O1 Cu1 S1 C23 -125.86(14) . . . . ?  
 O2 Cu1 S1 C23 -32.59(14) . . . . ?  
 O3 Cu1 S1 C23 54.41(14) 3\_666 . . . ?  
 O4 Cu1 S1 C23 145.55(14) 3\_666 . . . ?  
 O1 Cu1 S1 C24 -22.68(15) . . . . ?  
 O2 Cu1 S1 C24 70.59(14) . . . . ?  
 O3 Cu1 S1 C24 157.59(15) 3\_666 . . . ?  
 O4 Cu1 S1 C24 -111.27(15) 3\_666 . . . ?  
 O2 Cu1 O1 C2 1.7(3) . . . . ?  
 O3 Cu1 O1 C2 -84.3(11) 3\_666 . . . ?  
 O4 Cu1 O1 C2 -174.1(3) 3\_666 . . . ?  
 S1 Cu1 O1 C2 98.4(3) . . . . ?  
 O1 Cu1 O2 C4 -0.5(3) . . . . ?  
 O3 Cu1 O2 C4 173.8(3) 3\_666 . . . ?  
 O4 Cu1 O2 C4 105.3(13) 3\_666 . . . ?  
 S1 Cu1 O2 C4 -99.7(3) . . . . ?  
 Cu1 O1 C2 C3 -2.6(5) . . . . ?  
 Cu1 O1 C2 C1 176.5(2) . . . . ?  
 O1 C2 C3 C4 1.9(5) . . . . ?  
 C1 C2 C3 C4 -177.1(3) . . . . ?  
 O1 C2 C3 C6 -178.6(3) . . . . ?  
 C1 C2 C3 C6 2.4(5) . . . . ?  
 Cu1 O2 C4 C3 0.1(5) . . . . ?  
 Cu1 O2 C4 C5 -177.7(2) . . . . ?  
 C2 C3 C4 O2 -0.6(6) . . . . ?  
 C6 C3 C4 O2 179.9(3) . . . . ?  
 C2 C3 C4 C5 177.1(3) . . . . ?  
 C6 C3 C4 C5 -2.4(5) . . . . ?

C4 C3 C6 C13 -97.4(4) . . . . ?  
 C2 C3 C6 C13 83.1(4) . . . . ?  
 Cu1 O3 C8 C9 -7.1(5) 3\_666 . . . ?  
 Cu1 O3 C8 C7 174.3(2) 3\_666 . . . ?  
 O3 C8 C9 C10 -10.2(6) . . . . ?  
 C7 C8 C9 C10 168.3(3) . . . . ?  
 O3 C8 C9 C12 175.4(3) . . . . ?  
 C7 C8 C9 C12 -6.1(5) . . . . ?  
 Cu1 O4 C10 C9 14.3(5) 3\_666 . . . ?  
 Cu1 O4 C10 C11 -167.5(2) 3\_666 . . . ?  
 C8 C9 C10 O4 6.3(5) . . . . ?  
 C12 C9 C10 O4 -179.5(3) . . . . ?  
 C8 C9 C10 C11 -171.8(3) . . . . ?  
 C12 C9 C10 C11 2.4(5) . . . . ?  
 C10 C9 C12 C19 121.8(4) . . . . ?  
 C8 C9 C12 C19 -63.8(4) . . . . ?  
 C3 C6 C13 C22 43.2(5) . . . . ?  
 C3 C6 C13 C14 -138.7(3) . . . . ?  
 C22 C13 C14 C15 0.5(5) . . . . ?  
 C6 C13 C14 C15 -177.6(3) . . . . ?  
 C13 C14 C15 C16 0.3(5) . . . . ?  
 C14 C15 C16 C17 -178.6(3) . . . . ?  
 C14 C15 C16 C21 -0.3(5) . . . . ?  
 C15 C16 C17 C18 179.2(3) . . . . ?  
 C21 C16 C17 C18 0.9(5) . . . . ?  
 C16 C17 C18 C19 0.7(5) . . . . ?  
 C17 C18 C19 C20 -2.1(5) . . . . ?  
 C17 C18 C19 C12 177.8(3) . . . . ?  
 C9 C12 C19 C20 -43.3(5) . . . . ?  
 C9 C12 C19 C18 136.8(3) . . . . ?  
 C18 C19 C20 C21 1.9(5) . . . . ?  
 C12 C19 C20 C21 -178.0(3) . . . . ?  
 C17 C16 C21 C22 177.9(3) . . . . ?  
 C15 C16 C21 C22 -0.5(5) . . . . ?  
 C17 C16 C21 C20 -1.1(5) . . . . ?  
 C15 C16 C21 C20 -179.5(3) . . . . ?  
 C19 C20 C21 C22 -179.2(3) . . . . ?  
 C19 C20 C21 C16 -0.3(5) . . . . ?  
 C14 C13 C22 C21 -1.4(5) . . . . ?  
 C6 C13 C22 C21 176.7(3) . . . . ?  
 C16 C21 C22 C13 1.4(5) . . . . ?  
 C20 C21 C22 C13 -179.7(3) . . . . ?  
 C24 S1 C23 C24 59.9(3) . . . 3\_666 ?  
 Cu1 S1 C23 C24 164.3(2) . . . 3\_666 ?

C23 S1 C24 C23 -58.2(3) . . . 3\_666 ?  
 Cu1 S1 C24 C23 -157.9(2) . . . 3\_666 ?

\_diffn\_measured\_fraction\_theta\_max 0.898  
 \_diffn\_reflns\_theta\_full 25.0  
 \_diffn\_measured\_fraction\_theta\_full 0.898  
 \_refine\_diff\_density\_max 0.30  
 \_refine\_diff\_density\_min -0.44  
 \_refine\_diff\_density\_rms 0.071  
 # END OF CIF

### **Cu<sub>2</sub>(NBDPr)<sub>2</sub>**

\_audit\_creation\_method SHELXL-97  
 \_chemical\_name\_systematic ?  
 \_chemical\_name\_common ?  
 \_chemical\_melting\_point ?  
 \_chemical\_compound\_source 'local laboratory'  
 \_chemical\_formula\_moiety 'C52 H60 Cu2 O8, 2(C H2 Cl2)'  
 \_chemical\_formula\_sum 'C54 H64 Cl4 Cu2 O8'  
 \_chemical\_formula\_weight 1109.93

loop\_  
 \_atom\_type\_symbol  
 \_atom\_type\_description  
 \_atom\_type\_scatter\_dispersion\_real  
 \_atom\_type\_scatter\_dispersion\_imag  
 \_atom\_type\_scatter\_source  
 'C' 'C' 0.0033 0.0016 'International Tables Vol C Tables 4.2.6.8 and 6.1.1.4'  
 'H' 'H' 0.0000 0.0000 'International Tables Vol C Tables 4.2.6.8 and 6.1.1.4'  
 'Cl' 'Cl' 0.1484 0.1585 'International Tables Vol C Tables 4.2.6.8 and 6.1.1.4'  
 'Cu' 'Cu' 0.3201 1.2651 'International Tables Vol C Tables 4.2.6.8 and 6.1.1.4'  
 'O' 'O' 0.0106 0.0060 'International Tables Vol C Tables 4.2.6.8 and 6.1.1.4'

\_symmetry\_space\_group\_name\_H-M 'P -1  
 \_symmetry\_space\_group\_name\_Hall '-P 1'  
 \_symmetry\_cell\_setting 'Triclinic'

loop\_  
 \_symmetry\_equiv\_pos\_as\_xyz  
 'x, y, z'  
 '-x, -y, -z'

_cell_length_a	11.153(3)
_cell_length_b	11.089(4)
_cell_length_c	21.772(10)
_cell_angle_alpha	84.761(13)
_cell_angle_beta	83.255(13)
_cell_angle_gamma	84.734(14)
_cell_volume	2653.9(17)
_cell_formula_units_Z	2
_cell_measurement_temperature	110
_cell_measurement_reflns_used	7155
_cell_measurement_theta_min	2.5
_cell_measurement_theta_max	26.0
_exptl_crystal_description	plate
_exptl_crystal_colour	'olive green'
_exptl_crystal_size_max	0.10
_exptl_crystal_size_mid	0.10
_exptl_crystal_size_min	0.03
_exptl_crystal_density_meas	?
_exptl_crystal_density_diffn	1.389
_exptl_crystal_density_method	'not measured'
_exptl_crystal_F_000	1156
_exptl_absorpt_coefficient_mu	1.055
_exptl_absorpt_correction_type	'multi-scan'
_exptl_absorpt_correction_T_min	0.902
_exptl_absorpt_correction_T_max	0.969
_exptl_absorpt_process_details	'Denzo and Scalepack (Otwinowski & Minor, 1997)'
_exptl_special_details	?
_diffn_ambient_temperature	110
_diffn_radiation_wavelength	0.71073
_diffn_radiation_type	MoK $\alpha$
_diffn_radiation_source	'fine-focus sealed tube'
_diffn_radiation_monochromator	graphite
_diffn_measurement_device	'KappaCCD (with Oxford Cryostream)'
_diffn_measurement_method	'\w scans with \k offsets'
_diffn_detector_area_resol_mean	?
_diffn_standards_number	0
_diffn_standards_interval_count	?
_diffn_standards_interval_time	?
_diffn_standards_decay_%	<2
_diffn_reflns_number	31892

_diffn_reflns_av_R_equivalents	0.268
_diffn_reflns_av_signal/netI	0.6097
_diffn_reflns_limit_h_min	-13
_diffn_reflns_limit_h_max	13
_diffn_reflns_limit_k_min	-13
_diffn_reflns_limit_k_max	13
_diffn_reflns_limit_l_min	-25
_diffn_reflns_limit_l_max	25
_diffn_reflns_theta_min	2.5
_diffn_reflns_theta_max	26.1
_reflns_number_total	8915
_reflns_number_gt	2517
_reflns_threshold_expression	$I > 2\sigma(I)$

_computing_data_collection	'COLLECT (Nonius, 2000)'
_computing_data_reduction	'Denzo and Scalepack (Otwinowski & Minor, 1997)'
_computing_cell_refinement	'Denzo and Scalepack (Otwinowski & Minor, 1997)'
_computing_structure_solution	'SIR97 (Altomare, et al., 1999)'
_computing_structure_refinement	'SHELXL-97 (Sheldrick, 1997)'
_computing_molecular_graphics	'ORTEP-3 (Farrugia, 1997)'
_computing_publication_material	'SHELXL-97 (Sheldrick, 1997)'

#### \_refine\_special\_details

Refinement of  $F^2$  against ALL reflections. The weighted R-factor  $wR$  and goodness of fit  $S$  are based on  $F^2$ , conventional R-factors  $R$  are based on  $F$ , with  $F$  set to zero for negative  $F^2$ . The threshold expression of  $F^2 > 2\sigma(F^2)$  is used only for calculating R-factors(gt) etc. and is not relevant to the choice of reflections for refinement. R-factors based on  $F^2$  are statistically about twice as large as those based on  $F$ , and R-factors based on ALL data will be even larger.

_refine_ls_structure_factor_coef	Fsqd
_refine_ls_matrix_type	full
_refine_ls_weighting_scheme	calc
_refine_ls_weighting_details	'calc w=1/[ $\sigma^2(F_o^2) + (0.2000P)^2$ ] where $P=(F_o^2 + 2F_c^2)/3$ '
_atom_sites_solution_primary	direct
_atom_sites_solution_secondary	difmap
_atom_sites_solution_hydrogens	geom
_refine_ls_hydrogen_treatment	constr
_refine_ls_extinction_method	none
_refine_ls_extinction_coef	?



_refine_ls_number_reflns	8915
_refine_ls_number_parameters	298
_refine_ls_number_restraints	0
_refine_ls_R_factor_all	0.448
_refine_ls_R_factor_gt	0.194
_refine_ls_wR_factor_ref	0.529
_refine_ls_wR_factor_gt	0.450
_refine_ls_goodness_of_fit_ref	1.188
_refine_ls_restrained_S_all	1.188
_refine_ls_shift/su_max	0.006
_refine_ls_shift/su_mean	0.001

loop\_

_atom_site_label	
_atom_site_type_symbol	
_atom_site_fract_x	
_atom_site_fract_y	
_atom_site_fract_z	
_atom_site_U_iso_or_equiv	
_atom_site_adp_type	
_atom_site_occupancy	
_atom_site_symmetry_multiplicity	
_atom_site_calc_flag	
_atom_site_refinement_flags	
_atom_site_disorder_assembly	
_atom_site_disorder_group	
Cu1 Cu	0.8121(3) 0.5816(2) -0.03082(13) 0.0482(10) Uani 1 1 d . . .
Cu2 Cu	-0.0926(3) 0.1935(2) 0.53881(14) 0.0581(11) Uani 1 1 d . . .
O1 O	0.8312(12) 0.5739(12) 0.0567(6) 0.045(4) Uiso 1 1 d . . .
O2 O	0.8666(13) 0.4142(12) -0.0377(6) 0.046(4) Uiso 1 1 d . . .
O3 O	0.2182(12) 0.4109(11) 0.1130(6) 0.038(4) Uiso 1 1 d . . .
O4 O	0.2432(13) 0.2519(12) 0.0253(7) 0.049(4) Uiso 1 1 d . . .
O5 O	-0.0657(15) 0.1749(13) 0.4503(7) 0.062(5) Uiso 1 1 d . . .
O6 O	0.0672(13) 0.1461(12) 0.5486(7) 0.048(4) Uiso 1 1 d . . .
O7 O	0.1167(13) 0.7792(12) 0.3770(7) 0.048(4) Uiso 1 1 d . . .
O8 O	0.2519(15) 0.7533(13) 0.4720(7) 0.064(5) Uiso 1 1 d . . .
C1 C	0.882(2) 0.5036(19) 0.1552(10) 0.055(7) Uiso 1 1 d . . .
H1A H	0.8451 0.4376 0.1826 0.066 Uiso 1 1 calc R . .
H1B H	0.9686 0.5013 0.1623 0.066 Uiso 1 1 calc R . .
C2 C	0.8735(19) 0.4829(18) 0.0869(10) 0.037(6) Uiso 1 1 d . . .
C3 C	0.9145(19) 0.3724(17) 0.0691(10) 0.037(6) Uiso 1 1 d . . .
C4 C	0.9118(19) 0.3464(18) 0.0039(10) 0.041(6) Uiso 1 1 d . . .
C5 C	0.941(2) 0.2160(18) -0.0141(10) 0.054(7) Uiso 1 1 d . . .
H5A H	1.0294 0.1954 -0.0144 0.065 Uiso 1 1 calc R . .

H5B H 0.8999 0.1607 0.0183 0.065 Uiso 1 1 calc R . .  
 C6 C 0.967(2) 0.263(2) 0.1143(11) 0.066(8) Uiso 1 1 d . . .  
 H6A H 1.0360 0.2169 0.0915 0.079 Uiso 1 1 calc R . .  
 H6B H 0.9972 0.2957 0.1498 0.079 Uiso 1 1 calc R . .  
 C7 C 0.871(2) 0.1780(19) 0.1381(10) 0.053(7) Uiso 1 1 d . . .  
 C8 C 0.904(2) 0.0584(19) 0.1697(10) 0.058(7) Uiso 1 1 d . . .  
 H8 H 0.9878 0.0363 0.1717 0.070 Uiso 1 1 calc R . .  
 C9 C 0.829(2) -0.0191(19) 0.1951(10) 0.046(6) Uiso 1 1 d . . .  
 H9 H 0.8586 -0.0911 0.2176 0.055 Uiso 1 1 calc R . .  
 C10 C 0.7007(19) 0.0041(17) 0.1890(9) 0.035(6) Uiso 1 1 d . . .  
 C11 C 0.618(2) -0.0729(18) 0.2122(10) 0.044(6) Uiso 1 1 d . . .  
 H11 H 0.6444 -0.1475 0.2336 0.053 Uiso 1 1 calc R . .  
 C12 C 0.496(2) -0.0486(19) 0.2065(10) 0.049(6) Uiso 1 1 d . . .  
 H12 H 0.4416 -0.1079 0.2223 0.059 Uiso 1 1 calc R . .  
 C13 C 0.452(2) 0.0576(19) 0.1788(10) 0.046(6) Uiso 1 1 d . . .  
 C14 C 0.5359(19) 0.1442(18) 0.1569(9) 0.042(6) Uiso 1 1 d . . .  
 H14 H 0.5082 0.2208 0.1381 0.050 Uiso 1 1 calc R . .  
 C15 C 0.658(2) 0.118(2) 0.1628(11) 0.065(7) Uiso 1 1 d . . .  
 C16 C 0.741(2) 0.2079(19) 0.1365(10) 0.047(6) Uiso 1 1 d . . .  
 H16 H 0.7114 0.2846 0.1186 0.057 Uiso 1 1 calc R . .  
 C17 C 0.3207(19) 0.0919(17) 0.1757(10) 0.042(6) Uiso 1 1 d . . .  
 H17A H 0.2855 0.1150 0.2172 0.050 Uiso 1 1 calc R . .  
 H17B H 0.2832 0.0179 0.1680 0.050 Uiso 1 1 calc R . .  
 C18 C 0.269(2) 0.346(2) 0.2147(11) 0.062(7) Uiso 1 1 d . . .  
 H18A H 0.3035 0.2734 0.2381 0.074 Uiso 1 1 calc R . .  
 H18B H 0.3251 0.4107 0.2124 0.074 Uiso 1 1 calc R . .  
 C19 C 0.253(2) 0.3147(19) 0.1469(10) 0.047(6) Uiso 1 1 d . . .  
 C20 C 0.2800(18) 0.1945(17) 0.1277(10) 0.035(6) Uiso 1 1 d . . .  
 C21 C 0.279(2) 0.1752(19) 0.0652(11) 0.046(6) Uiso 1 1 d . . .  
 C22 C 0.3199(19) 0.0492(16) 0.0425(9) 0.038(6) Uiso 1 1 d . . .  
 H22A H 0.4035 0.0258 0.0527 0.045 Uiso 1 1 calc R . .  
 H22B H 0.2670 -0.0109 0.0653 0.045 Uiso 1 1 calc R . .  
 C23 C 0.820(2) 0.622(2) 0.1708(11) 0.067(8) Uiso 1 1 d . . .  
 H23A H 0.8261 0.6327 0.2144 0.101 Uiso 1 1 calc R . .  
 H23B H 0.7347 0.6236 0.1640 0.101 Uiso 1 1 calc R . .  
 H23C H 0.8583 0.6870 0.1444 0.101 Uiso 1 1 calc R . .  
 C24 C 0.905(2) 0.1925(19) -0.0752(10) 0.056(7) Uiso 1 1 d . . .  
 H24A H 0.9284 0.1075 -0.0831 0.084 Uiso 1 1 calc R . .  
 H24B H 0.9463 0.2457 -0.1079 0.084 Uiso 1 1 calc R . .  
 H24C H 0.8174 0.2089 -0.0750 0.084 Uiso 1 1 calc R . .  
 C25 C 0.153(3) 0.387(3) 0.2461(15) 0.123(12) Uiso 1 1 d . . .  
 H25A H 0.1644 0.4070 0.2879 0.185 Uiso 1 1 calc R . .  
 H25B H 0.0983 0.3223 0.2491 0.185 Uiso 1 1 calc R . .  
 H25C H 0.1192 0.4592 0.2228 0.185 Uiso 1 1 calc R . .

C26 C 0.317(2) 0.0436(18) -0.0231(10) 0.048(6) Uiso 1 1 d . . .  
 H26A H 0.3415 -0.0395 -0.0342 0.072 Uiso 1 1 calc R . .  
 H26B H 0.3727 0.0993 -0.0461 0.072 Uiso 1 1 calc R . .  
 H26C H 0.2345 0.0671 -0.0337 0.072 Uiso 1 1 calc R . .  
 C27 C 0.0133(19) 0.1193(18) 0.3571(10) 0.042(6) Uiso 1 1 d . . .  
 H27A H 0.0117 0.0317 0.3522 0.050 Uiso 1 1 calc R . .  
 H27B H 0.0891 0.1453 0.3334 0.050 Uiso 1 1 calc R . .  
 C28 C 0.024(2) 0.1303(17) 0.4205(10) 0.039(6) Uiso 1 1 d . . .  
 C29 C 0.1371(18) 0.0901(16) 0.4444(9) 0.035(6) Uiso 1 1 d . . .  
 C30 C 0.151(2) 0.1017(19) 0.5112(11) 0.051(7) Uiso 1 1 d . . .  
 C31 C 0.273(2) 0.0596(19) 0.5368(10) 0.052(7) Uiso 1 1 d . . .  
 H31A H 0.3400 0.0879 0.5066 0.063 Uiso 1 1 calc R . .  
 H31B H 0.2825 -0.0303 0.5413 0.063 Uiso 1 1 calc R . .  
 C32 C 0.243(2) 0.0400(19) 0.4048(10) 0.052(7) Uiso 1 1 d . . .  
 H32A H 0.2124 -0.0010 0.3719 0.063 Uiso 1 1 calc R . .  
 H32B H 0.2873 -0.0232 0.4304 0.063 Uiso 1 1 calc R . .  
 C33 C 0.335(2) 0.131(2) 0.3729(10) 0.052(7) Uiso 1 1 d . . .  
 C34 C 0.442(2) 0.081(2) 0.3457(10) 0.053(7) Uiso 1 1 d . . .  
 H34 H 0.4586 -0.0046 0.3446 0.063 Uiso 1 1 calc R . .  
 C35 C 0.527(3) 0.165(2) 0.3186(13) 0.087(9) Uiso 1 1 d . . .  
 H35 H 0.6020 0.1335 0.2983 0.104 Uiso 1 1 calc R . .  
 C36 C 0.509(2) 0.2830(19) 0.3201(10) 0.043(6) Uiso 1 1 d . . .  
 C37 C 0.596(2) 0.3625(19) 0.2881(11) 0.055(7) Uiso 1 1 d . . .  
 H37 H 0.6687 0.3297 0.2661 0.066 Uiso 1 1 calc R . .  
 C38 C 0.573(2) 0.487(2) 0.2901(11) 0.059(7) Uiso 1 1 d . . .  
 H38 H 0.6294 0.5401 0.2695 0.071 Uiso 1 1 calc R . .  
 C39 C 0.461(2) 0.537(2) 0.3235(11) 0.057(7) Uiso 1 1 d . . .  
 C40 C 0.3742(19) 0.4548(17) 0.3477(9) 0.038(6) Uiso 1 1 d . . .  
 H40 H 0.2960 0.4862 0.3640 0.046 Uiso 1 1 calc R . .  
 C41 C 0.400(2) 0.3296(19) 0.3485(10) 0.048(6) Uiso 1 1 d . . .  
 C42 C 0.313(2) 0.2512(18) 0.3723(9) 0.042(6) Uiso 1 1 d . . .  
 H42 H 0.2351 0.2840 0.3886 0.050 Uiso 1 1 calc R . .  
 C43 C 0.429(2) 0.675(2) 0.3268(12) 0.075(8) Uiso 1 1 d . . .  
 H43 H 0.4777 0.7312 0.3022 0.090 Uiso 1 1 calc R . .  
 C44 C 0.195(2) 0.738(2) 0.2771(12) 0.067(8) Uiso 1 1 d . . .  
 H44A H 0.2462 0.7971 0.2523 0.080 Uiso 1 1 calc R . .  
 H44B H 0.2289 0.6562 0.2657 0.080 Uiso 1 1 calc R . .  
 C45 C 0.213(2) 0.745(2) 0.3431(12) 0.058(7) Uiso 1 1 d . . .  
 C46 C 0.330(2) 0.7158(18) 0.3660(11) 0.046(6) Uiso 1 1 d . . .  
 C47 C 0.343(2) 0.7188(19) 0.4301(12) 0.054(7) Uiso 1 1 d . . .  
 C48 C 0.463(2) 0.678(2) 0.4548(12) 0.073(8) Uiso 1 1 d . . .  
 H48A H 0.4830 0.5915 0.4476 0.088 Uiso 1 1 calc R . .  
 H48B H 0.5261 0.7250 0.4306 0.088 Uiso 1 1 calc R . .  
 C49 C -0.088(3) 0.183(2) 0.3260(13) 0.098(10) Uiso 1 1 d . . .

H49A H -0.0752 0.1693 0.2818 0.147 Uiso 1 1 calc R . .  
 H49B H -0.0905 0.2701 0.3309 0.147 Uiso 1 1 calc R . .  
 H49C H -0.1639 0.1514 0.3447 0.147 Uiso 1 1 calc R . .  
 C50 C 0.283(2) 0.111(2) 0.6039(11) 0.071(8) Uiso 1 1 d . . .  
 H50A H 0.3608 0.0814 0.6184 0.107 Uiso 1 1 calc R . .  
 H50B H 0.2168 0.0833 0.6341 0.107 Uiso 1 1 calc R . .  
 H50C H 0.2765 0.2004 0.5994 0.107 Uiso 1 1 calc R . .  
 C51 C 0.083(3) 0.757(2) 0.2568(14) 0.096(10) Uiso 1 1 d . . .  
 H51A H 0.0893 0.7457 0.2123 0.144 Uiso 1 1 calc R . .  
 H51B H 0.0485 0.8394 0.2640 0.144 Uiso 1 1 calc R . .  
 H51C H 0.0294 0.6982 0.2795 0.144 Uiso 1 1 calc R . .  
 C52 C 0.466(2) 0.692(2) 0.5185(12) 0.078(8) Uiso 1 1 d . . .  
 H52A H 0.5464 0.6632 0.5303 0.117 Uiso 1 1 calc R . .  
 H52B H 0.4048 0.6442 0.5432 0.117 Uiso 1 1 calc R . .  
 H52C H 0.4485 0.7778 0.5262 0.117 Uiso 1 1 calc R . .  
 Cl1 Cl 0.4390(9) 0.6799(9) -0.0012(4) 0.131(4) Uani 1 1 d . . .  
 Cl2 Cl 0.4476(10) 0.7142(11) 0.1283(5) 0.157(4) Uani 1 1 d . . .  
 Cl3 Cl 0.1996(14) 0.4393(10) 0.5104(5) 0.200(6) Uani 1 1 d . . .  
 Cl4A Cl 0.1984(18) 0.4675(16) 0.6281(9) 0.125(6) Uiso 0.50 1 d P . .  
 Cl4B Cl 0.041(3) 0.495(3) 0.6017(15) 0.232(13) Uiso 0.50 1 d P . .  
 C1S C 0.418(4) 0.600(3) 0.0784(19) 0.152(15) Uiso 1 1 d . . .

loop\_

\_atom\_site\_aniso\_label  
 \_atom\_site\_aniso\_U\_11  
 \_atom\_site\_aniso\_U\_22  
 \_atom\_site\_aniso\_U\_33  
 \_atom\_site\_aniso\_U\_23  
 \_atom\_site\_aniso\_U\_13  
 \_atom\_site\_aniso\_U\_12  
 Cu1 0.044(2) 0.0493(19) 0.054(2) -0.0047(15) -0.0077(15) -0.0124(15)  
 Cu2 0.062(2) 0.0445(19) 0.070(3) -0.0021(16) -0.0114(18) -0.0120(16)  
 Cl1 0.116(8) 0.170(9) 0.109(8) 0.030(6) -0.012(6) -0.060(7)  
 Cl2 0.144(10) 0.205(11) 0.138(10) -0.061(8) -0.021(7) -0.046(8)  
 Cl3 0.318(19) 0.141(9) 0.134(10) -0.020(7) 0.061(11) -0.077(10)

\_geom\_special\_details

;

All esds (except the esd in the dihedral angle between two l.s. planes)  
 are estimated using the full covariance matrix. The cell esds are taken  
 into account individually in the estimation of esds in distances, angles  
 and torsion angles; correlations between esds in cell parameters are only  
 used when they are defined by crystal symmetry. An approximate (isotropic)  
 treatment of cell esds is used for estimating esds involving l.s. planes.

```

loop_
  _geom_bond_atom_site_label_1
  _geom_bond_atom_site_label_2
  _geom_bond_distance
  _geom_bond_site_symmetry_2
  _geom_bond_publ_flag
Cu1 O3 1.853(13) 2_665 ?
Cu1 O4 1.902(14) 2_665 ?
Cu1 O2 1.913(14) . ?
Cu1 O1 1.936(14) . ?
Cu2 O6 1.842(15) . ?
Cu2 O8 1.855(16) 2_566 ?
Cu2 O7 1.869(14) 2_566 ?
Cu2 O5 1.941(16) . ?
O1 C2 1.24(2) . ?
O2 C4 1.25(2) . ?
O3 C19 1.30(2) . ?
O3 Cu1 1.853(13) 2_665 ?
O4 C21 1.23(2) . ?
O4 Cu1 1.902(14) 2_665 ?
O5 C28 1.21(2) . ?
O6 C30 1.26(2) . ?
O7 C45 1.28(2) . ?
O7 Cu2 1.869(14) 2_566 ?
O8 C47 1.33(3) . ?
O8 Cu2 1.855(16) 2_566 ?
C1 C23 1.47(3) . ?
C1 C2 1.54(3) . ?
C1 H1A 0.9900 . ?
C1 H1B 0.9900 . ?
C2 C3 1.34(2) . ?
C3 C4 1.48(3) . ?
C3 C6 1.61(3) . ?
C4 C5 1.53(3) . ?
C5 C24 1.49(3) . ?
C5 H5A 0.9900 . ?
C5 H5B 0.9900 . ?
C6 C7 1.50(3) . ?
C6 H6A 0.9900 . ?
C6 H6B 0.9900 . ?
C7 C16 1.46(3) . ?
C7 C8 1.47(3) . ?
C8 C9 1.29(3) . ?

```

C8 H8 0.9500 . ?  
 C9 C10 1.45(3) . ?  
 C9 H9 0.9500 . ?  
 C10 C11 1.34(3) . ?  
 C10 C15 1.40(3) . ?  
 C11 C12 1.38(3) . ?  
 C11 H11 0.9500 . ?  
 C12 C13 1.35(3) . ?  
 C12 H12 0.9500 . ?  
 C13 C14 1.41(3) . ?  
 C13 C17 1.49(3) . ?  
 C14 C15 1.39(3) . ?  
 C14 H14 0.9500 . ?  
 C15 C16 1.46(3) . ?  
 C16 H16 0.9500 . ?  
 C17 C20 1.55(3) . ?  
 C17 H17A 0.9900 . ?  
 C17 H17B 0.9900 . ?  
 C18 C25 1.44(3) . ?  
 C18 C19 1.58(3) . ?  
 C18 H18A 0.9900 . ?  
 C18 H18B 0.9900 . ?  
 C19 C20 1.43(3) . ?  
 C20 C21 1.40(3) . ?  
 C21 C22 1.54(3) . ?  
 C22 C26 1.44(3) . ?  
 C22 H22A 0.9900 . ?  
 C22 H22B 0.9900 . ?  
 C23 H23A 0.9800 . ?  
 C23 H23B 0.9800 . ?  
 C23 H23C 0.9800 . ?  
 C24 H24A 0.9800 . ?  
 C24 H24B 0.9800 . ?  
 C24 H24C 0.9800 . ?  
 C25 H25A 0.9800 . ?  
 C25 H25B 0.9800 . ?  
 C25 H25C 0.9800 . ?  
 C26 H26A 0.9800 . ?  
 C26 H26B 0.9800 . ?  
 C26 H26C 0.9800 . ?  
 C27 C28 1.42(3) . ?  
 C27 C49 1.47(3) . ?  
 C27 H27A 0.9900 . ?  
 C27 H27B 0.9900 . ?

C28 C29 1.44(3) . ?  
 C29 C32 1.47(3) . ?  
 C29 C30 1.50(3) . ?  
 C30 C31 1.55(3) . ?  
 C31 C50 1.64(3) . ?  
 C31 H31A 0.9900 . ?  
 C31 H31B 0.9900 . ?  
 C32 C33 1.57(3) . ?  
 C32 H32A 0.9900 . ?  
 C32 H32B 0.9900 . ?  
 C33 C42 1.33(3) . ?  
 C33 C34 1.36(3) . ?  
 C34 C35 1.44(3) . ?  
 C34 H34 0.9500 . ?  
 C35 C36 1.31(3) . ?  
 C35 H35 0.9500 . ?  
 C36 C41 1.37(3) . ?  
 C36 C37 1.45(3) . ?  
 C37 C38 1.39(3) . ?  
 C37 H37 0.9500 . ?  
 C38 C39 1.45(3) . ?  
 C38 H38 0.9500 . ?  
 C39 C40 1.41(3) . ?  
 C39 C43 1.55(3) . ?  
 C40 C41 1.39(3) . ?  
 C40 H40 0.9500 . ?  
 C41 C42 1.39(3) . ?  
 C42 H42 0.9500 . ?  
 C43 C46 1.38(3) . ?  
 C43 H43 0.9500 . ?  
 C44 C51 1.37(3) . ?  
 C44 C45 1.49(3) . ?  
 C44 H44A 0.9900 . ?  
 C44 H44B 0.9900 . ?  
 C45 C46 1.45(3) . ?  
 C46 C47 1.42(3) . ?  
 C47 C48 1.52(3) . ?  
 C48 C52 1.41(3) . ?  
 C48 H48A 0.9900 . ?  
 C48 H48B 0.9900 . ?  
 C49 H49A 0.9800 . ?  
 C49 H49B 0.9800 . ?  
 C49 H49C 0.9800 . ?  
 C50 H50A 0.9800 . ?

C50 H50B 0.9800 . ?  
 C50 H50C 0.9800 . ?  
 C51 H51A 0.9800 . ?  
 C51 H51B 0.9800 . ?  
 C51 H51C 0.9800 . ?  
 C52 H52A 0.9800 . ?  
 C52 H52B 0.9800 . ?  
 C52 H52C 0.9800 . ?  
 Cl1 C1S 1.87(4) . ?  
 Cl2 C1S 1.82(4) . ?  
 Cl4A Cl4B 1.90(4) . ?

loop\_

\_geom\_angle\_atom\_site\_label\_1  
 \_geom\_angle\_atom\_site\_label\_2  
 \_geom\_angle\_atom\_site\_label\_3  
 \_geom\_angle  
 \_geom\_angle\_site\_symmetry\_1  
 \_geom\_angle\_site\_symmetry\_3  
 \_geom\_angle\_publ\_flag  
 O3 Cu1 O4 91.5(6) 2\_665 2\_665 ?  
 O3 Cu1 O2 87.5(6) 2\_665 . ?  
 O4 Cu1 O2 179.0(7) 2\_665 . ?  
 O3 Cu1 O1 175.8(6) 2\_665 . ?  
 O4 Cu1 O1 87.4(6) 2\_665 . ?  
 O2 Cu1 O1 93.6(6) . . ?  
 O6 Cu2 O8 178.0(6) . 2\_566 ?  
 O6 Cu2 O7 88.2(6) . 2\_566 ?  
 O8 Cu2 O7 92.0(7) 2\_566 2\_566 ?  
 O6 Cu2 O5 92.0(7) . . ?  
 O8 Cu2 O5 87.7(7) 2\_566 . ?  
 O7 Cu2 O5 176.7(6) 2\_566 . ?  
 C2 O1 Cu1 124.4(13) . . ?  
 C4 O2 Cu1 124.5(14) . . ?  
 C19 O3 Cu1 126.7(13) . 2\_665 ?  
 C21 O4 Cu1 130.2(15) . 2\_665 ?  
 C28 O5 Cu2 128.6(16) . . ?  
 C30 O6 Cu2 130.3(15) . . ?  
 C45 O7 Cu2 130.3(15) . 2\_566 ?  
 C47 O8 Cu2 129.3(16) . 2\_566 ?  
 C23 C1 C2 110.7(19) . . ?  
 C23 C1 H1A 109.5 . . ?  
 C2 C1 H1A 109.5 . . ?  
 C23 C1 H1B 109.5 . . ?



C2 C1 H1B 109.5 . . ?  
 H1A C1 H1B 108.1 . . ?  
 O1 C2 C3 130(2) . . ?  
 O1 C2 C1 113.4(18) . . ?  
 C3 C2 C1 116.1(19) . . ?  
 C2 C3 C4 119.4(19) . . ?  
 C2 C3 C6 125(2) . . ?  
 C4 C3 C6 116.1(18) . . ?  
 O2 C4 C3 127.0(19) . . ?  
 O2 C4 C5 112.4(19) . . ?  
 C3 C4 C5 119.2(18) . . ?  
 C24 C5 C4 115.1(18) . . ?  
 C24 C5 H5A 108.5 . . ?  
 C4 C5 H5A 108.5 . . ?  
 C24 C5 H5B 108.5 . . ?  
 C4 C5 H5B 108.5 . . ?  
 H5A C5 H5B 107.5 . . ?  
 C7 C6 C3 110.9(19) . . ?  
 C7 C6 H6A 109.5 . . ?  
 C3 C6 H6A 109.5 . . ?  
 C7 C6 H6B 109.5 . . ?  
 C3 C6 H6B 109.5 . . ?  
 H6A C6 H6B 108.0 . . ?  
 C16 C7 C8 115(2) . . ?  
 C16 C7 C6 125(2) . . ?  
 C8 C7 C6 120(2) . . ?  
 C9 C8 C7 126(2) . . ?  
 C9 C8 H8 117.0 . . ?  
 C7 C8 H8 117.0 . . ?  
 C8 C9 C10 120(2) . . ?  
 C8 C9 H9 120.1 . . ?  
 C10 C9 H9 120.1 . . ?  
 C11 C10 C15 117(2) . . ?  
 C11 C10 C9 123.7(19) . . ?  
 C15 C10 C9 119(2) . . ?  
 C10 C11 C12 123(2) . . ?  
 C10 C11 H11 118.6 . . ?  
 C12 C11 H11 118.6 . . ?  
 C13 C12 C11 122(2) . . ?  
 C13 C12 H12 119.2 . . ?  
 C11 C12 H12 119.2 . . ?  
 C12 C13 C14 117(2) . . ?  
 C12 C13 C17 124(2) . . ?  
 C14 C13 C17 118.9(19) . . ?

C15 C14 C13 120(2) . . ?  
 C15 C14 H14 119.8 . . ?  
 C13 C14 H14 119.8 . . ?  
 C14 C15 C10 120(2) . . ?  
 C14 C15 C16 118(2) . . ?  
 C10 C15 C16 121(2) . . ?  
 C15 C16 C7 119(2) . . ?  
 C15 C16 H16 120.7 . . ?  
 C7 C16 H16 120.7 . . ?  
 C13 C17 C20 119.7(18) . . ?  
 C13 C17 H17A 107.4 . . ?  
 C20 C17 H17A 107.4 . . ?  
 C13 C17 H17B 107.4 . . ?  
 C20 C17 H17B 107.4 . . ?  
 H17A C17 H17B 106.9 . . ?  
 C25 C18 C19 110(2) . . ?  
 C25 C18 H18A 109.6 . . ?  
 C19 C18 H18A 109.6 . . ?  
 C25 C18 H18B 109.7 . . ?  
 C19 C18 H18B 109.6 . . ?  
 H18A C18 H18B 108.2 . . ?  
 O3 C19 C20 127(2) . . ?  
 O3 C19 C18 111.2(18) . . ?  
 C20 C19 C18 121.8(19) . . ?  
 C21 C20 C19 119.1(19) . . ?  
 C21 C20 C17 121.9(18) . . ?  
 C19 C20 C17 118.7(19) . . ?  
 O4 C21 C20 125(2) . . ?  
 O4 C21 C22 115.1(19) . . ?  
 C20 C21 C22 119.9(19) . . ?  
 C26 C22 C21 113.7(17) . . ?  
 C26 C22 H22A 108.8 . . ?  
 C21 C22 H22A 108.8 . . ?  
 C26 C22 H22B 108.8 . . ?  
 C21 C22 H22B 108.8 . . ?  
 H22A C22 H22B 107.7 . . ?  
 C1 C23 H23A 109.5 . . ?  
 C1 C23 H23B 109.5 . . ?  
 H23A C23 H23B 109.5 . . ?  
 C1 C23 H23C 109.5 . . ?  
 H23A C23 H23C 109.5 . . ?  
 H23B C23 H23C 109.5 . . ?  
 C5 C24 H24A 109.5 . . ?  
 C5 C24 H24B 109.5 . . ?

H24A C24 H24B 109.5 . . ?  
 C5 C24 H24C 109.5 . . ?  
 H24A C24 H24C 109.5 . . ?  
 H24B C24 H24C 109.5 . . ?  
 C18 C25 H25A 109.5 . . ?  
 C18 C25 H25B 109.5 . . ?  
 H25A C25 H25B 109.5 . . ?  
 C18 C25 H25C 109.5 . . ?  
 H25A C25 H25C 109.5 . . ?  
 H25B C25 H25C 109.5 . . ?  
 C22 C26 H26A 109.5 . . ?  
 C22 C26 H26B 109.5 . . ?  
 H26A C26 H26B 109.5 . . ?  
 C22 C26 H26C 109.5 . . ?  
 H26A C26 H26C 109.5 . . ?  
 H26B C26 H26C 109.5 . . ?  
 C28 C27 C49 122(2) . . ?  
 C28 C27 H27A 106.9 . . ?  
 C49 C27 H27A 106.9 . . ?  
 C28 C27 H27B 106.9 . . ?  
 C49 C27 H27B 106.9 . . ?  
 H27A C27 H27B 106.7 . . ?  
 O5 C28 C27 116(2) . . ?  
 O5 C28 C29 125(2) . . ?  
 C27 C28 C29 119(2) . . ?  
 C28 C29 C32 122(2) . . ?  
 C28 C29 C30 119.7(19) . . ?  
 C32 C29 C30 118.1(19) . . ?  
 O6 C30 C29 123(2) . . ?  
 O6 C30 C31 117(2) . . ?  
 C29 C30 C31 119.8(19) . . ?  
 C30 C31 C50 112.5(18) . . ?  
 C30 C31 H31A 109.1 . . ?  
 C50 C31 H31A 109.1 . . ?  
 C30 C31 H31B 109.1 . . ?  
 C50 C31 H31B 109.1 . . ?  
 H31A C31 H31B 107.8 . . ?  
 C29 C32 C33 117.5(17) . . ?  
 C29 C32 H32A 107.9 . . ?  
 C33 C32 H32A 107.9 . . ?  
 C29 C32 H32B 107.9 . . ?  
 C33 C32 H32B 107.9 . . ?  
 H32A C32 H32B 107.2 . . ?  
 C42 C33 C34 121(2) . . ?

C42 C33 C32 123(2) . . ?  
 C34 C33 C32 116.4(19) . . ?  
 C33 C34 C35 116(2) . . ?  
 C33 C34 H34 122.2 . . ?  
 C35 C34 H34 122.2 . . ?  
 C36 C35 C34 124(3) . . ?  
 C36 C35 H35 117.9 . . ?  
 C34 C35 H35 117.9 . . ?  
 C35 C36 C41 118(2) . . ?  
 C35 C36 C37 121(2) . . ?  
 C41 C36 C37 121(2) . . ?  
 C38 C37 C36 119(2) . . ?  
 C38 C37 H37 120.5 . . ?  
 C36 C37 H37 120.5 . . ?  
 C37 C38 C39 120(2) . . ?  
 C37 C38 H38 119.9 . . ?  
 C39 C38 H38 119.9 . . ?  
 C40 C39 C38 118(2) . . ?  
 C40 C39 C43 120(2) . . ?  
 C38 C39 C43 122(2) . . ?  
 C41 C40 C39 122(2) . . ?  
 C41 C40 H40 119.0 . . ?  
 C39 C40 H40 119.0 . . ?  
 C36 C41 C42 119(2) . . ?  
 C36 C41 C40 120(2) . . ?  
 C42 C41 C40 121(2) . . ?  
 C33 C42 C41 122(2) . . ?  
 C33 C42 H42 119.2 . . ?  
 C41 C42 H42 119.2 . . ?  
 C46 C43 C39 120(2) . . ?  
 C46 C43 H43 120.2 . . ?  
 C39 C43 H43 120.2 . . ?  
 C51 C44 C45 122(2) . . ?  
 C51 C44 H44A 106.8 . . ?  
 C45 C44 H44A 106.8 . . ?  
 C51 C44 H44B 106.8 . . ?  
 C45 C44 H44B 106.8 . . ?  
 H44A C44 H44B 106.7 . . ?  
 O7 C45 C46 124(2) . . ?  
 O7 C45 C44 114(2) . . ?  
 C46 C45 C44 123(2) . . ?  
 C43 C46 C47 119(2) . . ?  
 C43 C46 C45 120(2) . . ?  
 C47 C46 C45 121(2) . . ?

O8 C47 C46 124(2) . . ?  
 O8 C47 C48 116(2) . . ?  
 C46 C47 C48 120(2) . . ?  
 C52 C48 C47 115(2) . . ?  
 C52 C48 H48A 108.4 . . ?  
 C47 C48 H48A 108.4 . . ?  
 C52 C48 H48B 108.4 . . ?  
 C47 C48 H48B 108.4 . . ?  
 H48A C48 H48B 107.5 . . ?  
 C27 C49 H49A 109.5 . . ?  
 C27 C49 H49B 109.5 . . ?  
 H49A C49 H49B 109.5 . . ?  
 C27 C49 H49C 109.5 . . ?  
 H49A C49 H49C 109.5 . . ?  
 H49B C49 H49C 109.5 . . ?  
 C31 C50 H50A 109.5 . . ?  
 C31 C50 H50B 109.5 . . ?  
 H50A C50 H50B 109.5 . . ?  
 C31 C50 H50C 109.5 . . ?  
 H50A C50 H50C 109.5 . . ?  
 H50B C50 H50C 109.5 . . ?  
 C44 C51 H51A 109.5 . . ?  
 C44 C51 H51B 109.5 . . ?  
 H51A C51 H51B 109.5 . . ?  
 C44 C51 H51C 109.5 . . ?  
 H51A C51 H51C 109.5 . . ?  
 H51B C51 H51C 109.5 . . ?  
 C48 C52 H52A 109.5 . . ?  
 C48 C52 H52B 109.5 . . ?  
 H52A C52 H52B 109.5 . . ?  
 C48 C52 H52C 109.5 . . ?  
 H52A C52 H52C 109.5 . . ?  
 H52B C52 H52C 109.5 . . ?  
 Cl2 C1S Cl1 103(2) . . ?

_diffn_measured_fraction_theta_max	0.844
_diffn_reflns_theta_full	26.1
_diffn_measured_fraction_theta_full	0.844
_refine_diff_density_max	1.10
_refine_diff_density_min	-0.71
_refine_diff_density_rms	0.16
# END OF CIF	

# **Cu(3,5-heptanedionate)**

_audit_creation_method	SHELXL-97
_chemical_name_systematic	Cu <sup>II</sup> (bis)dipropionylmethane
;	
_chemical_name_common	?
_chemical_melting_point	?
_chemical_compound_source	'local laboratory'
_chemical_formula_moiety	'C <sub>14</sub> H <sub>22</sub> Cu O <sub>4</sub> '
_chemical_formula_sum	'C <sub>14</sub> H <sub>22</sub> Cu O <sub>4</sub> '
_chemical_formula_weight	317.86
loop_	
_atom_type_symbol	
_atom_type_description	
_atom_type_scatter_dispersion_real	
_atom_type_scatter_dispersion_imag	
_atom_type_scatter_source	
'C' 'C' 0.0033 0.0016	'International Tables Vol C Tables 4.2.6.8 and 6.1.1.4'
'H' 'H' 0.0000 0.0000	'International Tables Vol C Tables 4.2.6.8 and 6.1.1.4'
'Cu' 'Cu' 0.3201 1.2651	'International Tables Vol C Tables 4.2.6.8 and 6.1.1.4'
'O' 'O' 0.0106 0.0060	'International Tables Vol C Tables 4.2.6.8 and 6.1.1.4'
_symmetry_space_group_name_H-M	'P -1'
_symmetry_space_group_name_Hall	'-P 1'
_symmetry_cell_setting	'Triclinic'
loop_	
_symmetry_equiv_pos_as_xyz	
	'x, y, z'
	'-x, -y, -z'
_cell_length_a	4.551(3)
_cell_length_b	8.685(6)
_cell_length_c	18.870(12)
_cell_angle_alpha	86.29(2)
_cell_angle_beta	89.54(3)
_cell_angle_gamma	78.56(3)
_cell_volume	729.5(8)
_cell_formula_units_Z	2
_cell_measurement_temperature	110
_cell_measurement_reflns_used	1690
_cell_measurement_theta_min	2.5

_cell_measurement_theta_max	22.9
_exptl_crystal_description	needle
_exptl_crystal_colour	'light blue'
_exptl_crystal_size_max	0.32
_exptl_crystal_size_mid	0.07
_exptl_crystal_size_min	0.02
_exptl_crystal_density_meas	?
_exptl_crystal_density_diffn	1.447
_exptl_crystal_density_method	'not measured'
_exptl_crystal_F_000	334
_exptl_absorpt_coefficient_mu	1.504
_exptl_absorpt_correction_type	'multi-scan'
_exptl_absorpt_correction_T_min	0.645
_exptl_absorpt_correction_T_max	0.971
_exptl_absorpt_process_details	'Denzo and Scalepack (Otwinowski & Minor, 1997)'
_exptl_special_details	?
_diffn_ambient_temperature	110
_diffn_radiation_wavelength	0.71073
_diffn_radiation_type	MoK $\alpha$
_diffn_radiation_source	'fine-focus sealed tube'
_diffn_radiation_monochromator	graphite
_diffn_measurement_device_type	'KappaCCD (with Oxford Cryostream)'
_diffn_measurement_method	'\w scans with \k offsets'
_diffn_detector_area_resol_mean	?
_diffn_standards_number	0
_diffn_standards_interval_count	?
_diffn_standards_interval_time	?
_diffn_standards_decay_%	<2
_diffn_reflns_number	5467
_diffn_reflns_av_R_equivalents	0.047
_diffn_reflns_av_sigmal/netl	0.0763
_diffn_reflns_limit_h_min	-4
_diffn_reflns_limit_h_max	4
_diffn_reflns_limit_k_min	-9
_diffn_reflns_limit_k_max	9
_diffn_reflns_limit_l_min	-20
_diffn_reflns_limit_l_max	20
_diffn_reflns_theta_min	2.5
_diffn_reflns_theta_max	22.9
_reflns_number_total	1944

_reflns_number_gt	1346
_reflns_threshold_expression	$I > 2\sigma(I)$
_computing_data_collection	'COLLECT (Nonius, 2000)'
_computing_cell_refinement	'Denzo and Scalepack (Otwinowski & Minor, 1997)'
_computing_data_reduction	'Denzo and Scalepack (Otwinowski & Minor, 1997)'
_computing_structure_solution	'SIR97 (Altomare et al., 1999)'
_computing_structure_refinement	'SHELXL-97 (Sheldrick, 1997)'
_computing_molecular_graphics	'Ortep-3 for Windows (Farrugia, 1997)'
_computing_publication_material	'SHELXL-97 (Sheldrick, 1997)'
_refine_special_details	
;	
Refinement of $F^2$ against ALL reflections. The weighted R-factor wR and goodness of fit S are based on $F^2$ , conventional R-factors R are based on F, with F set to zero for negative $F^2$ . The threshold expression of $F^2 > 2\sigma(F^2)$ is used only for calculating R-factors(gt) etc. and is not relevant to the choice of reflections for refinement. R-factors based on $F^2$ are statistically about twice as large as those based on F, and R-factors based on ALL data will be even larger.	
;	
_refine_ls_structure_factor_coef	Fsqd
_refine_ls_matrix_type	full
_refine_ls_weighting_scheme	calc
_refine_ls_weighting_details	'calc w=1/[ $\sigma^2(F_o^2) + (0.0504P)^2 + 2.3881P$ ] where $P = (F_o^2 + 2F_c^2)/3$ '
_atom_sites_solution_primary	direct
_atom_sites_solution_secondary	difmap
_atom_sites_solution_hydrogens	geom
_refine_ls_hydrogen_treatment	constr
_refine_ls_extinction_method	none
_refine_ls_extinction_coef	?
_refine_ls_number_reflns	1944
_refine_ls_number_parameters	175
_refine_ls_number_restraints	0
_refine_ls_R_factor_all	0.093
_refine_ls_R_factor_gt	0.057
_refine_ls_wR_factor_ref	0.136
_refine_ls_wR_factor_gt	0.122
_refine_ls_goodness_of_fit_ref	1.070
_refine_ls_restrained_S_all	1.070



_refine_ls_shift/su_max	0.000
_refine_ls_shift/su_mean	0.000

loop\_

_atom_site_label	
_atom_site_type_symbol	
_atom_site_fract_x	
_atom_site_fract_y	
_atom_site_fract_z	
_atom_site_U_iso_or_equiv	
_atom_site_adp_type	
_atom_site_occupancy	
_atom_site_symmetry_multiplicity	
_atom_site_calc_flag	
_atom_site_refinement_flags	
_atom_site_disorder_assembly	
_atom_site_disorder_group	

Cu1 Cu 1.0000 1.0000 0.0000 0.0219(4) Uani 1 2 d S . .  
 Cu2 Cu 0.5000 0.0000 0.5000 0.0227(4) Uani 1 2 d S . .  
 O1 O 0.8525(9) 0.8508(5) -0.0540(2) 0.0207(11) Uani 1 1 d . . .  
 O2 O 0.8286(9) 0.9337(5) 0.0871(2) 0.0224(11) Uani 1 1 d . . .  
 O3 O 0.2645(9) 0.0551(5) 0.4151(2) 0.0249(11) Uani 1 1 d . . .  
 O4 O 0.2480(9) 0.1565(5) 0.5529(2) 0.0236(11) Uani 1 1 d . . .  
 C1 C 0.5545(15) 0.6731(8) -0.0868(4) 0.0254(17) Uani 1 1 d . . .  
 H1A H 0.4081 0.7445 -0.1185 0.030 Uiso 1 1 calc R . .  
 H1B H 0.4486 0.5959 -0.0622 0.030 Uiso 1 1 calc R . .  
 C2 C 0.6633(14) 0.7678(7) -0.0323(4) 0.0196(16) Uani 1 1 d . . .  
 C3 C 0.5541(15) 0.7617(8) 0.0366(4) 0.0232(17) Uani 1 1 d . . .  
 H3 H 0.4065 0.6998 0.0463 0.028 Uiso 1 1 calc R . .  
 C4 C 0.6448(14) 0.8398(8) 0.0928(4) 0.0218(17) Uani 1 1 d . . .  
 C5 C 0.5327(15) 0.8095(8) 0.1676(4) 0.0260(18) Uani 1 1 d . . .  
 H5A H 0.3355 0.7784 0.1646 0.031 Uiso 1 1 calc R . .  
 H5B H 0.6738 0.7202 0.1916 0.031 Uiso 1 1 calc R . .  
 C6 C 0.8062(14) 0.5847(8) -0.1321(4) 0.0290(18) Uani 1 1 d . . .  
 H6A H 0.7206 0.5259 -0.1665 0.044 Uiso 1 1 calc R . .  
 H6B H 0.9492 0.5114 -0.1013 0.044 Uiso 1 1 calc R . .  
 H6C H 0.9097 0.6604 -0.1574 0.044 Uiso 1 1 calc R . .  
 C7 C 0.5013(17) 0.9501(9) 0.2120(4) 0.037(2) Uani 1 1 d . . .  
 H7A H 0.4310 0.9229 0.2596 0.055 Uiso 1 1 calc R . .  
 H7B H 0.3563 1.0379 0.1895 0.055 Uiso 1 1 calc R . .  
 H7C H 0.6962 0.9808 0.2158 0.055 Uiso 1 1 calc R . .  
 C8 C -0.1266(15) 0.1656(8) 0.3362(4) 0.0265(18) Uani 1 1 d . . .  
 H8A H -0.2291 0.0755 0.3341 0.032 Uiso 1 1 calc R . .  
 H8B H 0.0354 0.1514 0.3004 0.032 Uiso 1 1 calc R . .

C9 C 0.0190(14) 0.1547(8) 0.4087(4) 0.0216(16) Uani 1 1 d . . .  
 C10 C -0.1153(15) 0.2444(8) 0.4626(4) 0.0252(18) Uani 1 1 d . . .  
 H10 H -0.3026 0.3126 0.4522 0.030 Uiso 1 1 calc R . .  
 C11 C 0.0017(15) 0.2429(8) 0.5306(4) 0.0233(17) Uani 1 1 d . . .  
 C12 C -0.1670(16) 0.3538(9) 0.5835(4) 0.0305(19) Uani 1 1 d . . .  
 H12A H -0.1410 0.4622 0.5699 0.037 Uiso 1 1 calc R . .  
 H12B H -0.3835 0.3525 0.5803 0.037 Uiso 1 1 calc R . .  
 C13 C -0.3504(16) 0.3138(9) 0.3133(4) 0.039(2) Uani 1 1 d . . .  
 H13A H -0.4294 0.3032 0.2661 0.059 Uiso 1 1 calc R . .  
 H13B H -0.2511 0.4042 0.3117 0.059 Uiso 1 1 calc R . .  
 H13C H -0.5156 0.3297 0.3474 0.059 Uiso 1 1 calc R . .  
 C14 C -0.0651(17) 0.3123(9) 0.6601(4) 0.0350(19) Uani 1 1 d . . .  
 H14A H -0.1828 0.3880 0.6909 0.053 Uiso 1 1 calc R . .  
 H14B H 0.1478 0.3161 0.6642 0.053 Uiso 1 1 calc R . .  
 H14C H -0.0948 0.2061 0.6746 0.053 Uiso 1 1 calc R . .

loop\_

\_atom\_site\_aniso\_label  
 \_atom\_site\_aniso\_U\_11  
 \_atom\_site\_aniso\_U\_22  
 \_atom\_site\_aniso\_U\_33  
 \_atom\_site\_aniso\_U\_23  
 \_atom\_site\_aniso\_U\_13  
 \_atom\_site\_aniso\_U\_12  
 Cu1 0.0204(7) 0.0229(8) 0.0239(8) -0.0037(6) 0.0019(5) -0.0070(5)  
 Cu2 0.0199(7) 0.0238(8) 0.0236(8) -0.0037(6) 0.0000(5) -0.0018(5)  
 O1 0.016(3) 0.024(3) 0.023(3) -0.001(2) -0.0004(19) -0.005(2)  
 O2 0.019(3) 0.023(3) 0.027(3) -0.003(2) 0.001(2) -0.009(2)  
 O3 0.026(3) 0.024(3) 0.024(3) -0.003(2) -0.001(2) -0.002(2)  
 O4 0.019(3) 0.025(3) 0.027(3) -0.007(2) -0.003(2) -0.001(2)  
 C1 0.029(4) 0.023(4) 0.027(5) 0.001(3) 0.003(3) -0.012(3)  
 C2 0.021(4) 0.012(4) 0.023(4) 0.001(3) -0.001(3) 0.000(3)  
 C3 0.031(4) 0.015(4) 0.027(5) -0.003(3) 0.003(3) -0.014(3)  
 C4 0.023(4) 0.020(4) 0.019(4) 0.003(3) -0.002(3) 0.003(3)  
 C5 0.026(4) 0.029(4) 0.025(4) 0.002(4) -0.003(3) -0.008(3)  
 C6 0.027(4) 0.028(4) 0.032(5) -0.008(4) 0.000(3) -0.003(3)  
 C7 0.049(5) 0.037(5) 0.025(5) -0.002(4) 0.016(4) -0.011(4)  
 C8 0.024(4) 0.028(4) 0.026(5) -0.001(3) -0.003(3) -0.003(3)  
 C9 0.019(4) 0.018(4) 0.029(4) -0.003(3) 0.003(3) -0.004(3)  
 C10 0.024(4) 0.028(4) 0.020(5) 0.000(4) -0.002(3) 0.001(3)  
 C11 0.020(4) 0.019(4) 0.031(5) -0.002(3) 0.004(3) -0.005(3)  
 C12 0.029(4) 0.029(4) 0.034(5) -0.015(4) 0.004(3) -0.004(3)  
 C13 0.041(5) 0.041(5) 0.031(5) 0.001(4) -0.004(4) 0.006(4)  
 C14 0.048(5) 0.031(5) 0.022(5) 0.001(4) 0.009(4) 0.000(4)

\_geom\_special\_details

;

All esds (except the esd in the dihedral angle between two l.s. planes) are estimated using the full covariance matrix. The cell esds are taken into account individually in the estimation of esds in distances, angles and torsion angles; correlations between esds in cell parameters are only used when they are defined by crystal symmetry. An approximate (isotropic) treatment of cell esds is used for estimating esds involving l.s. planes.

;

loop\_

\_geom\_bond\_atom\_site\_label\_1

\_geom\_bond\_atom\_site\_label\_2

\_geom\_bond\_distance

\_geom\_bond\_site\_symmetry\_2

\_geom\_bond\_publ\_flag

Cu1 O2 1.918(5) 2\_775 ?

Cu1 O2 1.918(5) . ?

Cu1 O1 1.922(4) 2\_775 ?

Cu1 O1 1.922(4) . ?

Cu2 O3 1.915(4) . ?

Cu2 O3 1.916(4) 2\_656 ?

Cu2 O4 1.923(4) . ?

Cu2 O4 1.923(4) 2\_656 ?

O1 C2 1.277(8) . ?

O2 C4 1.278(8) . ?

O3 C9 1.271(7) . ?

O4 C11 1.276(8) . ?

C1 C2 1.503(9) . ?

C1 C6 1.534(9) . ?

C1 H1A 0.9900 . ?

C1 H1B 0.9900 . ?

C2 C3 1.389(9) . ?

C3 C4 1.403(9) . ?

C3 H3 0.9500 . ?

C4 C5 1.522(9) . ?

C5 C7 1.508(10) . ?

C5 H5A 0.9900 . ?

C5 H5B 0.9900 . ?

C6 H6A 0.9800 . ?

C6 H6B 0.9800 . ?

C6 H6C 0.9800 . ?

C7 H7A 0.9800 . ?

C7 H7B 0.9800 . ?  
 C7 H7C 0.9800 . ?  
 C8 C9 1.515(9) . ?  
 C8 C13 1.515(9) . ?  
 C8 H8A 0.9900 . ?  
 C8 H8B 0.9900 . ?  
 C9 C10 1.385(9) . ?  
 C10 C11 1.393(9) . ?  
 C10 H10 0.9500 . ?  
 C11 C12 1.527(9) . ?  
 C12 C14 1.520(10) . ?  
 C12 H12A 0.9900 . ?  
 C12 H12B 0.9900 . ?  
 C13 H13A 0.9800 . ?  
 C13 H13B 0.9800 . ?  
 C13 H13C 0.9800 . ?  
 C14 H14A 0.9800 . ?  
 C14 H14B 0.9800 . ?  
 C14 H14C 0.9800 . ?

loop\_  
 \_geom\_angle\_atom\_site\_label\_1  
 \_geom\_angle\_atom\_site\_label\_2  
 \_geom\_angle\_atom\_site\_label\_3  
 \_geom\_angle  
 \_geom\_angle\_site\_symmetry\_1  
 \_geom\_angle\_site\_symmetry\_3  
 \_geom\_angle\_publ\_flag  
 O2 Cu1 O2 179.999(1) 2\_775 . ?  
 O2 Cu1 O1 93.58(18) 2\_775 2\_775 ?  
 O2 Cu1 O1 86.42(18) . 2\_775 ?  
 O2 Cu1 O1 86.42(18) 2\_775 . ?  
 O2 Cu1 O1 93.58(18) . . ?  
 O1 Cu1 O1 180.000(1) 2\_775 . ?  
 O3 Cu2 O3 180.0(2) . 2\_656 ?  
 O3 Cu2 O4 93.43(18) . . ?  
 O3 Cu2 O4 86.57(18) 2\_656 . ?  
 O3 Cu2 O4 86.57(18) . 2\_656 ?  
 O3 Cu2 O4 93.43(18) 2\_656 2\_656 ?  
 O4 Cu2 O4 180.0(2) . 2\_656 ?  
 C2 O1 Cu1 125.6(4) . . ?  
 C4 O2 Cu1 125.4(4) . . ?  
 C9 O3 Cu2 126.1(4) . . ?  
 C11 O4 Cu2 125.4(4) . . ?

C2 C1 C6 113.6(5) . . ?  
 C2 C1 H1A 108.9 . . ?  
 C6 C1 H1A 108.9 . . ?  
 C2 C1 H1B 108.9 . . ?  
 C6 C1 H1B 108.9 . . ?  
 H1A C1 H1B 107.7 . . ?  
 O1 C2 C3 124.5(6) . . ?  
 O1 C2 C1 116.0(6) . . ?  
 C3 C2 C1 119.4(6) . . ?  
 C2 C3 C4 125.1(6) . . ?  
 C2 C3 H3 117.5 . . ?  
 C4 C3 H3 117.5 . . ?  
 O2 C4 C3 124.7(6) . . ?  
 O2 C4 C5 115.4(6) . . ?  
 C3 C4 C5 119.9(6) . . ?  
 C7 C5 C4 113.3(6) . . ?  
 C7 C5 H5A 108.9 . . ?  
 C4 C5 H5A 108.9 . . ?  
 C7 C5 H5B 108.9 . . ?  
 C4 C5 H5B 108.9 . . ?  
 H5A C5 H5B 107.7 . . ?  
 C1 C6 H6A 109.5 . . ?  
 C1 C6 H6B 109.5 . . ?  
 H6A C6 H6B 109.5 . . ?  
 C1 C6 H6C 109.5 . . ?  
 H6A C6 H6C 109.5 . . ?  
 H6B C6 H6C 109.5 . . ?  
 C5 C7 H7A 109.5 . . ?  
 C5 C7 H7B 109.5 . . ?  
 H7A C7 H7B 109.5 . . ?  
 C5 C7 H7C 109.5 . . ?  
 H7A C7 H7C 109.5 . . ?  
 H7B C7 H7C 109.5 . . ?  
 C9 C8 C13 118.5(6) . . ?  
 C9 C8 H8A 107.7 . . ?  
 C13 C8 H8A 107.7 . . ?  
 C9 C8 H8B 107.7 . . ?  
 C13 C8 H8B 107.7 . . ?  
 H8A C8 H8B 107.1 . . ?  
 O3 C9 C10 124.6(6) . . ?  
 O3 C9 C8 114.1(6) . . ?  
 C10 C9 C8 121.2(6) . . ?  
 C9 C10 C11 125.4(6) . . ?  
 C9 C10 H10 117.3 . . ?

C11 C10 H10 117.3 . . ?  
 O4 C11 C10 124.8(6) . . ?  
 O4 C11 C12 115.9(6) . . ?  
 C10 C11 C12 119.3(6) . . ?  
 C14 C12 C11 114.0(6) . . ?  
 C14 C12 H12A 108.7 . . ?  
 C11 C12 H12A 108.7 . . ?  
 C14 C12 H12B 108.7 . . ?  
 C11 C12 H12B 108.7 . . ?  
 H12A C12 H12B 107.6 . . ?  
 C8 C13 H13A 109.5 . . ?  
 C8 C13 H13B 109.5 . . ?  
 H13A C13 H13B 109.5 . . ?  
 C8 C13 H13C 109.5 . . ?  
 H13A C13 H13C 109.5 . . ?  
 H13B C13 H13C 109.5 . . ?  
 C12 C14 H14A 109.5 . . ?  
 C12 C14 H14B 109.5 . . ?  
 H14A C14 H14B 109.5 . . ?  
 C12 C14 H14C 109.5 . . ?  
 H14A C14 H14C 109.5 . . ?  
 H14B C14 H14C 109.5 . . ?

\_diffn\_measured\_fraction\_theta\_max  
 \_diffn\_reflns\_theta\_full  
 \_diffn\_measured\_fraction\_theta\_full  
 \_refine\_diff\_density\_max  
 \_refine\_diff\_density\_min  
 \_refine\_diff\_density\_rms  
 # END OF CIF

0.972  
 22.9  
 0.972  
 0.90  
 -0.44  
 0.105

## **Vita**

Sylvester Burton was born on September 25, 1954, to Arless and Francis Burton in Shreveport, Louisiana. He attended Southern University where he received his Bachelor of Science degree in chemistry in May of 1977. He pursued a career in the petroleum reservoir engineering industry from 1978 until 1983. He returned to Southern University in 1983 where he received his Master of Science degree in chemistry in December of 1986. He was formerly an Instructor of Chemistry at the University of Southwestern Louisiana from 1986 until 1992. In 1994 he returned to Southern University as an Instructor of Chemistry, and in 1997 he entered Louisiana State University and expects to receive the degree of Doctor of Philosophy in May of 2006.